Head Office: Università degli Studi di Padova

Department of Surgical, Oncological and Gastroenterological Sciences

PhD course in Clinical and Experimental Oncology and Immunology

XXXIV series

ROLE OF PROTEIN KINASE CK1α IN THE MULTIPLE MYELOMA ASSOCIATED BONE DISEASE

Thesis written with the financial contribution of

"Martino e Silvana Gesuato Foundation Scholarship"

Coordinator: Ch.mo Prof. Stefano Indraccolo, Department of Surgical, Oncological and Gastroenterological Sciences, Padova, Italy

Supervisor: Prof. Francesco Piazza, Department of Medicine, Padova, Italy

Co-Supervisor: Dott.ssa Sabrina Manni, Department of Medicine, Padova, Italy

Ph.D. student: ANNA FREGNANI

INDEX

ABSTRACT

Multiple myeloma (MM) is a malignant plasma cell (PC) neoplasm which displays also pathological bone involvement. The bone marrow (BM) microenvironment sustains the MM associated bone disease (MMABD) characterized by impaired bone homeostasis. The Wnt/β-catenin pathway plays a critical role on mesenchymal stromal cell (MSC) differentiation towards the osteoblastic lineage, stimulating *RUNX2*, the master gene regulator of this process. Moreover, the effect of MM cells on osteoblastogenesis appears to be mediated by their capability to inhibit RUNX2 expression in MSC.

The Ser/Thr protein kinase CK1α is overexpressed in MM cells supporting the tumor phenotype. Previous data demonstrated that CK1α inactivation causes MM cells apoptosis and cell cycle arrest, impinging on clonal expansion. Lenalidomide (Lena), an immunomodulatory drug (IMiD) used in MM therapy, is able to induce CK1α protein degradation in MM cells and although its effects on PCs has been intensively studied, its effects on the stromal compartment are still debated.

CK1α has a negative role on Wnt pathway promoting β-catenin proteasomal degradation. Therefore, in this study we aimed at investigating whether CK1α inactivation could support the MSC osteogenic transcriptional program and positively promote osteogenesis in a context of MM BM *niche*. Moreover, the study pointed to unravel the effects of Lena on the MSC osteogenic differentiation potential, to better understand its possible impact on MMABD.

We have demonstrated that CK1α inactivation in two different *CSNK1A1* shRNA IPTG inducible MSC cellular clones, called respectively MSC hTERT 6044 and HS-5 6044, promoted the potential osteogenic differentiation of MSC towards the osteoblastic lineage, through the upregulation of the early osteogenic *RUNX2* and the later *ALP*, *SPP1 and BGLAP* markers.

To deeply investigate if CK1α could regulate osteogenesis also in the BM context, we reproduced the BM *niche* through a co-culture model between the MM IL-6 dependent INA-6 cells and a feeder layer of stromal cells represented by the MSC hTERT or HS-5 cells. We discovered that in this model of co-culture, a specific CK1α inactivation in MM cells or in the MSC hTERT could induce MM cells apoptosis and could support the osteogenic transcriptional program, with the potential to counteract the MMABD. However, using HS-5 as stromal feeder layer gave opposite results. Indeed, only when CK1α silencing was achieved both in MM and in HS-5 cells in the co-culture model, the osteogenic differentiation block induced by malignant PCs was overcome.

Focusing our investigation on RUNX2 basal expression, we found that its expression in MM cells is mainly sustained by cell-to cell contact with stromal cells both with MSC hTERT and HS-5, rather than by soluble

factors. Oppositely, RUNX2 expression in the stromal compartment represented by MSC hTERT and HS-5 cell lines depicted two different *scenarios*. Indeed, in the MSC hTERT cell line both soluble factors and cell-to cell contact caused a reduction of RUNX2 expression, which is instead unaffected in the HS-5 cell line. The different immortalization methods used in the two cell lines could be responsible for this discrepancy, since only MSC hTERT and not HS-5 cells could express the p53 protein.

Next, we focused our study on Lena confirming that it is able to induce CK1α degradation also in MSC but it did not seem to have a positive role on the expression of osteoblastic related genes, thus likely limiting the osteogenic differentiation potential of MSC.

Our results indicate that CK1α inactivation could be a promising therapy not only to enhance the pro-apoptotic effect of Lena on the haematological disease, but also to interfere with the undesirable effects of this drug on the osteogenic differentiation potential, likely ameliorating MMABD.

ABBREVIATIONS

A

ALP	Alkaline phosphatase
APC	Adenomatous polyposis coli
AML	Acute myeloid leukemia

B

BCL-2	B Cell Lymphoma-2
BD	Bone Disease
BIRC3	Baculoviral IAP repeat containing 3
BM	Bone Marrow
BMSC	Bone Marrow Stromal Cells
BP	Bisphosphonates
BMP	Bone Morphogenetic Protein

C

CAM-DR	Cell-Adhesion-Mediated Drug Resistance
CBFA1/AML3	Runt-related transcription factor 2
CCL3	C-C motif ligand 3
CCR1	C-C motif chemokine receptor 1
CFU	Colony-forming unit
CLL	Chronic Lymphocytic Leukemia
CK1α	Casein kinase 1
COL1α1	Collagen1α1
CRAB	Calcium, Renal, Anemia and Bone abnormalities
CRCs	Colon rectal cancers

D

DEPTOR	Domain containing mTOR interacting protein
DKK-1	Dickkopf-1 related protein
DLX5	Distal-less homeobox 5
DVL	Dishevelled

E

ECM	Extracellular matrix
ERK	Extracellular signal-regulated kinases
EMM	Extramedullary multiple myeloma
EZH2	Enhancer of zeste 2 polycomb repressive complex 2 subunit

F

FADD	Fas-Associated protein with Death Domain
FDA	Food and Drug Admnistration
FISH	Fluorescent In Situ Hybridization
FOXO3	Forkhead box protein O3
FOXO1	Forkhead box protein O1

FZD	Frizzled

G

GFI-1	Growth Factor Independent 1 transcriptional repressor
GL11	Glioma-associated oncogene homolog1
GSK3-β	Glycogen Synthase Kinase 3 beta

H

HCC	Hepatocellular carcinoma
HDAC1	Histone deacetylase 1
HH	Hedgehog
HS	Heparan sulfate

I

ICAM1	Intercellular Adhesion Molecule 1
IGF-1	Insulin like Growth Factor-1
Ig	Immunoglobulin
IgH	Ig heavy chain
IHH	Indian Hedgehog
IKZF1	Ikaros
IKZF3	Aiolos
IL	Interleukine
IMiDS	Immunomodulatory drugs
IRF4	Interferon Regulatory Factor 4

L

Lena	Lenalidomide
LEF1	Lymphoid enhancer-binding factor-1
LFA-1	Leukocyte function-associated antigen 1
LRP	Low-density lipoprotein receptor Related Protein

M

mAb	Monoclonal antibody
MAPK	Mitogen-Activated Protein Kinase
M-CSF	Macrophage colony stimulating factor
MCLs	Multiple myeloma Cell Lines
MDMX	Mouse Double Minute 4 homolog
MDM2	Murine Double Minute chromosome 2
MDS	Myelodysplastic syndrome
MGUS	Monoclonal Gammopathy of Undetermined Significance
miRNAs	MicroRNAs
MIP1α	Macrophage Inflammatory Protein 1α
MM	Multiple Myeloma
MMABD	Multiple Myeloma Associated Bone Disease
MMP	Matrix metallopeptidase
MSC	Mesenchymal Stromal Cells

mTOR	Mammalian target of rapamycin

N

NHL	Non Hodgkin lymphoma
NCAM	Neuronal adhesion molecule
NF-κB	Nuclear Factor Kb
NK	Natural Killer

O

OCN	Osteocalcin
OCPs	Osteoclasts precursors
OPG	Osteoprotegerin
OPN	Osteopontin
OSX	Osterix

P

PCs	Plama Cells
PCL	Plasma Cells Leukemia
PKC	Protein Kinase
PI3K/AKT	Phosphatidylinositol-3 kinase/protein kinase B
PI	Proteasome Inhibitors
PIP3	Phosphatidylinositol (3,4,5) trisphosphate
PLC	Phospholipase C
Poma	Pomalidomide
PYGO	Pygopus
PTCH1	Protein patched homolog 1
PTH	Parathyroid hormone

R

RANKL	Receptor Activator of Nuclear factor Kappa-B Ligand
ROR	Receptor tyrosine kinase like orphan receptor
RUNX2	Runt-related transcription factor 2

S

SCL	Sclerostin
SFRP	Secreted Frizzled-related proteins
shRNA	Short hairpin RNAs
SMURF2	SMAD Specific E3 Ubiquitin Protein Ligase 2
SLAMF7	Signaling Lymphocytic Activation Molecule Family-7
SMAD	Small Mother Against Decapentaplegic
SMM	Smouldering multiple myeloma
SPARC	Osteonectin
SRE	Skeletal related events

T

TCF	T cell factor

TME	Tumor microenvironment
TNFα	Tumor necrosis factor-α
TGFβ	Transforming Growth Factor-β
TRAIL	TNF-related apoptosis inducing ligand

U

UPR	Unfolded Protein Response

V

VCAM1	α4β1- vascular cell-adhesion
VLA	Very Late Antigen
VEGF	Vascular Endothelial Growth Factor

W

WLS	Wntless

AMINO ACID ABBREVIATIONS

A	Ala	Alanine
C	Cys	Cysteine
D	Asp	Aspartic acid
E	Glu	Glutamic acid
F	Phe	Phenylalanine
G	Gly	Glycine
H	His	Histidine
I	Ile	Isoleucine
K	Lys	Lysine
L	Leu	Leucine
M	Met	Methionine
N	Asn	Asparagine
P	Pro	Proline
Q	Gln	Glutamine
R	Arg	Arginine
S	Ser	Serine
T	Thr	Threonine
V	Val	Valine
W	Trp	Tryptophan
Y	Tyr	Tyrosine

X generic amino acid

1. MULTIPLE MYELOMA

1.1 DEFINITION AND EPIDEMIOLOGY

Multiple myeloma (MM) is an hematological cancer of terminally differentiated plasma cells (PCs) that accounts for about 1% of all cancers and is the second most common hematological malignancy after non-Hodgkin lymphoma (NHL) [1]. It is a clonal disease characterized by uncontrolled growth of monoclonal PCs in the bone marrow (BM), that leads to the over-secretion of non-functional monoclonal immunoglobulins (Igs), called M-protein, or Ig free light chains [2]. Accumulation of Ig and interactions of the monoclonal PCs with others cells in the BM microenvironment, cause the widely known MM symptomatology [3].

The oncogenic transformation in MM occurs within the secondary lymphoid organs since the malignant PCs present a high rate of somatic mutations and, considering the nature of the monoclonal Ig, they are essentially IgG and IgA. Focusing on these pieces of evidence, it has been supposed that the PCs transformation occurs after the end of the somatic hypermutation and during the class switch recombination in the germinal centers [2]. Furthermore, neoplastic PCs are reliably differentiated from healthy PCs, based on their expression of monoclonal intracytoplasmic Ig, diminished CD27, CD38, and/or CD138, positivity for CD56, CD20, CD28, or CD117 and negativity for CD19 and/or CD45 [4].

MM is a disease of the older population: in the western World, the incidence has been reported to be approximately 5 cases per 100.000 and the median age of patients at diagnosis is about 66-70 years. The disease is less frequent in patients younger than 65 years of age (37% of cases) and is extremely rare in those less than 30 years (0,02% of cases). Interestingly, MM has one of the most pronounced differences between populations in both incidence and outcome. Indeed, the incidence of disease in the African American population is twice that of the Caucasian population and thrice in those younger than 50 years of age [5].

1.2 MULTISTEP AND HETEROGENEOUS DISEASE

From the clinical, cytogenetic and molecular point of view, MM is a very heterogeneous disease [2].

The heterogeneity in clinical presentation, course and survival often mirrors the cytogenetic abnormalities in the malignant clone. MM develops in a multistep process (Fig.1), evolving from a pre-malignant stage such as monoclonal gammopathy of undetermined significance (MGUS) and smouldering multiple myeloma (SMM) to the active MM and plasma cell leukemia (PCL) [1]. The premalignant condition MGUS is characterized by a serum protein level of less than 3 g per 100 mL and BM PCs less than 10%, without related clinical manifestations and the 1% per year overall risk of transformation to MM. Patients with serum M protein higher than 3 g per 100 mL, urine light-chain protein greater than 1 g per day and/or BM PCs equal or more than 10% present the diagnostic criteria for MM. The common clinical presentation of active MM

are bone pain and pathological fractures, anemia (bone marrow failure), recurrent infections, hypercalcemia, renal failure and abnormal bleeding, together referred to as CRAB (Calcium, Renal, Anemia and Bone abnormalities) [6]. Patients who present MM diagnostic criteria without characteristic symptoms are classified in SMM disease stage. Upon further progression, MM occurs at extramedullary sites describing the condition of PCL in which PCs circulate in peripheral blood [7].

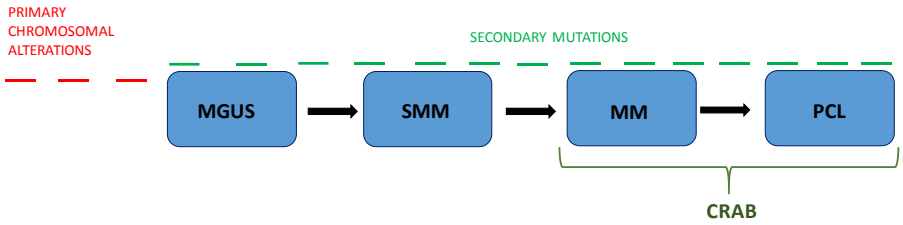

Fig.1 Schematic representation of MM multistep process.

Since 2000s, it has been possible a spread of knowledge about the genomic and molecular characterization of MM, thanks to metaphase karyotyping and Fluorescent In Situ Hybridization (FISH) until more high-throughput technologies such as gene expression profiling and next generation sequencing. Most of the genomic work unraveled MM heterogeneity that mirrors the complexity of clonal evolution [3]. The development of different minor subclones, in most cases undetectable at diagnosis, are the consequence of epigenetic changes and the therapeutic pressure. Indeed, the different clones acquire spontaneous genetic lesions, supporting disease progression via clonal competition and survival of the fittest clone, evolving via a classic Darwinian branching pattern of increasing genetic complexity [3][2].

Focusing on the MM genomic landscape, it is characterized by high instability caused by numerous chromosomal gains or losses, structural variations, cancer driver gene mutations, that can be recognized already at the premalignant states of the disease [8]. Common primary genetic events are chromosomal translocations (>90%), aneuploidy and primary trisomies. The secondary genetics events include copy number abnormalities, DNA hypomethylation and acquired mutations, that lead to tumor progression [1]. The pivotal chromosomal translocations involve the Ig heavy chain (*IgH*) locus on chromosome 14 (14q32.33) and one of several chromosomes among which 4, 6, 11, 14 and 20. In the resulting product, specific oncogenes are under the transcriptional control of the IgH enhancer. Among the main translocations, t(4;14), t(11;14), t(6;14), t(14;16), t(14;20) cause *MMSET/FGFR3*, *CCDN1*, *CCDN3*, *MAF* and *MAFB* oncogenes expression [8]. Primary chromosomal trisomies involve the odd-numbered chromosomes 3, 5, 7, 9, 11, 15, 19, 21, causing hyperdiploid karyotype. Considering the secondary cytogenetic abnormalities, the monosomy of chromosome 13 and del13q have been detected in 35-40% and 6-10% of patients respectively and they are associated with poor prognosis. The loss of tumor-suppressor TP53 activity occurs by del17q or by the presence of inactivating mutations and it is particularly associated with aggressive clinical course and poor overall survival [3]. Moreover, chromosomal alterations or focal amplifications on 8q24 chromosomal locus,

commonly cause oncogene *MYC* activation, leading to pleiotropic downstream effects, driving MM cell proliferation. *MYC*-oncogene aberrations have been detected in almost 50% of MM patients causing poor outcomes [8].

In addition to chromosomal aberrations, several gene mutations are frequently involved in myelomagenesis, guiding defects in cell-cycle progression (Fig.2). These pivotal mutations increase the instability of chromosomal structures through cell cycle perturbation. Among these, *KRAS*, *NRAS*, *BRAF* mutations affect the mitogen-activated protein kinase (MAPK) pathway and have been found in 40% of MM patients. Others mutations frequently found are *FAM46C* and *CCDN1* that codes for the proto-oncogene cyclin D1, an essential regulator of G1 to S phase progression [8]. Frequently, in the late stage of the disease, different mutations have been found to inactivate the regulation of the nuclear factor κB (NF-κB) pathway, inducing MM cells-BM cross talk perturbation [3]. Despite the overall agreement about the prognostic impact of cytogenetic abnormalities, it still unclear if these represent predictive biomarkers of the pathology (Fig.3) [1].

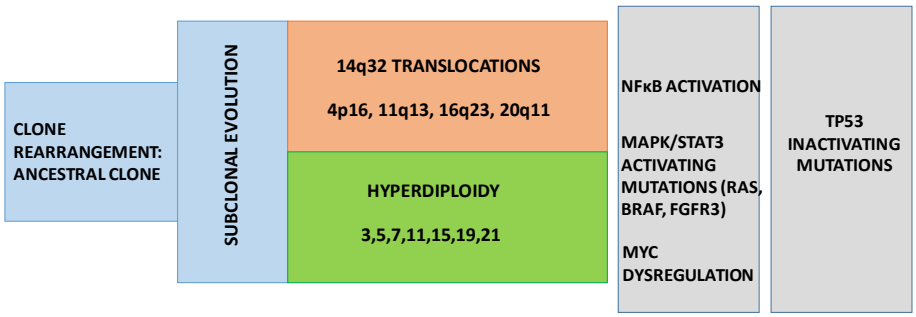

Fig.2 Oncogenetic model supports MM multistep process, (adapted from [2]).

Genomic Event	Genes Involved	Frequency in MM[†] (%)	Prognostic Value
Primary Abnormalities			
Trisomies	Odd-numbered chromosomes: 3, 5, 7, 9, 11, 15, 19 or 21	~45	Favorable[‡]
Translocations	t(11;14): CCND1	15	Neutral
	t(4;14): FGR3/MMSET	15	Adverse
	t(6;14): CCND3	2	Neutral
	t(14;16): MAF	5	Adverse
	t(14;20): MAFB	1	Adverse
Secondary Abnormalities			
Chromosome gains	1q: MCL1, CKS1B, ANP32E or BCL9	40	Adverse
	8q: MYC	15	Neutral
	11q: CCND1	15	Neutral
Chromosome losses	1p: CDKN2C or FAM46C	30	Adverse
	12p: CD27	15	Adverse
	14q: TRAF3	10	Not determined
	16q: CYDL or WWOX	30	Neutral
	17p:TP53	10	Adverse
	13q: RB1, DIS3, mir15a or mir16.1	40	Neutral
Translocations	Affecting MYC: t(8;14), t(8;11)	15	Adverse

Fig.3 Frequency and prognostic value of genomic alterations in MM, (adapted from [1]).

1.3 BONE MARROW MICROENVIRONEMNT

MM is characterized by PCs growth within the BM that mirrors the extreme addiction of MM clone to BM tumor microenvironemt (TME). Extramedullary MM (EMM) is a rare MM manifestation where PCs become independent of BM TME, thus infiltrating other organs or circulating in peripheral blood [9]. The most aggressive type of EMM is PCL, in which at least 20% clonal PCs is observed in blood [10]. More recently, this cut off threshold has been proposed to be 5%. Several mechanisms and different features are involved in the cross talk between malignant PCs and BM *niche,* including soluble cytokines, adhesion molecules and different signaling pathways [11]. The *niche* ecosystem is mainly populated by stromal cells, endothelial cells, hematopoietic cells, immune cells, osteoblasts, osteoclasts and extracellular matrix. The networking between all features in TME allows the activation of autocrine and paracrine signaling, promoting the malignant clone survival [9]. Diverse molecules are involved in MM cell adhesion to BM stromal cells (BMSC) including CD44 isoforms, neuronal adhesion molecule (NCAM), beta-1 integrins [very late antigen (VLA) 4, VLA5] and beta-2 integrins [leukocyte function-associated antigen 1 (LFA-1), intercellular adhesion molecule (ICAM1)] and chemokine receptors. In turn, cellular adhesion promotes secretion of cytokines, chemokines and other factors that favor angiogenesis and an immune suppressive microenvironment [9]. Focusing on soluble factors secreted in the BM *milieu*, the main are interleukine-6 (IL-6), tumor necrosis factor-α (TNF-α), Insulin like growth factor-I (IGF-I) and vascular endothelial growth factor (VEGF). These molecules are able to activate MM related signaling pathways among which Ras/Raf/MAPK cascade, the phosphatidylinositol-3 kinase (PI3K)/protein kinase B (AKT) signaling, MAPK/ extracellular signal-regulated kinases (ERK) and JAK/STAT pathways, which mediate growth, survival, drug resistance and migration of MM cells as well as

osteoclastogenesis and angiogenesis [7] [12]. The involvement of adhesion molecules and soluble factors on bone impairment will be widely discuss on chapter 2.3.

A critical microenvironmental factor involved in the development of genomic instability is hypoxia. It has been discovered that the BM microenvironment in MM is more hypoxic than the normal BM and it causes increased DNA damage, enhanced mutagenesis and functional impairments in the DNA repair pathways. Moreover, the consequence of poorly oxygenated *niche* and hypoxia is the induction of glycolytic metabolism that correlates to drug resistance in MM cases [8].

1.4 THERAPY

Despite the fact that survival in MM has improved significantly in the last 15 years, MM remains an incurable disease. Many patients achieve a stable remission through a combination of chemotherapy and autologous stem-cell transplantation, but in most cases, the disease relapses and becomes drug resistant. Another option for a minority of young and fit patients, is the allogenic stem-cell transplantation, even if relapse is still common [6]. For all these reasons, the introduction of new specific therapeutics molecules could significantly improve refractory and relapsed MM patients outcome [13]. Before the new therapeutic drug classes Melphalan was considered the standard of treatment for MM patients. To date, the therapy mainly accounts proteasome inhibitors (PI), immunomodulatory drugs (IMiDs) classes.

IMiDs

Thalidomide and its derivatives Lenalidomide (Lena) and Pomalidomide (Poma), belong to IMiDs class. These molecules bind and activate Cereblon E3 ubiquitin ligase, resulting in the ubiquitination and in the subsequent degradation of Ikaros (IKZF1) and Aiolos (IKZF3), two zinc finger transcription factors, which are fundamental for B cell maturation and MM cells survival. Indeed, the Lena-dependent degradation of IKZF1/IKZF3 leads to the expression of interferon regulatory factor 4 (IRF4), which in turn regulates the oncogene *MYC*. In addition, the Lena-induced degradation of IKZF1/IKZF3, is associated with increased IL-2 transcription and production, leading to proliferation of natural killer (NK) and CD4+T cells [14].

Moreover, IMiDs present anti-angiogenic properties, reducing both VEGF and IL-6 expression, thereby counteracting angiogenesis. IMiDs are also known to decrease the cell surface adhesion molecules, in particular ICAM-1, VCAM-1 and E–selectin, thus inhibiting the adhesion of MM cells to the BM microenvironment. IMiDs cause cell cycle arrest through the regulation of cyclin dependent kinase. Furthermore, these drugs are able to alter cytokine production in the BM TME, enhancing anti-inflammatory cytockine IL-10 release and contrasting TNF-α, IL-1, IL-12 production [15].

A

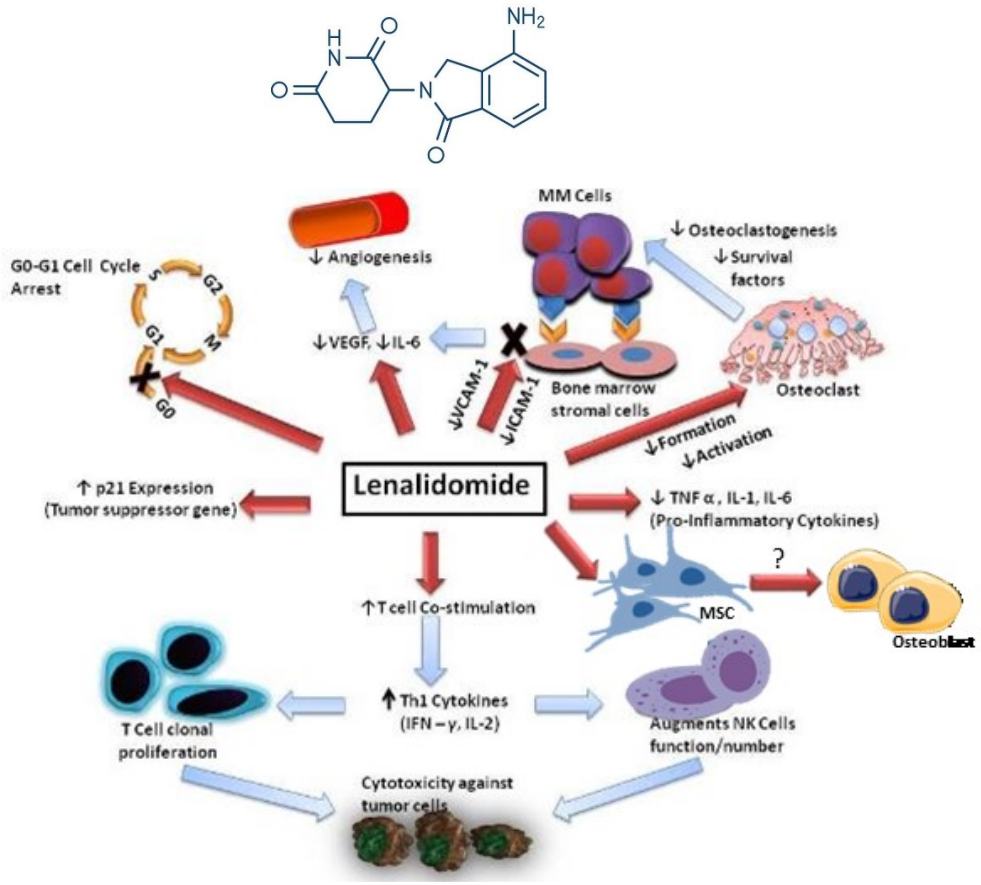

Fig.4 Molecular structure of Lenalidomide (A) and its mechanism of action (B), (adapted from [15]).

PROTEASOME INHIBITORS

The proteasome 26S, composed by 20S proteolytic core region and two 19S regulatory particles, is a multicatalytic enzyme complex involved in the adenosine triphosphate-dependent intracellular proteolysis. Indeed, the ubiquitin-proteasome pathway is able to disrupt each protein flagged with the polyubiquitin chain, tightly regulating cellular protein degradation [16]. The therapeutical strategy based on PI is based on the high proliferation and protein synthesis rate of the malignant PCs. Indeed, MM cells are more sensitive to proteasome inhibition compared to normal cells due to high secretion of Igs that are generally transported out of endoplasmic reticulum through the unfolded protein response (UPR). The cellular stress induced by PI, causes cell cycle arrest and apoptosis through the UPR pathway [16]. An important mechanism of action of PI is the inhibition of NF-κB signaling, overactive in MM pathogenesis. Moreover, different processes are affected by proteasome activity, including cell cycle control, pro inflammatory cytochine pathways, cell adhesion and proangiogenic signaling. Bortezomib is a PI widely used in MM therapy combinations, belonging to the first generation of such inhibitors. It is a peptide boronic acid and a reversible inhibitor of the β5 catalytic subunit (Fig.5) [17]. By contrast, the second-generation agent Carfilzomib is an IV peptide epoxyketone that irreversibly inhibits the β5 site. Ixazomib, is the third approved PI and it is the first orally

administered agent in this class to be investigated in the clinic and, like Bortezomib, is a peptide boronic acid [17].

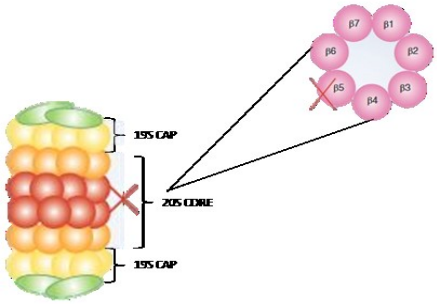

Fig.5 Schematic representation of proteasome. Zoom of central rings of the inner core.

The main drugs with anti-catabolic properties used to prevent skeletal-related events (SRE) and to treat bone disease (BD) in MM are Bisphosphonates (BP) and the molecule Denosumab. BP are pyrophosphate analogs able to bind to bone areas of exposed hydroxyapatite crystals, while Denosumab is a monoclonal antibody (mAb) that strongly binds Receptor Activator of Nuclear Factor kappa-B Ligand (RANKL) mimicking Osteoprotegerin (OPG) in the physiologic control of OPG/RANKL ratio. Other potential therapeutic targets for BD include anti Dickkopf-1 related protein (DKK-1), Sclerostin (SCL) antagonists (Romosozumab, currently in clinical trial) and anti-Transforming Growth Factor-β (TGF-β), which try to combine the antagonism to the reduction in bone resorption with the promotion of new bone formation delaying the burden of disease [18].
In the relapsed MM treatment settings, numerous new molecules in the last decade have been approved by Food and Drug Administration (FDA). The introduction of mAbs opened the possibility to the use also of the immunotherapeutic approach to cure MM patients. New drugs enrolled in therapy are used in multiple combinations, in order to target not only the malignant Pcs malignant clone, but also the permissive microenvironment [19]. Among these, Panobinostat, Elotuzumab, Daratumumab, Isatuximab and Selinexor have been recently approved for the treatment of relapsed MM. Particularly, Elotuzumab is a IgG-k mAb specific for Signaling Lymphocytic Activation Molecule Family F7 (SLAMF7), a surface glycoprotein receptor expressed on PCs and implicated in adhesion to stromal cells. Panobinostat is a deacetylase inhibitor, able to inhibit aggressome pathway, while Selinexor, blocking exportin 1, leads to accumulation and activation of various tumor suppressor. The mAbs Daratumumab and Isatuximab both target CD38, a transmembrane glycoprotein highly expressed on MM cells that acts as both receptor and an ectoenzyme [13][19].
Interestingly, in recent years, the definition of MM is changing towards to include disease' states historically considered precursors. Thus, the starting point of treatment could be the SMM state, resulting in improved both survival and patients quality life [20]. The future directions of innovative patient-specific therapy strategies, have to consider oncogenomics, gene/protein expression profile and high-throughput screening in order to use less toxic targeted agents combination and adjust them over time, based on the evolving clonal architecture [21].

2. MULTIPLE MYELOMA ASSOCIATED BONE DISEASE

2.1 BONE HOMEOSTASIS

Bone is continually remodeled by a dynamic process. Cells and extracellular matrix (ECM) build the bone, which becomes mineralized by the deposition of calcium hydroxyapatite, which confers rigidity and strength. The ECM makes up 90% of overall bone volume and it consists of organic and inorganic components. The inorganic part is composed by calcium, phosphorus and magnesium, mainly in the form of hydroxyapatite. The organic part predominantly contains type I collagen with glycoproteins, proteoglycans, growth factors that allow the matrix mineralization [22]. The major cell types that constitute adult skeleton are osteoblasts, osteocytes and osteoclasts. In a coupled and constant process, osteoblasts and osteoclasts, respectively form and resorb the bone [23]. A specific interconnected molecular orchestra of signaling pathways, regulates bone maturation, preventing bone disorders [24]. Focusing on the osteoblasts, these cells secrete and synthesize bone matrix, forming the whole bone. In 1970 *Friedenstaein et al.* were the first to discover the mesenchymal stromal cells (MSC), the osteoblasts progenitors, described as rare nucleated cells in the BM, with spindle-shaped morphology, able to adhere to plastic, creating fibroblastoid colonies (colony-forming unit-fibroblasts, "CFU-F") [25]. MSC are pluripotent cells able to differentiate in osteoblasts, chondrocytes and adipocytes. Due to their ability of differentiation, self-renewal and expansion, many studies are focusing on MSC as a future promising tool for treating bone pathology and damaged tissues/organs. Proliferative stage, cell maturation and matrix mineralization are the main phases of MSC osteogenic differentiation. The enrollment and the expansion of osteoprogenitors cells precede cell maturation in pre-osteoblasts upon ECM, which ends with the mineralization [24].

The main genes expressed by osteoblasts are Osterix (*SP7,* OSX) and Runt-related transcription factor 2 (*RUNX2*), identified as early osteoblast markers and controllers of the osteoblastic lineage. Focusing on OSX role, it acts in diverse fashions, controlling the commitment of MSC promoting primary crystal formation and regulating bone homeostasis. In fact, OSX upregulation maintains the cells in an immature and undifferentiated state. *SP7* transgenic mice displayed osteopenia and reduced bone matrix mineralization not only in embryos, but in postnatal phase too, with a sever impairment of bone formation. Moreover, it has been demonstrated an auto-regulatory loop of OSX, able to maintain a sufficient level of *SP7* at early phase of differentiation and its down-regulation at the later [26]. Besides *OSX* and *RUNX2*, a distinctive pattern of genes are expressed towards osteoblastic lineage, such as alkaline phosphatase (*ALP*), Collagen type Iα1 (*COL1A1,* COL1α1) and Osteopontin (*SPP1,* OPN), a non-collagenous matrix protein. Considering the late differentiation markers, Osteocalcin (*BGLAP*, OCN) is the most abundant non-collagenous bone matrix protein. Furthermore, Osteonectin (*SPARC*) is a phosphate binding secreted protein that operates with OCN in the deposition of mineral by regulating the number of hydroxyapatite crystals [23].

TGF-β/bone morphogenetic protein (BMP) pathway closely cooperates with Wnt/β-catenin signaling, in the control of osteoblastogenesis. TGF-β/BMP pathway activates both canonical Smad (small mother against decapentaplegic) dependent signaling (TGF-β/BMP ligands-receptors-Smads) and MAPK, the non-canonical Smad-independent signaling pathway (p38/MAPK). Both signaling promote *RUNX2* gene expression and therefore MSC differentiation [27]. Among BMPs family, BMP2, 4, 5, 6, 7, 9 have main roles in osteogenesis. Particularly, BMP signaling promotes every stages of the differentiation also interplaying with fibroblast growth factor signaling [28]. On the contrary, TGF-β controls only the early phases, inhibiting the terminal differentiation.

Additionally, also Notch and Hedgehog (Hh) signaling are involved in bone homeostasis. Regarding Notch signaling, the proteolytically cleaved Notch protein NCID, expressed in osteoblastic cell lines, impairs their osteogenic differentiation, blocking an artificial LEF1/TCF (lymphoid enhancer-binding factor 1 /T cell factor) target promoter [29].

In endochondral bone, the commitment of MSC into the osteoblast lineage is dependent on Hh signaling. Among involved molecules in Hedgehog pathway, Indian Hedgehog (Ihh), glioma-associated oncogene homolog1 (GLI1) and protein patched homolog 1 (PTCH1) are the main whose expression is enhanced by RUNX2 [30]. Several epigenetic factors, such as microRNAs (miRNAs), control the signaling pathways involved in osteogenesis, by a post-transcriptionally modulation, increasing or reducing osteogenesis gene expression [24]. Ultimately, the osteoblasts have a double fate: they could remain quiescent or became osteocytes [23][31].

The osteocytes are the most abundant cells in bone (90-95% of totally cells) derived from mature osteoblasts and embedded within the mineralized matrix. Osteocytes survive in *lacunae* and communicate with BM via the canalicular system. The release of transforming growth factor-β1 (TGF-β1) by the osteoclasts, allows the maturation of osteocytes starting from the osteoblasts [32].

Osteocytes are the main mechanosensing cells with high ability to detect mechanical stimuli and subsequently to activate the osteoblastic and osteoclastic effector cells. Furthermore, they take part to bone homeostasis regulating calcium/phosphate levels and through the release of factors acting by paracrine fashion. Particularly, SCL, DKK-1 and RANKL/TNF-related activation-induced cytokine, are the main molecules secreted by osteocytes that promote osteoclast differentiation [33] [34] [35] [36].

Jilka et al. have demonstrated that parathyroid hormone (PTH) amino-teminal peptide 1-34, stimulates bone formation in mice and rats [37]. PTH, directly stimulates survival signaling in osteoblasts through RUNX2-dependent expression of anti-apoptotic genes, such as B-cell lymphoma 2 (*BCL-2*). Moreover, PTH inhibits SCL expression in osteocytes, activating Wnt signaling and Notch Jagged1 ligand in osteoblasts, thus participating to molecular orchestra affecting bone homeostasis [38]. Osteoblastic cells not only regulate osteocytes formation, but also osteoclasts. Differently from osteoblasts, osteoclasts are multinucleated cells with hematopoietic origin from the mononuclear monocyte-macrophage lineage. These cells are able to

degrade bone, starting its remodeling and increasing the resorptive activity. Macrophage-colony stimulating factor (M-CSF) and RANKL are the main cytokines released from osteoblasts that allow osteoclasts formation from osteoclasts precursors (OCPs). In addition, also T and B-lymphocytes express RANKL, regulating osteoclast formation [39]. During the early phase of OCPs differentiation, M-CSF binds c-fms receptor, activating MAPK and ERK signaling, while, in the last phase, RANKL binds RANK receptor starting osteoclastogenesis [40]. In addition to RANKL, osteoblasts produce OPG as a decoy receptor for RANKL, inhibiting RANKL-RANK binding through OPG/RANKL ratio upregulation. This biological triad, belonging to TNF superfamily, was discovered in 1990s and it is one of the most important signaling in the bone remodeling system [40]. Furthermore, there are many other genes and transcription factors such as TNF receptor associated factor 6 [41], c-Fos, Nf-kB, nuclear factor of activated T cells c1, phospholipase Cγ and Fc Receptor γ-Chain/DAP12, that induce differentiation of OCPs into osteoclasts [32]. *Y. Ikeuchi et al.* demonstrated that RANKL-RANK signaling regulates also osteoblastogenesis by its reverse signaling. Mature osteoclasts secrete RANK in small extracellular vesicles, that bind RANKL and promote osteoblastogenesis by triggering RANKL reverse signaling, which activates *RUNX2* gene in the end [42]. In addition, hormones (*e.g.* vitamin D, estrogen, glucocorticoids) and different cytokines take part to the molecular scenario that controls bone homeostasis. Among cytokines, TNF-α, interleukin IL-1, IL-6, IL-4, IL-11, IL-17 regulate osteoclasts maturation [43].

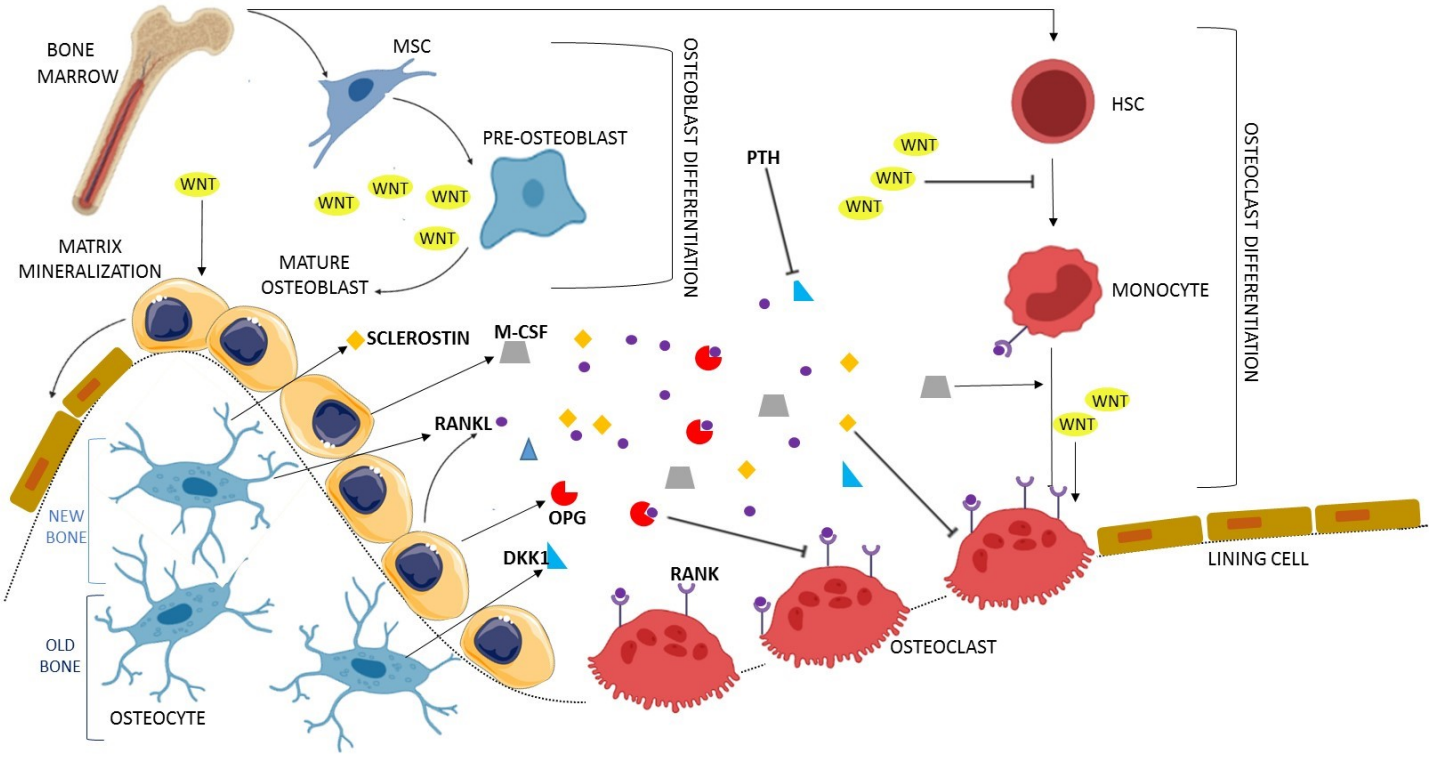

Fig.6 Schematic representation of bone homeostasis.

2.2 RUNT RELATED TRANSCRIPTION FACTOR 2

RUNX2 is the master gene regulator of skeletogenesis: the guardian of MSC commitment towards the osteoblastic lineage [23]. RUNXs transcription factors family consists of three members, RUNX1 (AML1/CBFA2/PEBP2αB), RUNX2 (AML3/CBFA1/PEBP2αA) and RUNX3 (AML2/CBFA3/PEBP2αC).

"Runt domain", with 128-amino acids, is responsible for both heterodimerisation and DNA binding: α subunit allows DNA interaction, indeed the β stabilizes and enforces the binding [44]. It has been observed RUNXs compromised expression in several cancer types. The involvement of RUNX2 in the control of gene expression in cancer development, progression and metastasis is widely documented in different tumors. RUNX2 overexpression correlates with osteosarcoma develop as well as breast, prostate, melanoma and thyroid metastasis carcinomas [45]. About hematological malignancies, evidences confirm the role of RUNX2 in T-cell lymphoma, acute myeloid leukemia (AML) and MM [45]. *S.Colla et al*. have confirmed that RUNX2/CBFA1 expression and activity in MM cells sustain angiogenesis, cell survival and tumor progression OPN mediated [46]. Furthermore, RUNX2- PI3K/AKT axis, is an important driving force for tumor progression. In particular, PI3K/AKT regulates RUNX2 expression and activity through both a direct and an indirect mechanism, respectively rising RUNX2 DNA binding and controlling proteins indirectly related to RUNX2 stability such as SMAD Specific E3 Ubiquitin Protein Ligase 2 (SMURF2), Forkhead box protein O1 (FOXO1), Forkhead box protein O3 (FOXO3), Glycogen synthase kinase 3 *beta* (GSK3β). In a mutual activation, RUNX2 enhances

PI3K/AKT signaling by up-regulating p85, p110β, AKT protein levels and components of mTORC2 complex, corroborating PI3K-AKT-RUNX2 feedback loop. Moreover, *T. Fujita et al.* demonstrated that RUNX2 induces osteoblast and chondrocyte differentiation and enhances cell migration and chemotaxis through PI3K/AKT signaling [47][48][49].

Focusing on the genomic characterization, *RUNX2* human gene has been identified and localized on chromosome 6p21 by *D.Levanon et al.* in 1994 [50]. *RUNX2* gene transcription is controlled by two different promoters, P1 (distal promoter) and P2 (proximal promoter), generating two mRNAs, differing in the 5' UTRs regions and N-terminal sequences: type I *RUNX2* mRNA is controlled by the P2 promoter while type II *RUNX2* mRNA by the P1 promoter. The two isoforms described in human, bind the same consensus *cis*-acting elements, but have distinct functions in control of skeletogenesis: RUNX2-I is sufficient for early osteoblastogenesis and intramembranous bone formation (it is expressed predominantly in undifferentiated MSC and pre-osteoblasts), indeed RUNX2-II is mandatory for the terminal stage of osteoblastic maturation and endochondral bone formation [51]. Mutant mice, completely lacking both RUNX2-I and RUNX2-II, did not show osteoblast formation and mineralized skeleton. On the contrary, mice selectively lacking the Runx2-II isoform maintained intramembranous and cortical bone formation, providing evidences of the diverse functions of the *RUNX2* gene isoforms [51] [52]. Corroborating the close dependence between RUNX2 expression and osteoblast differentiation, *RUNX2* mutated gene is associated with cleidocranial dysplasia, an autosomal dominant bone disease, mapping on chromosome 6p21, characterized by skeletal ossification disorders affecting both intramembranous and endochondral bone formation [53].

RUNX2 is the first gene to be expressed on MSC commitment towards osteoblastogenesis and it is able to control osteoblastic specific genes expression. In fact, RUNX2 activation in human MSC stimulates the expression of the osteoblastic markers OSX, COL1α1, ALP, OPN and OCN [23].

As reported by *Geoffroy et al.*, RUNX2 has been identified as transcriptional activator of *BGLAP* gene. They have discovered two diverse osteoblast-specific sequences, OSE1 and OSE2 in the BGLAP promoter: particularly, OSE2 contained an identical sequence to RUNX2 DNA binding site [54]. *COL1A1* and *SPP1* osteogenic genes, predominantly expressed in osteoblastic cells, are controlled by RUNX2 expression too, since it has been identified the same Osf2/Cbfa1 binding sites in their genes promoters [55]. In addition, genes coding for OPG and RANKL show in their promoter, a RUNX2 binding site, indicating a molecular connection between osteoblastogenesis and osteoclastogenesis in which RUNX2 plays a main role [56] [57]. Among other several target genes of RUNX2 there are Baculoviral IAP repeat containing 3 (*BIRC3*), shown to be up regulated in some osteosarcomas, *IL-11*, involved in the development of craniofacial bones and Matrix metallopeptidase (*MMP) 9/13,* coding metallo-matrix protease, implicating in bone formation [58].

Interestingly, *Drissi et al.* have demonstrated a transcriptional autoregulation loop of *RUNX2* gene since overexpression of CBFA1 protein was able to downregulate the same CBFA1 promoter activity and a single CBFA1 binding site was sufficient for its transcriptional auto suppression [59].

The pivotal pathway that controls RUNX2 expression, thus promoting osteogenesis, is Wnt/β-catenin signaling. *T.Gaur et al*. have reported that RUNX2/CBFA1/AML3 is a target of β-catenin/TCF1, suggesting a direct regulation between canonical Wnt pathway and the early events of osteogenesis [60]. By a mutational analysis, it has been demonstrated a functional TCF regulatory element responsive to Wnt resides in *RUNX2* gene promoter. In this study has been shown that Secreted Frizzled Related Protein 1 (SFRP1)-null mouse displayed endogenous RUNX2 and TCF1 up regulated, exhibiting increased Wnt signaling activation thus enhanced osteoblastic differentiation. In mouse embryonic fibroblast, in pluripotent MSC and in osteoprogenitor cells *in vitro*, *RUNX2* is a direct target of the canonical WNT pathway [60].

Many others factors participate in the cross talk that regulates RUNX2 expression. Focusing on paracrine and autocrine factors, PTH is one of the upstream regulators of RUNX2 [37]. 1,25-(OH) 2-vitamin D3/VDR/VDRE pathway determines RUNX2 expression in human bone cells [61]. As recently reviewed from *C.Mazziotta et al.* epigenetic factors, such as miRNAs, manage the osteogenic differentiation directly targeting RUNX2. MiR-30, miR-133, miR-133a, miR-133a-5p, miR-135a as well as miR-338-3p, miR-137-3p, miR-204 and miR-628-3p negatively contrast osteoblastogenesis, suppressing RUNX2 expression.

Furthermore, different components of BMP/TGFβ/Smad signaling pathways, interact with *RUNX2* gene promoter, activating or repressing its expression. For example, Smad3, is a RUNX2 activator, on the contrary BMP4/7 induce its repressor [44].

2.3 BONE DISEASE

The physiological complexity of bone homeostasis unravels that it could be easily damaged. Bone homeostasis perturbation gives rise to bone disease, the major cause of MM morbidity, involving 80–90% of patients during their tumor course. Osteolytic bone lesions, leading to SRE, characterize the MM associated bone disease (MMABD). Among SRE, pathological fractures, severe bone pain and hypercalcemia, negatively affect patients' quality life and survival [62]. Clinical studies revealed that MM patients who presented osteolytic bone lesions, showed osteogenic markers reduction together with an increase of bone resorption markers [63]. As mentioned in 2.1 chapter, many biological features participate to the bone microenvironment cross talk, maintaining bone homeostasis through the balance between bone formation and resorption. Simultaneous increase of osteoclast proliferation/activity and inhibition of osteoblast, drive bone disease development. Histomorphometric studies have demonstrated that bone lesions evolution is correlated with high PCs infiltration, leading to bone deregulation [64]. Particularly, a close mutual dependence between MM cells and TME characterizes the disease. Indeed, MM cells secrete factors increasing the bone compartment deregulation, establishing a permissive TME for MM clone expansion [65]. Osteoclastogenesis is stimulated by many soluble factors released by MM cells such as IL-1β, IL-3, IL-6, IL-11, and IL-17, as well as TNF-α, C-C motif ligand 3 (CCL3), annexin2, and stromal cell-derived factor-1 alpha, which suppress osteoblasts activity [18]. Particularly, IL-3 induces the production of activin A, a TGF-β member, that

acts as a mediator for the effects of IL-3 on osteoclastogenesis, able to prevent the differentiation of MSC into mature osteoblasts [12]. Other several factors have been described as potential osteoblasts inhibitors both in mouse and in human system such as secreted Frizzled-related proteins (sFRP)-1, sFRP-2, sFRP-3, sFRP-4, noggin and IL-7. *N.Giuliani et al.* have demonstrated that IL-7 enrichment of MM plasma, compared with healthy controls, is involved in the osteoclast activation. Indeed, IL-7 up-regulates RANKL activation and inhibits both pluripotential CFU-F and colony-forming units osteoblasts by decreasing RUNX2/CBFA1 activity, leading to osteoclastogenesis and worsening MMABD [64]. Additionally, *B. A. Nierste et al.* have discovered high levels of DKK-1 in MM plasma, able to contrast osteoblast differentiation through Wnt/β-catenin cascade inhibition. Indeed, blocking both DKK-1 and IL-7 in MSC-hTERT human cell line recovered osteoblastogenesis [66]. As reported in chapter 2.1, RANKL secretion in TME is extremely important to regulate RANK/OPG bone homeostatic axis, widely investigated in MMABD context. Among cells involved in osteoclastogenesis, activated T lymphocytes secrete RANKL, increasing bone resorption, through NF-κB and *c*-Jun N-terminal kinases activation. Indeed, MM patients who present severe osteolytic bone lesions, show up regulated RANKL levels, suggesting a role of T cells role in bone disease [67][62]. Moreover, MM cells express themselves RANKL, inducing its further release from osteoblasts/MSC, reducing OPG secretion [47] [48]. Thus, high level of RANKL/OPG ratio correlates with advanced bone disease stage, delineating a poor prognosis [65]. Furthermore, it has been demonstrated that OPG control cell viability, through the block of TNF-related apoptosis inducing ligand (TRAIL), a potent inducer of apoptosis in MM [70]. MM cells are able to produce also hepatocyte growth factor inhibiting BMP-induced osteoblastogenesis both in murine and human MSC [71].

Not only soluble factors participate in MMABD evolution; more molecules drive MM/BM cells adhesion interactions, uncoupling the bone remodeling process. One of the major integrin involved in cell-to-cell contact is VLA-4, expressed on MM cells. *In vitro* studies showed that addition of VLA-4 mAb in a MM/MSC co-culture system, drastically reduced MM cells adhesion to MSC, thus RANKL induction. In a murine model of MM-induced bone disease, neutralizing VLA-4 mAb, prevented enhanced production of osteoclast-stimulating activity and bone destruction. Oppositely, MM cells binding on MSC through α4β1- vascular cell-adhesion (VCAM1), increased the expression of RANKL, impairing OPG/RANK axis and promoting bone osteolysis [21] [70]. In addition, other adhesion molecules are involved in osteoblastogenesis inhibition such as neural cell adhesion molecule (NCAM)-NCAM interactions between MM cells and MSC/osteoblastic cells [71]. Furthermore, the adhesion molecules activity impact also on RUNX2 expression, downregulating it, thus contrasting osteoblastogenesis. Particularly, it has been observed enhanced RUNX2 inhibitory effect by MM cells on osteoblast formation in a co-culture system with conserved cell contacts compared to the same system without adhesion between cells. These data have suggested how the adhesion mechanisms could be the predominant fashion in controlling MMABD pathogenesis [64].

Trotter et al. firstly discovered higher levels of RUNX2 m-RNA and protein in primary MM cells than PCs isolated from healthy/MGUS donors [72]. *RUNX2* gene knock down or overexpression unraveled how it sustains clone growth and bone disease *in vivo*, corroborating the close dependency of MM RUNX2 overexpression with a more aggressive phenotype. Indeed, RUNX2 knock down in MM cells significantly reduced different pattern of cytokines, chemokines and growth factors involved in tumor progression and bone metastasis, such as EGF, IL-9, SDF-1, VEGF, OPN, RANKL and MMP9, counteracting MMABD progression [72].

Interestingly, the MSC compartment of MM patients are permanently functionally compromised even in the absence of MM clone, with eradicated PCs disease. It has been discovered a different genomic profile of MSC between MM patients and healthy donors, suggesting a possible role of genomic alterations of MSC in MM pathogenesis and persistent BD. Indeed, an altered stromal compartment would able to modify the cross talk with the clonal PCs, favoring a specific clonal selection of MSC able to promote the tumor growth [73].

Recent studies are focusing on the role of epigenetic changes in MM progression. Growth Factor Independent 1 Transcriptional Repressor (Gfi-1) binds RUNX2 promoter in multiple sites, blocking its transcription and repressing the MSC differentiation towards the osteoblastic lineage. Particularly, Gfi-1 recruits different histone modifiers [Histone Deacetylase 1 (HDAC1), Lysine-specific Demethylases and Enhancer Of Zeste 2 Polycomb Repressive Complex 2 Subunit (EZH2)], repressing chromatin changes in RUNX2, even in the absence of MM cells. A specific Gfi-1 knockdown or HDAC1/EZH2 inhibition in pre-osteoblasts cells prevented RUNX2 repression, opening clinically possibilities to counteract osteolytic bone lesions [74].

Considering the central role of Wnt/β-catenin pathway in the control of osteogenic differentiation, it has been unraveled a close relationship between MMABD development and Wnt/β-catenin pathway inhibitors. Elevated levels of DKK-1 and SCL, both Wnt/β-catenin inhibitors, have been found in sera of MM patients who presented MMABD with osteolytic lesions. Indeed, besides other cells type resident in the BM *niche* (chapter 2.1), the MM PCs are able to produce themselves Wnt/β-catenin cascade inhibitors , favoring the uncoupling of the bone homeostasis and worsening bone disease [75][12]. Another mechanism that contributes to MMABD involves the macrophage inflammatory protein 1α (MIP-1α). MIP-1α is a chemokine produced by MM cells and able to induce cell adhesion and migration, acting as a chemotactic factor. Increased levels of MIP-1α were found in sera of MM patients that positively correlates with major bone destruction. Indeed, the chemokine promotes osteoclast formation through both RANKL and IL-6 stimulation. Moreover, MIP-1α is able to bind C-C motif chemokine receptor 1 (CCR1) on osteoclasts and CCR5 receptor on MM cells. Blocking both CCR1 and CCR5 reduces bone destruction and the adhesion of MM cells to bone marrow, ameliorating the MMABD [21]. Focusing on the other players present in the BM, *in vitro* studies have demonstrated that adipocytes sustain MM engraft and growth through the release of different soluble factors such as IL-6, TNF-α and insulin, thereby contributing to MMABD. TNF-α inhibits the osteoblastogenic transcriptional program inducing apoptosis of mature osteoblasts and stimulating osteoclast differentiation

by Nf-κB, PI3K/AKT and MAPK pathways activation. High levels of TNF-α have been detected in TME of MM patients with BD, able to exert a catabolic effect on bone. In addition, the osteocytes have a pivotal role to contribute to MMABD, being the main source of RANKL release, thus inducing osteoclastogenesis. Bone biopsies from MM patients displayed increased osteocyte apoptosis, caused by MM cells able to activate Notch and TNF-α signaling pathways in osteocytes. In turn, enhanced osteocyte apoptosis, strengthens RANKL expression, thus osteoclasts recruitment and activation [12].

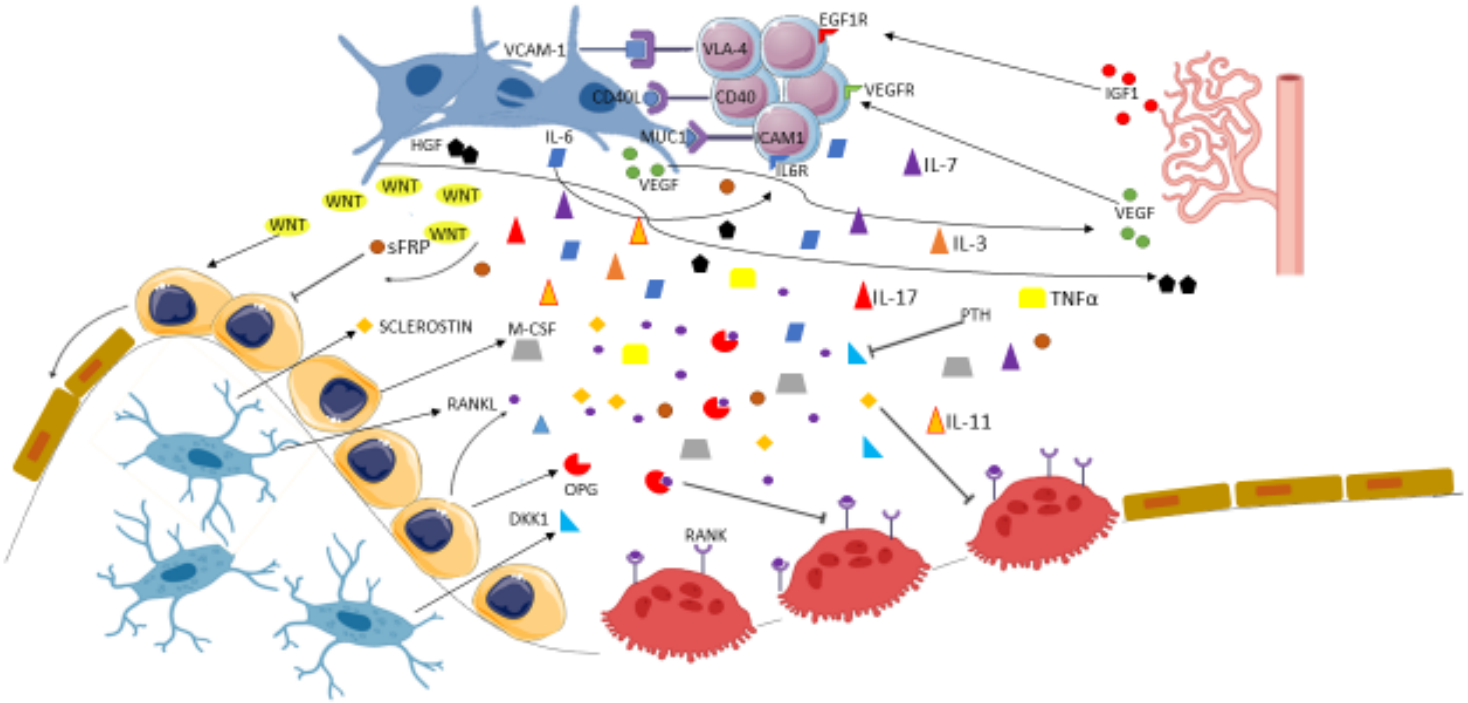

Fig.7 Schematic representation of cross talk between MM clone and TME.

2.4 ROLE OF LENALIDOMIDE IN MMABD

Although Lena mechanism of action on MM PCs has been studied intensively, its effects on the stromal compartment in the TME context has not yet been investigated. Indeed, the impact of IMiDs use on MSC differentiation and bone remodeling is still debated and controversial. *A. Bolomsky et al.*, investigating the impact of IMiDs on bone formation, discovered that treatment with Lena and Thalidomide of MSC reduced ALP activity and matrix mineralization, counteracting osteoblast development *in vitro*. Moreover, they unraveled beta A, DKK-1, activin A and gremlin 1 upregulation and a concurrent downregulation of the major positive osteoblast regulators such as *RUNX2* and distal-less homeobox 5 (DLX5), underlying the negative effects of Lena on osteoblastogenesis [76]. Another study has identified activin A secretion to be critical in MM-induced osteolysis. It has been demonstrated that Lena acts on BMSC via Akt-mediated increase in Jun N-terminal kinase-dependent signaling. The result is an increased activin A secretion that could be abrogated by the addition of activin A-neutralizing antibody, which effectively restored osteoblast function and inhibited MM-induced osteolysis [77]. On the contrast, *M. Bolzoni et al.* found a positive role for the use of

of IMiDs on osteoblastogenesis. *In vivo* studies, have demonstrated that Lena and Poma treatments blunted RANKL upregulation, normalizing the impaired RANKL/OPG ratio in human osteoprogenitor cells co-cultured with MM cells and inhibited CCL3 production by MM cells [78]. Furthemore, after Lena and Poma treatments, the pro-osteoclastogenic property of MM cells co-cultured with pre osteoblasts was reduced, by downregulating adhesion molecules on MM cells [78]. The IMiDs role on the regulation of adhesion molecules has been demonstrated also by *KC Anderson'* group. They identified PU.1 and pERK as major targets of Lena, resulting in osteoclastogenesis inhibition. Notably, in patients' sera, not only RANKL secretion was significantly decreased, but OPG was increased, counterbalancing the compromised RANKL/OPG ratio [79]. Focusing on the impact of IMiDs treatment on MSC, *S. Munemasa et al.* concluded that Lena is able to kill malignant PCs without inducing any cytotoxicity to osteoblast differentiation, since neither ALP activity nor mineralized nodule formation were impaired [80].

The expression of cell surface molecules and the chemokine secretion of MSC can be modulated by Lena treatment. In particular, GPI-anchored protein CD73, associated with MSC migratory behavior, could promote the osteogenic differentiation of MSC in response to Lena. Moreover, CD29 is another interesting target of Lena, involved both in cell–cell interactions and adhesion to the extracellular matrix and soluble factors regulation [81].

3. WNT/ β-CATENIN PATHWAY

3.1 THE SIGNALING PATHWAY

Wnt/β-catenin cascade controls a plethora of cellular processes, including proliferation, differentiation, migration and stem-cell renewal [82]. In 1991 the "Wnt" was first coined "Wnt" combing *wingless,* a Drosophila segment polarity gene, and the mouse proto-oncogene *INT1* [83].

The Wnt ligands family is composed by 19 different secreted lipid-modified glycoproteins that act in a paracrine or autocrine fashion. Human Wnt ligands are very similar in size (between 39 and 46 kDa) with highly conserved cysteine hydrophobic residues domain and N-terminal signal peptide for secretion. Considering the hydrophobic nature of Wnt proteins, they exist in association with cell membrane and ECM [84][82]. All Wnt ligands undergo a process of post-translational modification before secretion. Glycosylation, acylation and palmitoylation are the mainly modifications that occur in the endoplasmic reticulum, whereas there are other modifications that have been reported in very specific subgroups of Wnt ligands [82]. Acylation is one of the most essential post translational modification that allows the Wnt transportation from the Golgi to cell surface and the subsequent binding to a specific Frizzled (FZD) receptor, composed by a large cysteine rich domain (10 residues) on the cells surface [84].

The signaling pathway has been classified in canonical and non-canonical, considering its β-catenin dependence. In summary, in the non-canonical Wnt pathway, Wnt ligands (e.g. WNT-5A,11) bind the Receptor Tyrosine Kinase Like Orphan Receptor (ROR)1/ROR2 receptors. The different pathways, that can be activated independently from β-catenin, act in cytoskeletal rearrangements such as Planar Cell Polarity/Jun N-terminal kinase, in the regulation of cell migration and in Ca^{2+} intracellular release, such as WNT/Ca^{2+} pathway linked to PLC/Protein Kinase C (PKC) [85].

Focusing on Wnt/β-catenin canonical pathway, it exists in two different states: on/off. In the "Wnt-off" state, a cytosolic multi-protein destruction complex consisting of the scaffold protein Axin1, adenomatous polyposis coli (APC) and 2 protein kinases, casein kinase 1α (CK1α) and GSK3β, regulates the β-catenin phosphorylation and its subsequent proteasomal degradation. The destruction complex mediates the phosphorylation of β-catenin by CK1α on Ser45, which primes it for its subsequent phosphorylation by GSK3β on Ser33, Ser37, Thr41. Thus, the phosphorylated β-catenin, is ubiquitinated by F-box E3 ubiquitin ligase β-Trcp and subsequently degraded by the proteasome. In "off-state", Wnt transcriptional program is blocked due to β-catenin nuclear absence [86]. On the contrary, in the "Wnt-on" state, a specific Wnt ligand (*e.g.* WNT-2,3,3A and 8) binds to FZD receptor and low-density lipoprotein receptor related protein 5/6 (LRP5/6), in order to activate the signaling. Human LRP5 and LRP6 belong to type I transmembrane receptors which share 71% amino acid sequence identity, characterized by an extracellular low-density lipoprotein receptor ligand-binding repeat [87]. The hetero-trimer WNT/FZD/LRP recruits other proteins, composing the "signalosome" in order to activate the Wnt/β-catenin cascade. Among other proteins involved in the signaling cascade, CK1ε/δ kinase phosphorylate the phosphoprotein Dishevelled (DVL), recruited to the receptor complex and favoring its disruption. These events block β-catenin degradation and allow its cytosolic stabilization. Thus, β-catenin enters the nucleus and associates with TCF/LEF1 and others co-activators, such as Pygopus (PYGO), BCL9, earthbound1/jerky and CREB binding protein. This association triggers the transcription of gene such as *CYCLIN D1*, *C-MYC*, *CDKN1A* involved in the regulation of cell proliferation, survival and differentiation [88] [89]. Among β-catenin target genes *AXIN2* is homolog of *AXIN1* and it is responsible of a negative feedback loop upon pathway activation [82].

The Wnt signaling pathway outcomes are affected by different variables such as Wnt ligands concentration, signaling pathways associated and Wnt molecules antagonists present in the microenvironment. Considering the different pathways involved, a networking of Wnt, PI3K/Akt, Notch, Hedgehog cascades influence Wnt/β-catenin signaling. Focusing on Wnt competitor, sFRPs 1-5 bind to extracellular Wnt, acting as decoy receptors; DKKs 1-4 and SCL bind to extracellular sub regions of the LRP co-receptor, antagonizing Wnt binding [35][36].

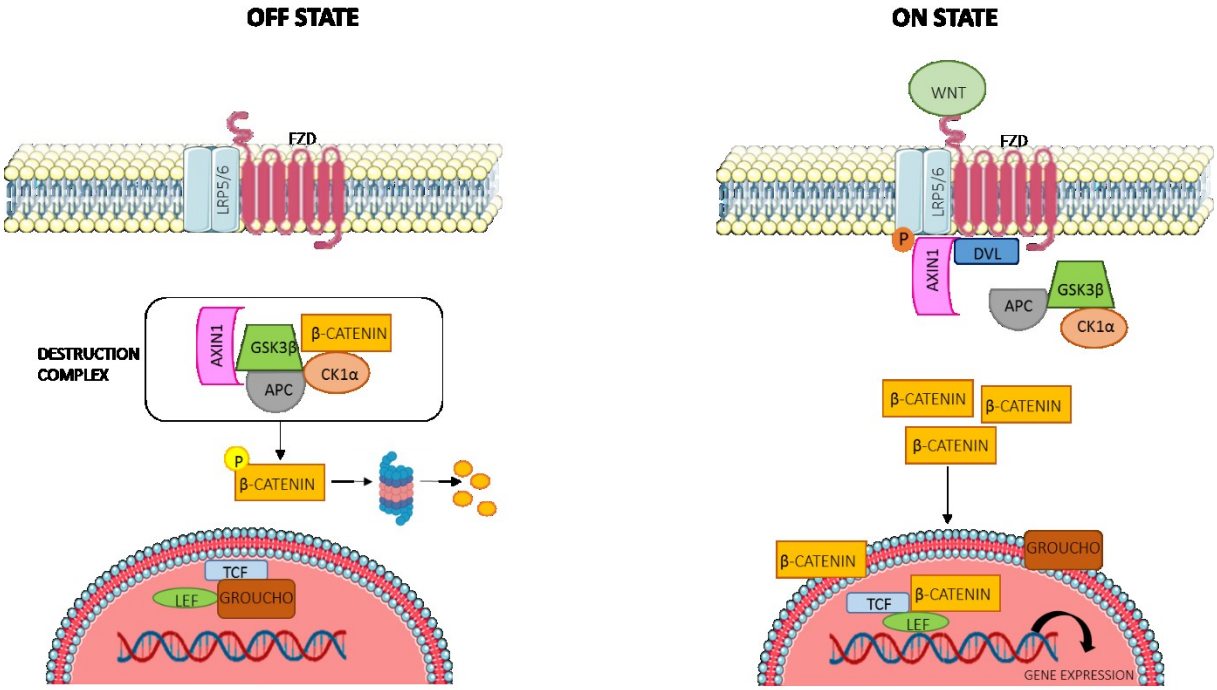

Fig.8 Schematic representation of Wnt/β-catenin pathway.

3.2 WNT/β-CATENIN SIGNALING PATHWAY IN CANCER

Several evidences have shown that aberrant activation of WNT/β-catenin signaling is correlated to different disease states, including cancer [86].

In the 1980 it was discovered that the proto-oncogene *INT1 (*Wnt1*)* induced mammary adenocarcinoma in mice, confirming the close relationship between Wnt signaling and cancer development [90].

The pivotal role of Wnt pathway in the onset and in cancer progression has been discovered in different type of neoplasia, including solid tumors and hematological malignancies. The signaling deregulation consists in diverse mutations and epigenetic mechanisms resulting in loss of function of β-catenin destruction complex, with its abnormal nuclear localization, leading to early event in carcinogenesis [88].

Aberrant Wnt signaling has been associated to colon rectal cancer (CRCs) as an oncogenic hallmark. Particularly, it has been demonstrated how APC mutations are the main drivers of the pathway upregulation in CRCs development and in other colonic disorders [91].

The canonical Wnt signaling promotes liver cancer pathogenesis, including hepatocellular carcinoma (HCC) and cholangiocarcinoma. In fact, β-catenin gene *CTNNB1* has been reported as one of the most frequently mutated genes in primary HCC (20–35 % of HCC cases) [92].

Regarding melanoma cancer, Wnt mutations have not been reported as a driving force both initiation and progression, but the signaling supports an important cross talk with others pathways involved in melanoma development and progression such as MAPK/ERK and PI3K/AKT [93].

Focusing on hematological cancers, Wnt signaling is central for the hematopoietic stem cells self-renewal and homeostasis and for hematopoietic progenitors maturation. Aberrant Wnt signaling has been confirmed in different hematological malignancies such as AML, chronic myelogenous leukemia, acute lymphoblastic leukemias, Chronic Lymphocytic Leukemia (CLL), different lymphomas subtypes and MM. The aberrations rely on β-catenin overexpressed and constitutively activated, affecting cell proliferation. Both Wnt canonical and non-canonical pathways modulate cell proliferation, invasion and resistance to therapy [85].

In cancer cells agents that target addiction to Wnt/β-catenin cascade scenario (Wnt-driven cancer), are explored as promising therapeutic possibility in various cancer therapy [85][88].

A panoramic overview of the several molecules, classified in the main macro categories, recently investigated in preclinical and clinical trials, is reported in below Fig.9.

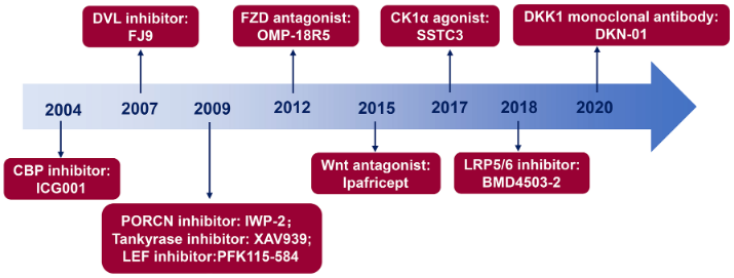

Fig.9 Timeline of the discovered diverse categories of Wnt/β-catenin signaling pathway targeted in cancers, (adapted from [88]).

3.3 WNT/β-CATENIN SIGNALING IN MULTIPLE MYELOMA

As mentioned before, dysregulation of Wnt/β-catenin signaling pathway is also reported in MM pathobiology. Indeed, impaired Wnt/β-catenin cascade is relevant to MM cells growth, migration and differentiation. Particularly, *Derksen et al.* firstly identified Wnt pathway involvement in the pathogenesis of lymphoid cancer. They demonstrated that all MM cell lines (MCLs) tested and the major part of primary MM samples studied, overexpressed β-catenin, including high levels of its non-phosphorylated counterpart, able to transduce Wnt signals. Other studies corroborated these results, showing how β-catenin small interfering RNA inhibited MM cell growth in xenograft model [94]. Moreover, treatment of MCLs with Wnt/β-catenin small molecules inhibitors such as AV-65 [94], PKF115-584 [95] or CGK012 [96] exerted anti-proliferative activity, increasing apoptosis and impairing MM tumor growth. In addition, *C. Bjorklund et al.* have reported how Wnt/β-catenin takes part to cell-adhesion-mediated drug resistance (CAM-DR) of MM. The persistent and acute Lena treatment increased β-catenin activity, leading CYCLIN D1 and C-MYC expression and conferring resistance to treatment. Moreover, Lena induces CK1α degradation and GSK3 inactivation, inducing enhanced β-catenin activity. The same study reports *CD44* as a downstream Wnt target gene

involved in CAM-DR by increasing MM adhesive potential properties to BM. Conversely, β-catenin silencing by short hairpin RNAs (shRNA), overcome drug resistance and restored MCLs sensitivity to Lena [97].

Differently from other Wnt-driven tumors where *APC* and/or *CTNNB1* genes are recurrently mutated and able to drive the oncogenic Wnt signaling, any mutations have been reported in MM cells, whereas the signaling is overactive and represents a hallmark of the disease. Analyzing the mutational status of Wnt pathway components in MM, other mutations have been identified with a low frequency and unknown pathogenic significance, corroborating that the oncogenic Wnt signaling is driven by alternative mechanisms. Interestingly, MCLs and purified primary MM cells, express several diverse Wnt ligands, such as Wnt3, 4, 5a, 5b, 6, 7, 8a, 10a, 10b, 11,14, 16a, suggesting an autocrine loop of pathway activation. Moreover, different BM cells in the microenvironment release Wnt molecules, further sustaining Wnt/β-catenin pathway by a paracrine loop [98][99] [100].

As reported in chapter 2.3, the cross talk between the MM clone and the BM milieu is crucial for both clone growth and BD progression. The canonical Wnt/β-catenin is a "double edged sword" since in the BM *niche* it sustains MM tumorigenesis and counteracts bone formation through Wnt antagonists secretion [98]. Wnt soluble antagonists act as potential tumor suppressor and *C.Chim et al.* also unraveled their contribution to MM pathogenesis by an epigenetic dysregulation mechanism. Indeed, the study demonstrated the presence of aberrant promoter methylation of Wnt inhibitors WIF1, DKK3, APC, SFRP1, SFRP2, SFRP4 and SFRP5 in primary MM samples. An aberrant methylation, leading gene silencing, sustains constitutive Wnt signaling activation, contributing to MM pathogenesis [99].

Heparan sulfate (HS) proteoglycan syndecan-1 (CD138) is a critical player in the MM BM *niche*. HS chains are connected with MM cells growth and survival through the regulation of many factors and signaling cascades involved in BM environment, among which Wnt/β-catenin pathway. Physiologically, HS chains bind Wnt hydrophobic ligand, promoting FZD receptors interaction. Knockdown of HS inhibits MM cells growth both *in vivo* and *in vitro*, decreasing Wnt/β-catenin activity dependent cell proliferation [101]. Other events support MM cells addiction to autocrine and paracrine Wnt ligands. Gene expression analysis reported that 60% of MM samples overexpressed *BCL-9* gene, mapping on chromosome 1, whose q region amplification is frequently detected in MM. *BCL-9* overexpression correlates with enhanced MM tumor growth/migration/invasion trough the recruitment of PYGO transcription factor to β-catenin/TCF complex, thus initiating Wnt target genes transcription. Similar *to BCL-9* overexpression, loss of *CYLD* gene is among the most MM prevalent genetic abnormalities. The loss of *CYLD*, overactives both NF-κB and Wnt pathways, implementing their signal transduction [98].

Regarding the role of non canonical Wnt signaling pathway in MM pathogenesis, recently it has been demonstrated how the overexpression of ROR-2 in MM cells exerts a key role in PCs adhesion to the BM microenvironment, mainly through the PI3K/AKT pathway. In fact, a specific inhibition of PI3K/AKT axis is able to reduce ROR-2 induced adhesion, mobilizes MM cells from the BM and delays disease progression

[102]. Moreover, *Y.W Qiang et al.* have better characterized the downstream Wnt signaling pathway, considering the main role of Wnt ligands in MM migration and invasion. They discovered that Ras homolog family member A, Protein Kinase C α (PKCα), PKCβ, and PKCμ, are required for induction of migration, without the involvement of β-catenin [103].

3.4 WNT/β-CATENIN SIGNALING PATHWAY IN BONE DEVELOPMENT

Numerous cellular events during embryonic development and adult tissue homeostasis are controlled by the Wnt/β-catenin pathway [86].

Commitment from MSC, differentiation, bone matrix formation and mineralization are the most features of osteoblast physiology led by canonical Wnt/β-catenin, confirming its pivotal role in bone development. Both developmental process and postnatal health/diseases are regulated by Wnt/β-catenin, in fact, the signaling impairment induces compromised bone mass [104].

Bone formation can occur via endochondral or intramembranous mechanism and β-catenin is involved in both processes [84].

Importantly, as reported by *Rodda and McMaho*, Wnt/β-catenin signaling is necessary in the early phases of bone formation; oppositely, in the later phases, it need to be downregulated to allow final maturation of osteoblast and favoring bone mineralization [105].

Considering LRP5/6 Wnt/β-catenin receptor, it has been confirmed its involvement in genetic disorders of skeletal mass. Loss and gain of function mutations occurred in LRP5, respectively causing low bone mass in osteoporosis-pseudoglioma syndrome and high bone mass formation in human [87].

Osteoblasts, osteocytes, chondrocytes and bone marrow cells secrete various Wnt ligands with a different role in the control of bone mass. Frequently, activators and repressors of Wnt signaling are co-expressed in the same type of cell, indicating the complexity of the pattern involved in bone homeostasis/regenerating [106]. Among the main Wnts ligand, Wnt-1, Wnt-10b and Wnt-3a, have been widely recognized as activator of canonical Wnt signaling, promoting bone formation. Despite Wnt-3a is always been considered as a Wnt canonical agonist, it could also activate non-canonical Wnt/β-catenin cascade, inducing in both cases osteoblast differentiation and inhibition of adipocyte differentiation [104] [107].

The discovery of Wntless (Wls/Evi) as a new transmembrane protein present in the plasma membrane and/or Golgi apparatus, has defined its importance for Wnt ligands secretion. [108] In fact, this multi-pass transmembrane protein control the transport and the secretory vesicles of Wnt modified proteins [84].

In *WLS* conditional knock out mice the trabecular and cortical bone masses were reduced with a low bone formation. Considering *WLS*-deficient osteoblast cultures, the mineralization was impaired, confirming the WNT main role for the maturation and mineralization of osteoblasts [36] [109]. Moreover, through genome wide association studies, two single nucleotide polymorphism in *WNT* locus associated with a reduced bone mass have been identified [110].

S. Kang et al. demonstrated that retroviral transfection of Wnt-10b into ST2 BM stromal cells, increased bone noduli formation and osteoblastic differentiation due to elevated expression of the osteoblastic transcription factors RUNX2, OSX, and DLX5 with a decreased expression of adipogenic transcription factors CCAAT/enhancer binding protein *α* and peroxisome proliferator-activated receptors γ [111]. Thus, β-catenin promotes MSC progression towards the osteoblastic lineage simultaneously suppressing the differentiation into adipogenic and chondrogenic lineages. Targeted *CTNNB1* gene, using a specific conditional gene deletion or activation in skeletal progenitors, influences bone formation and resorption, confirming the β-catenin key role in bone remodeling [87].

Wnt/β-catenin signaling pathway is involved both in osteoblastogenesis and in osteoclastogenesis processes. β-catenin signaling activation in osteoclasts is regulated by canonical Wnts ligands secreted from osteoblasts, thus controlling osteoclasts differentiation.

It has been reported that Wnt-3a affects osteoclast differentiation via an indirect mechanism involving RANKL downregulation. In osteoblastic cells, overexpression of β-catenin, inhibited RANKL promoter activity. Since in the human RANKL promoter have been identified consensus TCF/LEF binding sites, RANKL could be consider as a potential target of Wnt signaling in osteoblastic cells [112]. As reported, in addition of Wnt-3a, also Wnt-16 negatively regulated osteoclastic formation. In fact, Wnt-16 induces OPG expression, through the activation of Wnt/β-catenin signaling in osteoblastic cells, counteracting bone resorption. Moreover, Wnt-16 acts also in OPG-independent manner, directly inhibiting RANK signal in osteoclast precursors. In contrast of of both Wnt-3A and Wnt-16, Wnt-5A enhances RANK expression in osteoclast precursor, promoting osteoclast formation through non-canonical Wnt/β-catenin pathway activation [36]. β-catenin deletion in mice osteoblast/osteocytes causes low expression levels of OPG, corroborating the role of β-catenin in controlling OPG gene expression.

It has been reported that WLS inactivation, in osteoblasts progenitor, enhances osteoclast differentiation due to alterations of the OPG/RANK axis [110]. As widely described in literature, SCL and DKK-1 antagonize WNT/β-catenin signaling, binding the LRP5/6 receptor.

The DKK proteins family interacts with sub regions of LRP5/6, thus preventing the signalosome (WNT/FZD/LRP) formation, counteracting the signaling [87]. Moreover, in the several cells lines such as L cells, Rat2 cells and HEK293T cells, *M. Semenov et al.* have demonstrated that Wnt pathway inhibition by DKK-1 is independent of LRP6 internalization and degradation [113].

Focusing on the osteoclastogenesis process, β-catenin exerts a dual regulation: it is up regulated in progenitors proliferating phase, on the contrary, down regulated when the differentiation towards osteoclastic lineage starts. Therefore, β-catenin uses a dosage-dependent control: its activation is required for osteoclasts proliferation, but its suppression is necessary to osteoclast differentiation. Thus, Wnt signaling regulates osteoclastogenesis through a dual mechanism: the indirect osteoblastic OPG release (OPG/RANKL axis) and the direct effect on osteoclasts [114].

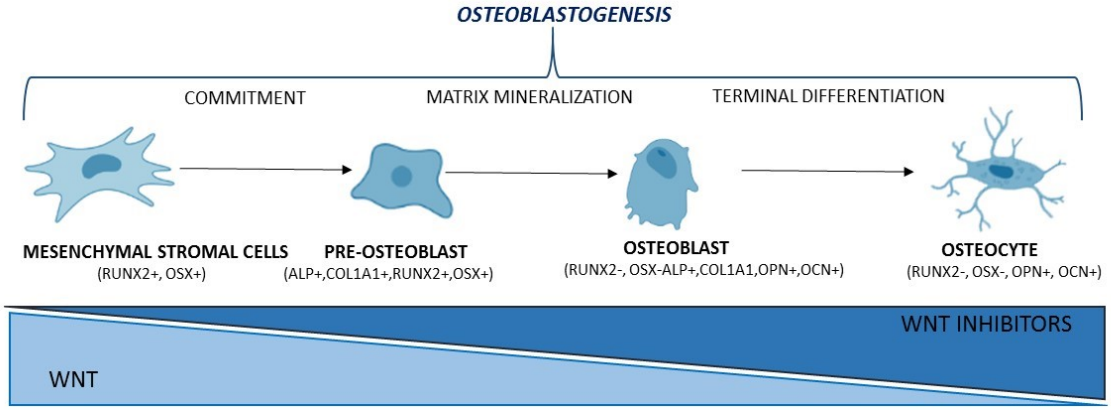

Fig.10 Wnt/β-catenin pathway guides osteoblastogenesis.

4. PROTEIN KINASE CK1α

4.1 PROTEIN KINASE CK1 FAMILY

According to *G.Manning et al.* the human genome encodes for more than 500 protein kinases, which mediate the most part of the signal transduction in eukaryotic cells [115]. Protein kinases, through phosphorylation, a common posttranslational modification, control a large scale of cellular functions, including metabolism, transcription, cell cycle progression, apoptosis and differentiation. Mutations and dysregulation of protein kinases could be involved in cancer initiation, progression and development of metastatic disease. As such, protein kinases could represent an attractive chance for developing molecules to use for targeted therapy in the modern medicine [115] [89].

The serine/threonine (Ser/Thr) protein kinase CK1 family, belonged to the group of acidotropic kinases, includes 7 mammalian CK1 different isoforms and their associated splice variants: α, β (not present in humans), γ1, γ2, γ3, δ and ε [116]. Structurally, they exhibit high degree of homology within catalytic domain, on the contrary N-terminal and C-terminal domains diverge in length (9-76 and 24-200 amino acids). The substrate specificity and the regulation of kinase activity, is mainly controlled by the C-terminal domain [117]. The wide range of CK1 substrates mirrors the kinases involvement in multiple cellular processes among which circadian rhythm, DNA repair, vesicular transport, signal transduction pathways, cell division, apoptosis and survival. Particularly, the diverse CK1 isoforms cooperate with many proteins belonging to several oncogenic signaling, such as Hedgehog, Wnt/β catenin, NF-kB, TGF-β/Smad and p53 pathways [118]. Each CK1 family member is able to be a positive regulator or a negative one, on the same signaling pathway, in a specific isoform dependent manner [89]. For instance, considering Wnt/β-catenin pathway, all CK1 isoforms are

involved either as inhibitors or as activators. It has been established how CK1ε and CK1δ are positive regulators of Wnt signaling by phosphorylating DVL and promoting β-catenin stabilization; on the contrary CK1α, acting as a component of the β-catenin destruction complex, is a negative regulator of the pathway [119][89].

More than 140 molecules have been reported to be *in vitro* and *in vivo* substrates for CK1 isoforms, highlighting the pleiotropic role of this kinases' family [116]. All CK1 family isoforms are a monomeric constitutively active enzyme and, by using ATP as exclusively source, each member catalyzes the transfer of a phosphate on to Ser/Thr residues of their substrates. The canonical CK1α consensus sequence is pS/pT-X-X-S/T where X is any amino acid and S/T indicate CK1-phosphorylation residues. Furthermore, also a non-canonical S-L-S motif with a concurrent cluster of C-terminal acidic residues it has been shown to be phosphorylated by CK1 family [120].

CK1 isoforms are constitutively activated kinases, but they can be also modulated. Compartmentalization and subcellular localization bring the kinases in proximity of substrates and guide their interaction [121]. The inhibitory auto phosphorylation, in C-terminal domain and site-specific phosphorylation, mediated by cellular kinases, are other mechanisms affecting CK1 activity [116].

Considering the key role of CK1 isoforms in signaling pathways pivotal in the control of tissue development and homeostasis, their dysfunctional activity has been linked to many human diseases, including cancer and neurodegenerative disorders [120]. Focusing on the hematological disorders, the CK1 isoforms are involved in malignant B lymphocyte biology, in particular in B-cell-derived pathogenesis (e.g CLL, DLBCL), in AML and MM, acting as pro-survival drivers [117] [120][122].

Despite the wide knowledge about the CK1 family downstream signaling, little is known about the upstream regulators of CK1 activity and about its physiological role in the ontogenesis of cells and tissues [117][116].

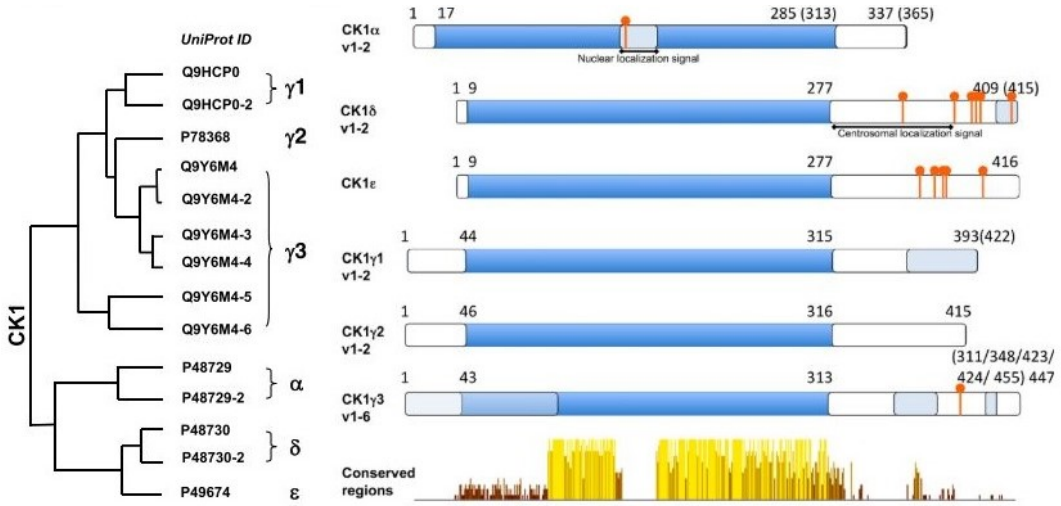

Fig.11 Structure of CK1 family (adapted from [118]).

4.2 PROTEIN KINASE CK1α

In humans, protein kinase CK1α, the smallest isoform of the CK1 family (37 kDa), is encoded by the *CSNK1A1* gene, which maps to the long arm of chromosome 5 (5q32). CK1α splice variants have been identified in vertebrates and mammalians. The four protein isoforms CK1α, CK1αL, CK1αS and CK1αLS, differ for the presence or absence of a 28-amino acid "L" insert in the kinase domain and a 12-amino acid "S" insert flanking the C terminal domain. These splice variants are characterized by diverse kinase activities, functions, subcellular localization and biochemical properties [121]. Constitutively active, CK1α mRNA is ubiquitously expressed in all human tissues under physiological conditions, with the higher level in esophagus and skin. Furthermore, the kinase is mainly localized in the cytosol compartment, suggesting its primarily role in the cytoplasm [123].

4.3 PROTEIN KINASE CK1α IN CELLULAR MOLECULAR PATHWAYS

The involvement of CK1α in the control of diverse molecular signaling pathways mirrors its pleiotropic feature.

- **THE WNT/β-CATENIN SIGNALING PATHWAY**

  Protein kinase CK1α is a negative regulator of Wnt/β-catenin signaling pathway. Briefly, CK1α belongs to the β-catenin destruction complex, since the kinase mediates the phosphorylation of β-catenin on Ser45, which primes it for its subsequent phosphorylation by GSK3β on Ser33, Ser37, Thr41. Among the proteins involved in the Wnt/β-catenin signaling cascade, CK1ε/δ phosphorylate DVL, favoring its disruption and allowing β-catenin cytosolic stabilization. For the full explanation, see chapter 3.1.

- **AKT SIGNALING PATHWAY**

  One of the major signaling cascades involved in the control of basic intracellular functions, such as cell proliferation, growth, cell size, metabolism, and motility is the PI3K/AKT/mammalian target of rapamycin (mTOR) pathway. Since the PI3K/AKT/mTOR pathway is pivotal during cell life span, it is one of the most frequently over-activated/genetically altered cascade in human cancers and currently studied to develop promising clinical inhibitors [124]. AKT/protein kinase B (PKB) is the downstream effector of PI3K that phosphorylates the phosphatidylinositol 4-5 bisphosphate generating the phosphatidylinositol (3,4,5) trisphosphate (PIP3). The levels of the second messenger PIP3 are tightly regulated by phosphatases, among which Phosphatase and TENsin homolog, which removes phosphate from the 3-OH position. The complete activation of AKT is dependent on two different specific phosphorylations: the first, that partially activates the kinase, is performed by phospho-inositide-dependent kinase-1 (PDK1) on the Thr308 residue in the kinase domain, while the

second is performed by mTOR on the Ser473 residue, in the regulatory tail allowing full activation of the kinase [125]. It has been reported that CK1α regulates AKT pathway through the phosphorylation of DEP Domain Containing mTOR Interacting Protein (DEPTOR), an inhibitor of mTOR. CK1α dependent phosphorylation of DEPTOR leads to its proteasomal degradation, resulting in activation of the mTOR signaling [121] [126]. *Manni et al.* have demonstrated that CK1α inhibition in MM cells reduces the Ser473 phosphorylation on AKT and the total AKT protein levels, as a consequence of a p53-caspase mediated mechanism [127].

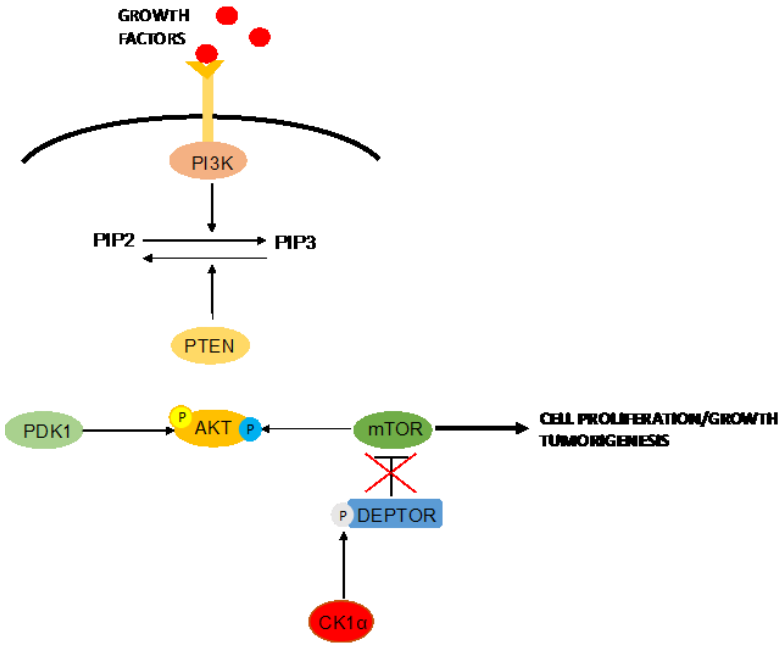

Fig.12 Schematic representation of CK1α role in AKT signaling pathway.

- **NF-κB PATHWAY**

The NF-κB pathway displays an essential role for lymphocyte activation and proliferation. CK1α is pivotal in NF-κB signaling pathway because of its regulatory action on the CBM1 complex. It has been found that CK1α associates with the CBM1 complex, composed by CARD11/BCL10/MALT1 upon antigen receptor stimulation, causing NF-κB downstream activation [117]. The CBM1 complex modulates IκB kinase activation, which phosphorylates the NF-κB inhibitor IκB, causing its proteasomal degradation. Thus, the related members of NF-κB family are free to translocate in the nuclei and activate its transcription target genes. CK1α, however, seems to act as a bifunctional regulator of the pathway. Indeed, the kinase not only promotes the signaling through its role as a scaffold of CBM1 complex, but also phosphorylates CARD11 on Ser608, decreasing NF-κB signaling [128]. At least 17% of primary MM tumors and 42% of MCLs present mutations in several major components of the NF-κB pathway and its regulators. These mutations achieve MM PCs independency from BM TME *niche* and from ligand-induced activation of the NF-κB pathway.

Considering hematological diseases, not only MM, but also B-cell lymphoid malignancies, such as Hodgkin's lymphoma, DLBCL, are also known for constitutive activation of the NF-κB pathway [129].

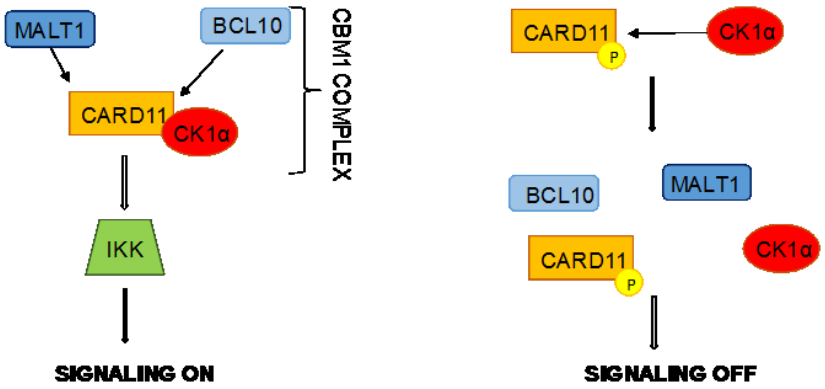

Fig.13 Schematic representation of NF-κB signaling pathway.

- **HEDGEHOG SIGNALING PATHWAY**

  Hh signaling pathway is fundamental for both embryonic development and adult cells since it contributes to maintain the epithelia and tissue regeneration. Consequently, aberrant activation of Hh signaling can be associated to tumorigenesis and cancer, including hematological diseases, such as MM and AML [130][131]. Within the mammalian Hh pathway, the ligands Sonic hedgehog (Shh), Ihh and Desert hedgehog (Dhh), bind PTCH, the negative regulator of the pathway, complexed with the positive Hh regulator Smoothened Homologue Precursor (SMO). Upon PTCH stimulation, SMO and PTCH disassociate, releasing the GLI factors from the inhibitory kinase complex composed by the kinases CK1, GSK3 and PKA. Thus, GLI transcription factors are free to translocate to the nucleus, inducing Hh target gene transcription [120]. As documented in Wnt/β-Catenin pathway, CK1 isoforms have both positive and negative regulatory influence on the Hh signaling cascade too. Particularly, in the absence of Hh ligands, SMO binds to PTCH and the GLI transcription factors are phosphorylated by the kinases CK1, GSK3 and PKA to trigger their proteolysis. On the contrary, G Protein-coupled Receptor kinase 2 and CK1α isoform positively regulate Hh pathway through the phosphorylation of SMO, thus promoting the release of GLI factors [120].

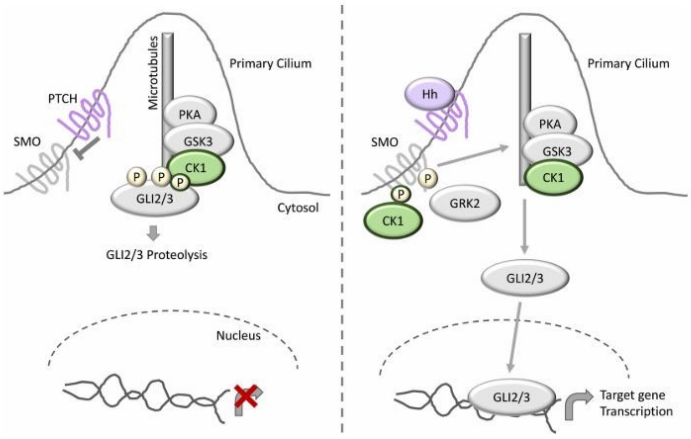

Fig.14 Schematic representation of Hedgehog pathway (adapted from [120]).

- **APOPTOTIC SIGNALING PATHWAYS/CELL CYCLE PROGRESSION/DNA DAMAGE RESPONSE**

  Protein kinase CK1α is widely involved in programmed cell death through the regulation of pivotal apoptotic signaling pathways. In particular, it has been shown to have an anti-apoptotic function since it phosphorylates p75 TNF and Fas-Associated protein with Death Domain (FADD), thus contrasting their apoptotic activities [132]. In addition, CK1α is a component of Fas-mediated apoptosis, in which the activation of caspase 8, through BH3-interacting domain death agonist (BID) protein, leads to cytochrome c-mediated apoptosis. Accordingly, CK1α mediates the inhibitory phosphorylation of BID, blocking caspase 8 activity and the apoptotic process [116]. Likewise, CK1α both promotes cell survival through the interaction with the retinoid X receptor (RXR) and inhibits TRAIL induced apoptosis by modification of the TNF receptor or FADD at the death-inducing signaling complex (DISC) [118]. Furthermore, CK1α has been reported to phosphorylate receptor-interacting protein kinase 3 on Ser227 to activate necroptosis, a form of immunogenic cell death [120].

In the context of DNA damage, CK1 family members are involved in DNA-damage associated signaling transduction, in order to activate p53 function and initiate the activation of the pathways ensuring centrosome activity and genomic stability [123]. CK1α is a major regulator of p53 activity. Indeed, under normal conditions, the kinase directly phosphorylates the N-terminal region of p53 in multiple sites [133]. Moreover, by an indirect fashion, CK1α stimulates the binding of Murine double minute chromosome 2 (MDM2) to p53, therefore inhibiting p53 function. Furthermore, CK1α phosphorylates Mouse double minute 4 homolog (MDMX), on Ser289, which is necessary for MDMX-p53 interaction, thus inhibiting p53 DNA-binding and its transcriptional activity [123]. *Manni et al.* have demonstrated that CK1α inhibition/silencing in MM cells, causes cell cycle arrest and cell apoptosis through the increase of p53, p21 and a reduction of MDM2 levels [127]. Similarly, *Jaras et*

al. discovered that *CSNK1A1* knockdown increased p53 activity and myeloid differentiation in AML, suggesting that the kinase is a new potential therapeutic approach for the treatment of AML [134].

Focusing on the different phases of cell cycle (G1, S, G2, M) in eukaryotic cells, the CK1 family plays a pivotal role in the regulation of several functions linked to cell cycle progression, spindle-dynamics and chromosome segregation. CK1α has been shown to be located at the centrosome, microtubule asters and kinetochore [116]. In particular, CK1α displays a cell cycle-dependent subcellular localization and association with cytosolic vesicles and nucleus during the interphase and associates with the spindle during mitosis [123]. Moreover, it has been discovered that CK1α is a positive regulator of the G2-M transition and it is upregulated during metaphase. Less is known about the CK1α function in meiosis [123].

4.4 LENALIDOMIDE

R.Schneider et al. have demonstrated that CK1α is degraded by Lena in myelodysplastic syndrome (MDS) characterized by the deletion of long arm of chromosome 5. The biological mechanism involved in CK1α degradation after Lena treatment, requires Cereblon and the activatation of the Cereblon E3 ubiquitin ligase activity, in the same manner of IKZF1 and IKZF3 degradation (chapter 1.4) [135]. In addition, CK1α could be degraded by Lena not only in del(5q) MDS but also in MM. Indeed, as demonstrated by *Manni et al.*, there is a time-dependent Lena-induced degradation of CK1α in MM cells. Moreover, CK1α silencing or inhibition in MM cells boosts Lena induced cytotoxicity in a synergistic mode, overcoming BM TME protection [127].

4.5 CK1α PROTEIN KINASE IN DISEASES

Being CK1α a multifunctional kinase involved in distinct cellular physiological processes, perturbation of its expression/activity is frequently correlated with the develop of pathological cellular features [123].
Database searches indicate that somatic mutations occurring on the *CSNK1A1* gene are very rare. *Schneider et al*., by performing whole-exome sequencing on 21 deleted region for del(5q) MDS samples, identified two cases with somatic mutations in *CSNK1A1*, occurring on E98K on the remaining allele of chromosome 5q. Moreover, additional mutations have been detected on E98V, D140Y and on D140A in a case with MDS with a normal karyotype [135]. Recently, it has been reported that these recurrent hot-spot mutations confer survival and tumorigenic advantage through p53 inhibition and loss of function in suppressing Wnt/β-catenin pathway [136]. Despite little is known about *CSNK1A1* mutations, literature reports other malignancies where they have been identified with a low frequency. *Dulak et al.* discovered a missense mutation on E98K in esophageal adenocarcinoma [137] and *Sato et al.* determined another mutation on D140H in the clear-cell renal carcinoma [138]. Furthermore, others missense substitutions, on the CK1α encoding gene, have been

investigated in the adult T cell leukemia/lymphoma (D140H) [139] and in colon cancer (D136N) [140]. Despite of CK1α is rarely mutated in tumors, the pivotal role of the kinase in the main pathways involved in the control of cell fate (chapter 4.3) ascribes to CK1α the feature of "conditionally essential malignant gene", in the paradigm of "non-oncogene" addiction (NOA) [122]. Focusing on the NOA concept, the tumorigenic state of cells depends on the activity of a wide variety of genes and pathways, not oncogenic themselves, but essential to support the oncogenic phenotype of cancer cells that become "addicted". Differently, the viability of normal cells do not require the same degree of addiction, thus highlighting the possibility to explore new therapeutic approaches for cancer drug targets [141].

As widely reviewed by *Jiang et al.*, RNA sequencing databases revealed that CK1α mRNA is expressed in various cancer cell lines and in most cancer tissue [123]. CK1α kinase, negatively regulating Wnt/β-catenin pathway, is an important key regulator in metastatic melanoma cancer. *In vitro* and *in vivo* studies, knockdown of CK1α in melanoma cells enhanced the tumorigenic potential and the invasiveness capacity of cancer cells through the stabilization of β-catenin [142][143]. CK1α has also been implicated in lung, breast, esophageal, skin, urothelial and prostate cancers. Moreover, the kinase promotes colon cancer progression and stimulates renal cell carcinoma growth and metastasis [123]. CK1α activity is described not only in cancer initiation and progression, but also in neurodegenerative disorders. For instance, the kinase is responsible for the pathological hyper-phosphorylation of tau protein, in Alzheimer's disease and for the phosphorylation of α-sinuclein, playing an important role also in the pathogenesis of Parkinson's disease [123].

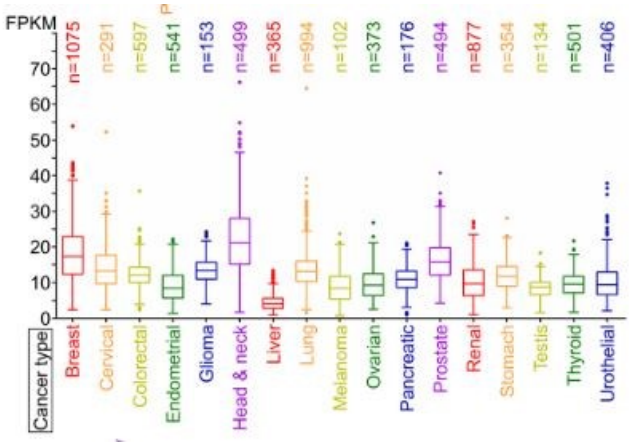

Fig.15 RNA sequencing data of CK1α levels in different cancer types. FPKM: fragments per kilobase of exon per million reads (adapted from [123]).

Focusing on cancer of blood origin, the involvement of CK1α has been investigated since its overexpression and overactivation has been demonstrated in acute and chronic leukemias, Mantle Cell Lymphoma (MCL) [144], DLBCL and in MM. As reported in chapter 4.3, CK1α activity supports signaling cascades, such as NF-κB, PI3K/AKT, RAS-MAP kinase, Wnt/β-catenin and others, essential for tumor selection and clonal evolution

in the context of blood cancers pathogenesis [122]. Specifically, in ABC-DLBCL disease and in MCL [144] , CK1α interacts with CARD11, promoting the formation of the CBM1 complex, thus constitutively activating the NF-kB pathway, required for cell proliferation and survival [128]. Considering AML, *Jaras at al.* demonstrated that CK1α is essential for human AML cells since it leads to enforced cell differentiation, reduces Ribosomal Protein S6 phosphorylation and increases p53 activation, selectively eliminating leukemic cells [134].

Interestingly, the protein kinase CK1α could be a potential target in MM for anti-tumor therapy [132] [127]. *CSNK1A1* gene is expressed in MM and in MCLs, suggesting a role of CK1α in the disease progression. Moreover, the studies demonstrated that CK1α inhibition triggered G0/G1-phase arrest, prolonged G2/M phase and apoptosis, affecting several cell proliferation and apoptosis pathways, including p53 expression [132] [127]. *Manni et al*. too, by analyzing a large cohort of MM cases, found high levels of the kinase, and confirmed that CK1α activity is essential for MM cells survival even in the protective BM *niche.* Indeed, CK1α disruption increases both p53 and caspase activity, and reduces the expression of β-catenin and AKT levels. CK1α inactivation in MM enhances the cytotoxic effect of both Bortezomib and Lena treatment *in vitro* studies [127].

4.6 CK1 PROTEIN KINASE INHIBITORS

Given the pro-survival role of the protein kinase CK1α in MM, its inhibition could represent a clinically meaningful therapeutic approach of this B cell malignancy. Several studies have shown that protein kinases could represent suitable therapeutic targets, since they are druggable with small molecules [145]. So far, there are no inhibitors that selectively target CK1α or other CK1 isoforms, due to the high degree of homology in the kinase domain between the different isoforms. Nonetheless, small molecule compounds are useful research tools for investigating CK1 functions, and most of these agents are ATP-competitive inhibitors [123]. *Rena et al.* identified D4476 (4-[4-(2,3-dihydro-benzo[1,4]dioxin-6-yl)-5-pyridin-2-yl-1H-imidazol-2-yl]benzamide) as a CK1s inhibitor, more potent and specific than IC261 or CKI-7, with an IC50 of 200-300nM [146]. It has been reported that D4476 inhibits CK1δ and also CK1α *in vitro* and in cells, not affecting the activity of others kinases such as ERK2, JNK, PKA, PDK1. For all these reasons, D4476 is the best CK1 inhibitor commercially available, widely used in preclinical studies to describe CK1α biology [89]. Furthermore, recently, the compound A51 was discovered as a novel dual inhibitor of CK1α and CDK7/9 with an anti-leukemic effect in preclinical models [147].

5. AIM

MM represents the second most common hematological malignancy after NHL. The role of the BM *niche* is crucial for both clonal PCs expansion and for the progression of the MM associated bone disease (MMABD). MMABD is the major cause of MM morbidity, found in 80–90% of patients, worsening patients quality of life [62]. Despite the recent advances in developing new treatment options, many patients still show insufficient response rates and often experience relapses [6].

Therefore, there is an urgent need to explore novel "druggable" targets to develop more effective therapeutic strategies both for the hematological neoplasm and for the MMABD.

CK1α is a Ser/Thr kinase overexpressed and overactive in MM PCs [127]. Among the different pathways controlled by CK1α and fundamental in MM pathogenesis there is the Wnt/β catenin signaling cascade. This pathway is known to play a pivotal roles in the early phases of MSC osteogenic differentiation, which is compromised in the MMABD [104].
It has been demonstrated that Lenalidomide, an IMiD currently used in MM therapy, is able to induce CK1α proteasomal degradation by a novel mechanism [14]. Although Lenalidomide mechanism of action on PCs has been intensively studied, its effects on the stromal compartment in the context of BM *niche* are still debated. Indeed, the impact of the use of IMiDs on MSC differentiation and bone remodeling is still controversial [78], [76].

The work of this thesis aims at clarifying the effects of CK1α inactivation on MSC osteogenic transcriptional program modulation. Specifically, to determine whether CK1α inactivation in the context of the BM *niche*, could promote osteogenesis, potentially counteracting the MMABD.
Moreover, the study focuses to unravel the possible effects of Lena treatment on the MSC osteogenic differentiation potential, in order to better investigate its possible impact on the MMABD.

Overall, the aim of the project is to evaluate whether CK1α could represent a potential new molecular target not only in the anti-tumour therapy of MM, but also in the regulation of osteoblastogenesis in the context of MMABD.

6. MATERIAL AND METHODS

6.1 CELL LINES

Different MM and MSC cell lines have been used:

- INA-6: was established from the pleural effusion of an 80-year-old PCL patient and is dependent either on exogenous human IL-6 or human BMSC for its growth and survival, similarly to primary MM cells. It was provided by Dott. M. Gramatzki (University of Kiel, Germany). These cells are mutated in *NRAS* gene [148];

- H929: an IgA-producing cell line established from a malignant effusion in a 62-year-old Caucasian woman with myeloma. Rearrangement of c-myc proto-oncogene has been described in this cell line and it is able to grow independently of IL-6 growth factor. These cells display wt *p53* gene and carried *NRAS* mutation [149];

- HS-5: a stromal cell line established from bone marrow, stroma of a healthy 30-year-old man. The cell line was purchased from the American Type Culture Collection (Rockville, USA);

-MSC hTERT: a stromal cell line obtained from unfractionated bone marrow mononuclear cells of a healthy donor expressing GFP [150].

6.2 CELL CULTURES

Multiple myeloma cells lines INA-6/H929 and HS-5 stromal cells were cultured with the appropriate media in 25 cm^2 flasks (Falcon) in a final volume of 10 mL. Differently, MSC hTERT were cultured in 75 cm^2 flasks (Falcon) in a final volume of 20 mL. They were maintained in incubator at 37°C in a modified atmosphere with 5% of CO^2. INA-6 were cultured in RPMI 1640 (EuroClone, Italy) with HEPES and L-Glutamin and supplemented with 10% v/v of heated inactivated fetal bovine serum (FBS) (EuroClone, Italy), antibiotics (penicillin 100 U/mL and streptomycin 100 µg/mL) (EuroClone, Italy) and IL-6 (2,5 ng/mL) (Sigma-Aldrich, Steinhelm, Germania); H929 were cultured in RPMI 1640 (EuroClone, Italy) with HEPES and L-Glutamin and supplemented with 10% v/v of heated inactivated FBS (EuroClone, Italy), antibiotics (penicillin 100U/mL and streptomycin 100µg/mL) (EuroClone, Italy) and 0,05mM of 2-mercaptoethanol); HS-5 were cultured in Dulbecco's Modified Eagle's Medium (DMEM) addicted with FBS to a final concentration of 10% and antibiotics (penicillin 100U/mL and streptomycin 100µg/mL) (EuroClone, Italy); MSC hTERT were cultured in RPMI 1640 (EuroClone, Italy) addicted with FBS to a final concentration of 10%, antibiotics (penicillin 100U/mL and streptomycin 100µg/mL) (EuroClone, Italy) and hydrocortisone (10-6 mol/L) (Sigma-Aldrich, Steinhelm, Germania). HS-5 and MSC hTERT cell lines grow in adhesion and support proliferation of MM cells when they are in a co-culture with MM cells. All the procedures of cell handling were performed under a

sterile hood. Each cell line was periodically tested for mycoplasma contamination using the MycoAlert® Mycoplasma Detection Kit (Lonza, Rockland, USA).

6.3 BONE MARROW STROMAL CELLS ISOLATION AND CULTURE

Patients were charged to the University of Padova Hospital. Informed consent was obtained from patients according to the declaration of Helsinki and the laboratory protocol was supervised by the institutional scientific review board, University-Hospital of Padova. BMSC were isolated from iliac crest aspirate of patients under local anesthesia. The blood samples were collected in a heparinized tube, then transferred to a sterile 15 mL polystyrene tube and lysed in an equal volume of EasySep RBC Lysis Buffer (StemCell Technologies, Vancouver, Canada) for 30' at room temperature. Subsequently the samples were centrifuged at 1300 rpm for 3' to pellet the cells. Then, the supernatant was discarded, and the cells resuspended in growth medium DMEM (Euroclone), 10% FCS, penicillin (100 U/mL) and streptomycin (100 µg/mL) (Gibco Laboratories). The suspension was transferred to a flask at the density of $1x10^3$ cells/cm^2, cultured at 37° C and 5% CO^2 in a humid environment to allow the attachment to the culture flask for 7 days. At this time-point, non-adherent fraction was discarded, and adherent cells were fed every week with fresh medium. Alternatively, after the purification of PCs from BM aspirated obtained with the Human Whole Blood CD138+ Selection Kit (EasySep, Stem Cell Technologies), BMSC were obtained keeping the CD138- fraction in DMEM 10%.

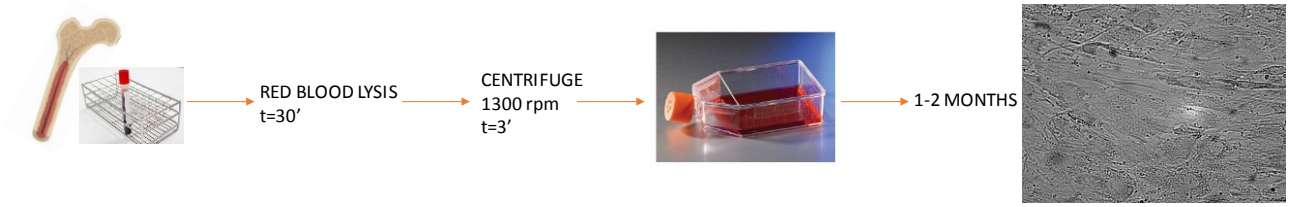

Fig.16 Schematic representation of BMSC isolation.

6.4 GENERATION OF ISOPROPIL β-D-1-THIOGALACTOPYRANOSIDE (IPTG) INDUCIBLE CK1α shRNA MM CELL CLONES

We generated CK1α inducible cellular clones using MISSION Lentiviral Particles Protocol provided by Sigma-Aldrich. The power of the lentiviral delivery system lies in the ability to create stable cell lines from both dividing and non-dividing cells. The lentiviral particles deliver their payload into the target cells, and then, the contents are integrated at high efficiency into the host genome. Stable integrants are selected using puromycin resistance. Three independent CK1α directed shRNA lentiviral particles were chosen, which gave rise to three distinct CK1α shRNA IPTG inducible cellular clones, named shRNA 6044, shRNA 6287 and shRNA 6042. The procedure of transduction was the following: INA-6 cells were seeded at appropriate density in

media containing 8 µg/mL of polybrene. shRNA lentiviral particles were added to the cells at multiplicity of infection (MOI) of 5. Cells were centrifuged at 1000 x g for 45' at 32 °C. The media was removed and replaced with 100µL of fresh growth media (without polybrene). After incubation overnight at 37 °C, 5% CO^2, the media was removed and replaced with fresh growth media containing puromycine 0.5µg/mL. A titration curve for puromycine resistance was previously performed by an Antibiotic Kill Curve Assay in our laboratory. 0.5µg/mL puromycine was the minimal concentration that killed INA-6 cells. Cells were maintained in puromycine containing media until they had emerged from the selection and non-transduced cells had died. For the experiments in this thesis the CK1α shRNA 6044 IPTG inducible cellular clone, called INA-6 6044 was used.

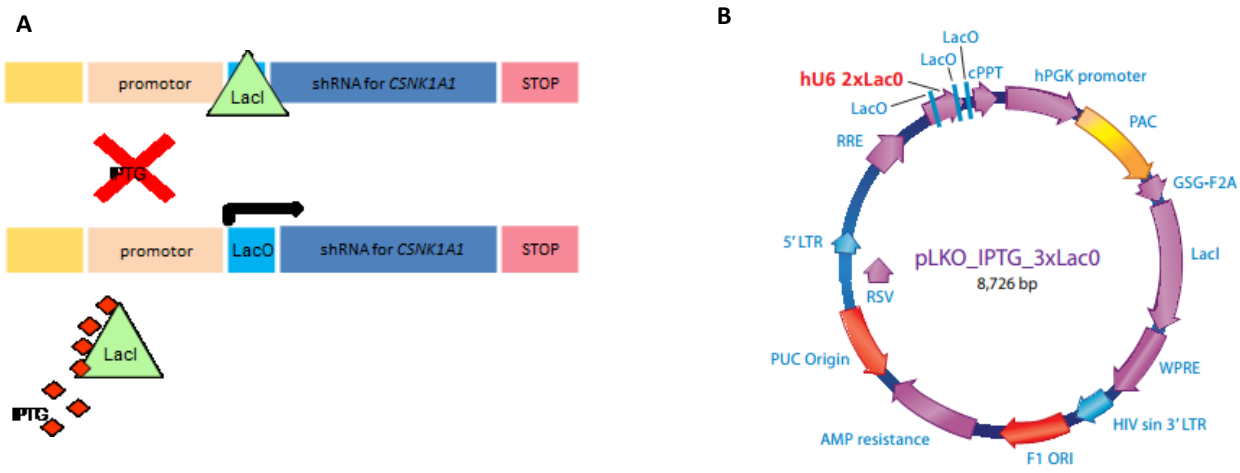

Fig.17 A. Schematic representation of CK1α silencing through RNA interference. In the absence of IPTG LacI binds to LacO preventing expression of the shRNA. When IPTG is present, the allosteric LacI repressor changes conformation, releasing itself from lacO modified human U6 promoter, and subsequently allows expression of the shRNA. **B. pLKO_IPTG_3xLacO plasmid used to generate IPTG inducible MM cell clones.**

6.5 GENERATION OF ISOPROPIL β-D-1-THIOGALACTOPYRANOSIDE (IPTG) INDUCIBLE CK1α shRNA MSC CLONES

The same protocol described in chapter 6.4 was applied for the generation of MSC hTERT and HS-5 inducible cellular clones. Two independent CK1α directed shRNA lentiviral particles were chosen, which gave rise to two distinct CK1α shRNA IPTG inducible cellular clones, named shRNA 6044, shRNA 6287 for HS-5 cells and named shRNA 6044, shRNA 6042 for MSC hTERT cells. A MOI of 4 and 3 were used for the transduction of MSC hTERT and HS-5 respectively. For the experiments presented in this thesis the CK1α shRNA 6044 IPTG inducible cellular clones, called MSC hTERT 6044 and HS-5 6044 were used.

6.6 GENERATION OF mCHERRY+ MSC CLONES

Stromal cells HS-5 and HS-6 6044 were infected with lentiviral particles containing the EX-NEG-Lv216 plasmid (GeneCopoeia, Rockville, MD, USA) (Fig.18) After 14 days of infection, the expression of the mCherry protein was controlled both by Olympus CKX53 Microscope (Olympus Corporation, Tokyo, Japan) and by FacsAria IIIu flow cytometer (BD, Becton-Dickinson, Italy) to create a stable mcherry HS-5 and HS-5 6044 clones. The percentage of infection was about 85%. To have a pure mcherry + HS-5 cell population, all mcherry positive cells were sorted by FacsAriaIIu flow cytometer and a stable clone was generated.

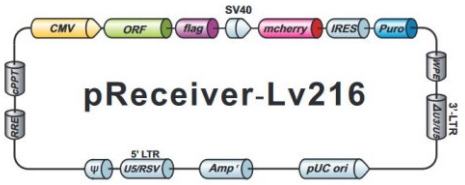

Fig.18 pReceiver-Lv216 plasmid used to generate mcherry+ HS-5 clones.

6.7 CELL CO-CULTURE: MODEL OF MM BONE MARROW MICROENVIRONMENT

Co-cultures of MM cells and stromal cells were obtained culturing the stromal cell line HS-5 or MSC hTERT and the MM IL-6 dependent INA-6 cell line. $3x10^5$ HS-5/ MSC hTERT cells were plated and cultured for 24 hours in order to allow cell adhesion. The day after the growing media was removed and replaced with 2 mL of RPMI containing $2,0×10^6$ PCs. IL-6 was not added because both HS-5 and MSC hTERT provided it. Cells were maintained at 37°C in incubator with 5% of CO^2 flow. The co-culture phase is preceded by a pre-induction phase with IPTG 500µM for seven days for INA-6 WT/INA-6 6044 cells (fig.19A) or MSC hTERT 6044/HS-5 6044 (fig.19B) cells, depending on the co-culture model performed. $1,5x10^6$ INA-6 cells were plated in 1,5 mL RPMI with FCS 10% supplemented with penicillin (100 U/mL), streptomycin (100 µg/mL) (Gibco Laboratories) and IL-6 2,5 ng/mL (Sigma-Aldrich), while both MSC hTERT and HS5 were plated at a concentration of $3x10^4$ in 2 mL in RPMI FCS 10% supplemented with penicillin (100 U/mL), streptomycin (100 µg/mL) (Gibco Laboratories) and hydrocortisone (only for MSC hTERT (Sigma). The cell culture medium and IPTG were refreshed every 2 days. At the end of the co-cultures, cell sorting by FACSARIA IIIu (Becton-Dickinson) was used to obtain MSC and MM pure populations. The three models of co-culture have been performed following different protocols as represented in Figure 19.

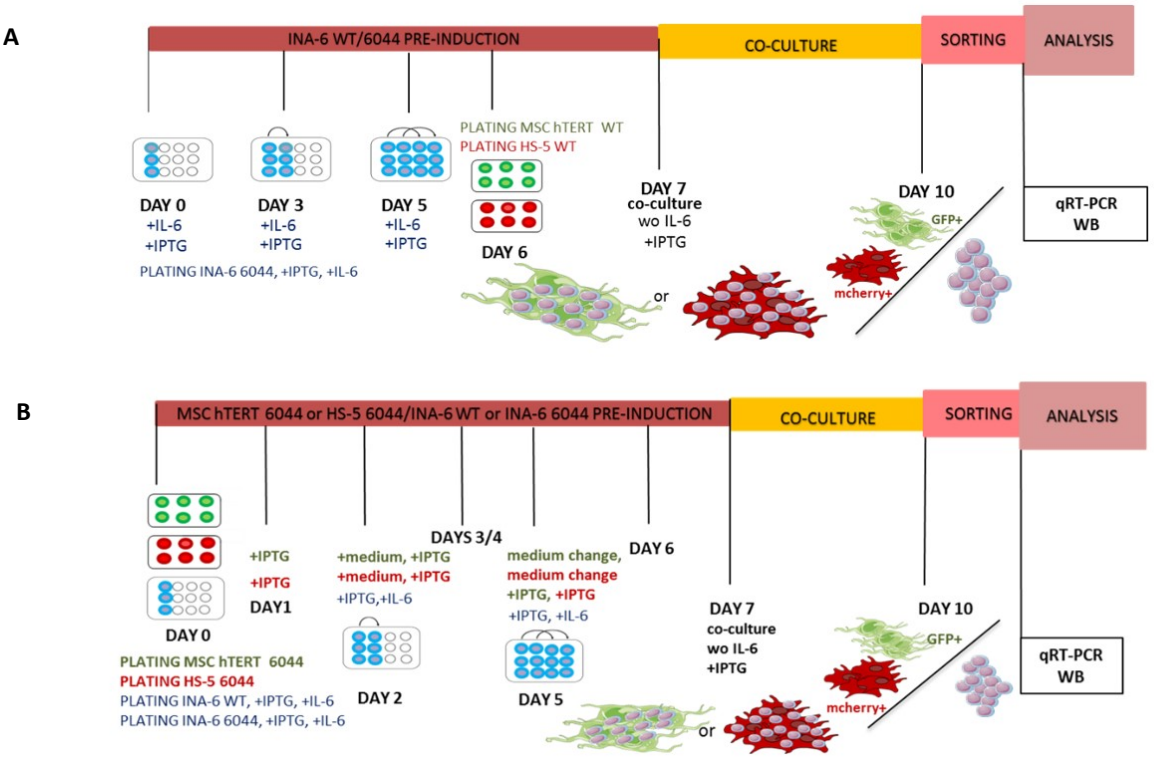

Fig.19 The figure summarizes the protocols applied in the co-culture experiments between MM and MSC. A. Protocol used for model 1 in which CK1α silencing was obtained in MM cells. B. Protocol used for both models 2 and 3 where CK1α silencing was achieved in MSC or in both cell populations respectively.

In the different co-cultures models, CK1α silencing was achieved in the MM compartment following the protocol showed in Fig.19A (model 1, Fig.20), in MSC compartment (model 2, Fig.20) or in both cell populations (model 3, Fig.20), following the protocol showed in Fig.19B.

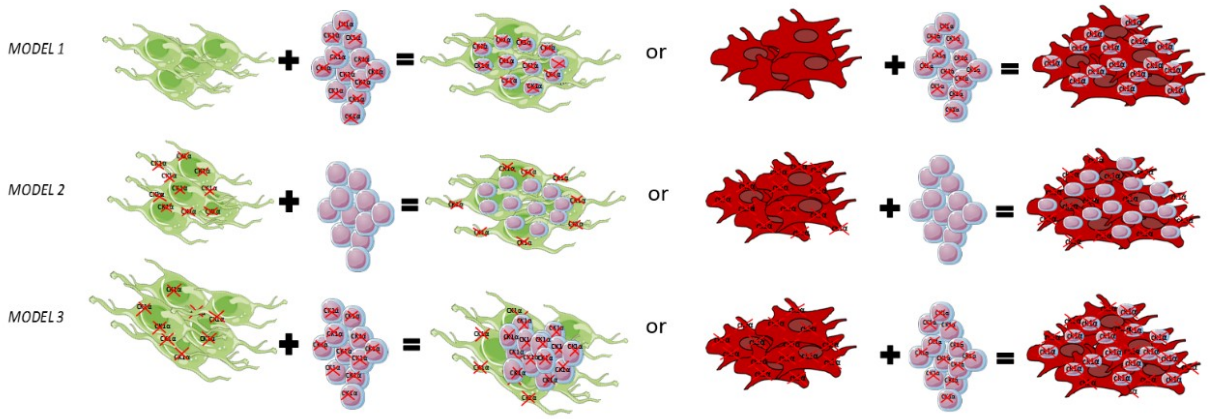

Fig.20 Schematic representation of the three models of co-culture experiments between INA-6 MM cells and the stromal compartment created by MSC hTERT or HS-5 cells.

In addition, the same experimental protocol of model 3, has been reproduced by using a transwell system (Greiner Bio-one, Italy). This tool prevents cell-to cell contact between MM cells and stromal cells in the co-culture, allowing their cross talk only through soluble factors in the medium. At the end of the co-culture, the two cells populations have been harvested without cell-sorting.

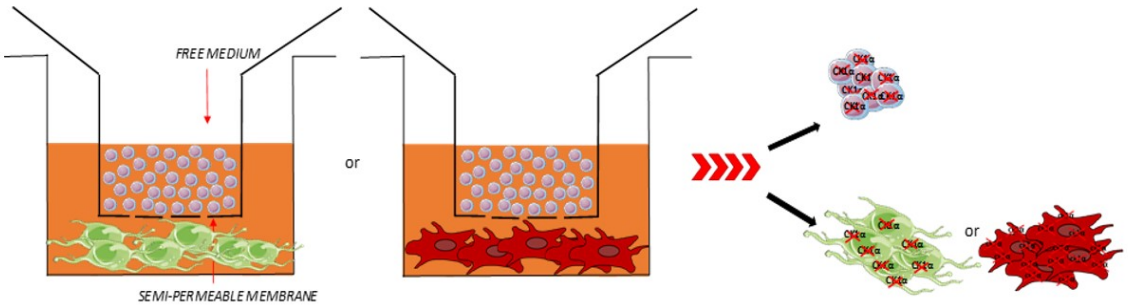

Fig.21 Schematic representation of co-culture experiments using the transwell system.

6.8 CELL TREATMENTS

-CK1α SILENCING IN IPTG INDUCIBLE CLONES

To obtain CK1α silencing, IPTG was added to MM cells (INA-6) and to MSC (HS-5 or MSC hTERT) and refreshed every 2-3 days. IPTG was used at a concentration of 0,5mM for each cell line. Cells were collected at different time points. For INA-6 clones and co-culture experiments with HS-5 or MSC hTERT, INA-6 or stromal cells were pre-induced with IPTG for 7 days and subsequently plated on a feeder layer of MSC hTERT/HS-5 cells in the continuous presence of IPTG for another three days. Cells were collected after a total induction of IPTG for 10 days.

-LENALIDOMIDE TREATMENT IN MSC LINES

Both HS-5 and MSC hTERT were cultured in 6 well plates and treated with Lena for 7 days. (Selleck Chemicals, USA) at different concentrations ranging from 1 to 10μM. As control the cells were treated also with dimethylsulfoxide (DMSO, Sigma-Aldrich), the vehicle in which the drug was dissolved. The H929 Lena sensitive cells were treated with Lena 10μM for 7 days as positive control.

-LENALIDOMIDE TREATMENT IN PRIMARY MSC

Primary MSC isolated from patient samples were cultured in DMEM medium addicted with FBS to a final concentration of 10% and antibiotics (penicillin 100U/mL and streptomycin 100μg/ml) in a 6 well plate.. Achieved the confluence, Lena was added at a concentration of 2,5μM for 7 days. Lena treatment and medium were refreshed every 2 days. As control, the cells were treated also with DMSO. H929 cells were treated with Lena 10μM for 7 days as positive control of Lena activity.

-WNT-3A STIMULATION

3X10^5 HS-5 and MSC hTERT were plated and cultured for 72 hours to allow cells adhesion and cell growth. Cell medium (RPMI 1640 for MSC hTERT cells or DMEM for HS-5 cells, both added with 10% of FBS and antibiotics penicillin 100U/mL and streptomycin 100µg/ml) was changed with starvation medium (RPMI 1640/DMEM additioned with 5% of FBS and antibiotics) for 24h. After the starvation phase, both MSC lines were treated with Recombinant Human WNT-3A Protein (R&D System, USA) at final concentration of 200 ng/mL. Cells were collected at different time points of treatment: after 8 hours for MSC hTERT and after 4 hours for HS-5 cells.

-**DOXORUBICIN TREATMENT**

5X10^5 HS-5/MSC hTERT and 1.5X10^6 INA-6 6044 were cultured in plate 6 wells and 12 wells respectively for 24 hours to allow cell growth. The day after, Doxorubicin 1.2µM was added at the culture medium for 18 hours.

6.9 FLOW CITOMETRY

ANNEXIN V/PI STAINING

In order to detect the rate of apoptosis, cells were labelled with Annexin V(AV) and Propidium Iodide (PI) (Immunostep Biotech, Spain). Annexin V is a member of the annexin family of intracellular protein capable of binding phosphatidyl serine (PS) in a calcium-dependent manner. While normally PS can be found on the intracellular leaflet of healthy cells, during early apoptosis it translocates to the external leaflet, since membrane asymmetry is lost. However, AV binding itself cannot distinguish apoptotic from necrotic cells, therefore PI is used. PI is a fluorescent dye that binds to DNA. Early apoptotic cells will exclude PI, differently from necrotic and late apoptotic cells which will be stained positively, due to the passage of this dye to the cell nucleus when the cellular membrane integrity is lost. $1x10^5$ cells were resuspended in 100 µL of binding buffer (Bender MedSystem, Vienna); 1.3 µL of AV-FITC (1µg/µL) was then added and cells were incubated for 10’ in the dark at room temperature. 100 µL of binding buffer were further added to the cell suspension and, immediately before flow cytometry, cells were stained with 3 µL of PI (1µg/µL). Fluorescence Activated Cell Sorting (FACS) analysis was performed using a FACS-CANTO Cell Cytometer and the FACS Diva software (Becton-Dickinson, Italy).

CELL CYCLE ANALYSIS

Cell Cycle analysis was performed by PI staining. Thanks to PI propriety to intercalate DNA content in the cell and to emit fluorescence in PE with a direct proportionality, it is estimated the percentage of cells in the

different phases of cell cycle. 1×10^6 cells were fixed adding ice cold ethanol 70% v/v drop by drop under vortex condition. The samples were incubated for 30' on ice and subsequently at least 2h at -20°. After washing 2 times in PBS, samples were stained with PI (50µg/mL) and RNAse 0.2mg/mL (Sigma-Aldrich, Italy) for 30'. After PI staining analysis was performed using FACS-CANTO Cell Cytometer and the FACS Diva software (Becton-Dickinson, Italy).

CELL SORTING

Cell sorting, a FACS separation method, was used to obtain MSC and MM pure populations from MSC hTERT/INA-6 or HS-5/INA-6 co-culture models. This technique allows obtaining fast, high pure cell populations through a specific cell protein expression/coloration or through cell dimension, thus considering cell forward and side scattering. MSC hTERT and HS-5 cell lines have been genetically modified in order to express GFP and mcherry, respectively. This specific protein expression allows the separation of the fluorescent MSC compartment from MM cells, (which are without fluorescence and with smaller dimensions than MSC counterpart).

For this purpose, a homogeneous suspension (MSC hTERT/HS-5 with INA-6 contamination) was prepared in PBS, which was then sorted by FACSARIA IIIu (Becton-Dickinson). The pure MSC compartment selected was finally collected in 15 mL polyethylene tubes, previously primed with FCS, containing PBS with 2% of FCS and subsequently stored at -80°C until the analysis.

6.10 RNA PURIFICATION

RNA was purified using RNeasy Mini Kit (Qiagen) according to manufacturer procedures. This procedure represents a well-established technology that combines the selective binding properties of a silica-based membrane with the speed of microspin technology. Biological samples are first lysed and homogenized in the presence of a highly denaturating guanidine-thiocyanate-containing buffer, in order to immediately inactivate RNases to ensure purification of intact RNA. Ethanol is added to provide appropriate binding conditions. The mix of sample and ethanol is then added to a RNeasy Mini spin column, where the total RNA binds to the membrane and contaminants are efficiently washed away. RNA is then eluted in water and then quantified by means of Nanodrop 1000 (Thermo Scientific, Wilmington, DE, USA), measuring the concentration (ng/µL). Purity of RNA was estimated through the ratio of the readings at 260 nm and 280nm (A_{260}/A_{280}) and 260 nm and 230 nm (A_{260}/A_{230}). Expected A_{260}/A_{280} are commonly in the range of 2.0-2.2 and indicate pure RNA. Expected A_{260}/A_{230} are commonly in the range of 2.0 and indicate the absence of protein, phenol or other contaminants in the sample.

6.11 REVERSE TRANSCRPTION REACTION

Reverse transcription is a reaction exploited by a RNA-dependent polymerase capable of synthesizing a complementary strand of DNA, called cDNA, using a RNA strand as template. The *Reverse Transcription System* (Promega Corporation, Madison, WI, USA), has been used to efficiently transcribe RNA into cDNA. This kit provides the reagents necessary for the reaction, specifically $MgCl_2$ 25mM, buffer RT 10x, dNTPs mix 10mM, RNases inhibitor 40 µg/µL, oligonucleotides (oligodT), Reverse Transcriptase enzyme and 1 µg of RNA for a final volume of 20 µL for each sample. Samples were incubated in the GeneAmp PCR System 2700 (Applied Biosystem, Foster City, CA, USA) for 15' at 42 °C and at 95 °C for 5'. Samples were stored at -80 °C.

6.12 QUANTITATIVE REAL-TIME PCR

The quantitative Real-Time PCR (qRT-PCR) is a method for gene quantification characterized by high sensibility and specificity. It is called "Real-Time PCR" because it allows the scientist to observe in real time the increase in the amount of DNA as it is amplified. This is possible because the qRT-PCR system combines a thermal cycler and an optical reaction module that detects and quantifies fluorophores. Molecules added to the PCR mix, as SYBR Green, bind the amplified DNA and emit a signal that increases in proportion to the rise of the amplified DNA products. An amplification curve is obtained where cycle numbers are found in abscissa and the fluorescence normalized on internal fluorophore in ordinate. At the beginning of the reaction there are only little changes in fluorescence, and this is the baseline region; the increasing in fluorescence above this threshold underlines amplified product formation. From this point on, the reaction maintains an exponential course that degenerates in plateau at the end of the reaction. In the midway cycles, the curve has a linear course: this is the most important phase since the amount of amplified DNA is correlated with the amount of cDNA expressed at the beginning in the sample. In this linear region a threshold of fluorescence is chosen and from this value it is possible to obtain the Ct (threshold cycle), namely the number of cycles of amplification necessary for the sample to reach that threshold of emission. If the amount of cDNA present at the beginning in the sample is high, the curve will rise earlier and Ct values will be smaller. As detector dye we used SYBR Green that emits low fluorescence if present in solution; on the contrary the signal becomes stronger if the dye binds to double strand DNA. However, SYBR Green is not a selective dye and binds to all DNA, even to primer dimers. For this reason, it is recommended the introduction of a further step after amplification, called dissociation protocol. During this step, temperature rises gradually until all the double strands are denatured. This method allows the identification of contaminants or unspecific amplification products since they show different melting points. There is also a dye called ROX that works as an internal reference used by the instrument to normalize the SYBR Green fluorescence.

For the evaluation of gene expression, we chose a relative quantification method, using the **ΔΔCt** formula:

1) **ΔCt** = **Ct (target gene)** - **Ct (reference gene)**

2) **ΔΔCt** = **ΔCt (of treated sample)** - **ΔCt (of untreated sample**), the internal calibrator)

3) **2^-ΔΔCt**

The "2"value in the last formula represents the higher efficiency for reaction that means a doubling of the product at every cycle of amplification. The thermal cycler used was the QuantStudio 5 Detection System (Applied Biosystem, CA, USA) with the QuantStudio ™ Design and Analysis Software v.1.4.3. The reagents of the reaction mix were:

• Luna Universal qPCR Master Mix (M3003) 4 µl

• Forward primer (4 pmol/µl) 0,5 µl

• Reverse primer (4 pmol/µl) 0,5 µl

• H2O 2 µl

• cDNA 1µl

Luna Universal qPCR Master Mix (M3003) contains all reagents (except primers and template) needed for running the qRT-PCR. Hot Start *Taq* DNA Polymerase is a hot start polymerase with the following amplification protocol: UDG activation 50°C 2' ⟶ Polymerase activation 95°C 10' ⟶ Denaturation 95°C 15'' for 40 cycles ⟶ Annealing and amplification 60°C 1'. Dissociation protocol: increasing temperature from 60°C to 95°C.

GENE	CODIFIED PROTEIN	FORWARD PRIMER (5'-3')	REVERSE PRIMER (5'-3')
RUNX2	RUNX2	TAAGAAGAGCCAGGCAGGTG	TAGTGCATTCGTGGGTTGG
ALP	ALP	GACCCTTGACCCCCACAAT	GCTCGTACTGCATGTCCCCT
SPP1	OPN	CTCAGGCCAGTTGCAGCC	CAAAAGCAAATCACTGCAATTCTC
BGLAP	OCN	GAAGCCCAGCGGTGCA	CACTACCTCGCTGCCCTC
CSNK1A1	CK1α	GGCACTGCCCGATATGCTA	CTCGGCGACTCTGCTCAATAC
AXIN2	AXIN2	GTGTGAGGTCCACGGAAACT	TGGCTGGTGCAAAGACATAG
GAPDH	GAPDH	AATGGAAATCCCATCACCATCT	CGCCCCACTTGATTTTGG

Table I. Primers used for qRT-PCR analysis.

In the table above are reported the sequences of the primers used for the qRT-PCR. GAPDH was used to normalize the reaction. The sequences were found using Primer Express program (Applied Biosystem) and BLAST: Basic Local Alignment Search Tool.

6.13 TOTAL CELL PROTEIN EXTRACTION

In order to obtain total protein, cells were harvested and centrifuged at 5000rpm for 5' at 4°C. The obtained pellet was then lysed in a buffer containing: Tris-HCl 20 mM, NaCl 150 mM, EDTA 2 mM, EGTA 2 mM , Triton X-100 20% 1:40, dithiothreitol (DTT) 1 mM diluted 1:200 (Amhersham Biosciences, UK), cocktail proteases inhibitor diluted 1:100, okadaic acid 1 µM 1:100 (Sigma-Aldrich, Steinheim, Germany), cocktail of

phosphatase inhibitors diluted 1:100 (Halt^{TM} Phosphatase Inhibitor Cocktail, Pierce Biotechnology, Rockford, USA). The lysis was performed for 30' on ice and cells were vortexed every 10'. Then, cells were centrifuged at 13000rpm for 10' and the lysate was collected. Its protein concentration was determined with Bradford method.

6.14 BRADFORD METHOD FOR PROTEIN QUANTIFICATION

The colorimetric system of Bradford (Sigma Aldrich, Steinheim, Germany) is employed to establish protein concentration. This assay is based on the ability of Comassie Brilliant Blue to change its absorbance maximum from 465 nm to 595 nm when binding to proteins, bringing the acquisition in the range of visible. The content of proteins is quantified with high sensitivity if it is in the range of 1-5µg/mL. The calibration curve and its equation are obtained plotting the absorbance values against the concentration of the reference protein in a Cartesian graph. Through the Lambert-Beer law, $A=\varepsilon cl$ (where c is the protein concentration of the sample, l is the length of the optic path, e the molar absorptivity and A is the absorbance) it is possible to calculate e the molar absorptivity, which is essential to define the protein concentration of the sample. The tare of the spectrophotometer was obtained using a solution of Bradford staining diluted 1:1 in milliQ water as blank; 1 µL of protein extract was added to 1 mL of Bradford reagent dilution and the protein concentration was determined reading the absorbance at λ=595 nm and using the Lambert-Beer law.

6.15 WESTERN BLOTTING

Western Blotting (WB) is a common technique used to detect and analyze proteins, which are separated according to their molecular weight (MW) in Dodecyl Sulfate-Polyacrylamide Gel Electrophoresis (SDS-PAGE) and subsequently transferred to a poly-vinylidene fluoride membrane (PVDF, Pierce Biotechnology, USA), where they can specifically be visualized. Proteins are first stained with primary antibodies (Ab), specific to the target protein, and then secondary antibodies, which allow the recognition of the constant Fc region of primary Ab. The protein samples extracted from the cells were resuspended in a buffer containing Tris 1.5 M, SDS 20%, Bromophenol Blu 0.05%, DTT 6%, β-mercaptoethanol 1:20, and they were heated at 100 °C for 5'. Migration of proteins was performed on manual gels at 10% of polyacrylamide, using a Tris-Glycine based running buffer TGS (Tris 25 mM, glycin 192 mM, SDS 0.1 % (pH 8.39). The SeeBlue Plus2 Prestained Standard

(Invitrogen, Carlsbad, CA) was used as moleuclar weight, distinguishing proteins with MW comprised between 4 and 250 kDa. After gel electrophoresis, proteins were transferred to a 1' methanol activated PVDF membrane at 350mA for 1 hour and 50' at 4°C, using a blotting buffer 1X made of Tris 25mM, glycine 192 mM (pH 8.3) and methanol 20%. In order to prevent unspecific binding of the primary antibodies, the membrane was saturated in TBS (0.137 M Sodium Chloride, 0.0027 M Potassium Chloride and 0.025 M Tris-Tween 0.1% (TBST)), supplemented with 5% w/V milk for 1 hour and then incubated with the primary antibody in agitation overnight at 4°C. The day after the membrane was washed in TBST for 30' and then incubated with the secondary antibody for 1 hour. The secondary antibody dilution was 1:4000 (anti-rabbit, made in goat, Cell Signaling Technology, USA) or 1:20000 (anti-mouse made in goat, KPL , USA) in TBST with the addition of 5% of milk. At the end of the incubation time, the membrane was washed for 30', to get rid of the antibody aspecific bonds. Secondary antibodies were conjugated with horseradish peroxidase (HRP, which catalyzes the oxidation of luminol (Pierce ECL Western Blotting Substrate, Thermo Scientific, LiteAblot TURBO, Euroclone, and Westar Supernova ECL Substrate) from the luminol peroxide detection reagent in a luminescent compound. It has a high substrate specificity and gives low background. The chemiluminescence acquisition of the bands was performed using the Image Quant LAS 500 machine (GE Healthcare, USA) and the densitometry analysis of the bands was performed with the Image Quant TL software (GE Healthcare, USA). In order to investigate more than on protein on the same membrane, stripping was performed. It allows to remove the primary and the secondary antibodies from a WB membrane, incubating it with the Restore Western Blot Stripping Buffer (Pierce Biotechnology, Inc) at 37 °C in agitation.

6.16 PRIMARY ANTIBODIES

For protein detection primary antibodies detecting RUNX2 (Santa Cruz Biotechnology, USA), CK1α (Cell signaling Technology, USA), β-Catenin (Cell Signaling Technology, USA), GAPDH (Millipore, Germany), p21 (Santa Cruz, USA), p53 (Invitrogen/Thermo Fisher, USA).

6.17 SECONDARY ANTIBODIES

Anti-rabbit IgG HRP-linked antibody (Cell signaling Technology, USA) HRP labeled goat anti-mouse IgG (KPL, USA), HRP labeled mouse anti-goat IgG (Santa Cruz, Biotechnology, USA) were used at 1:3000, 1:10.000, 1:1000 respectively.

6.18 OSTEOGENIC DIFFERENTIATION

Both MSC hTERT 6044 and HS-5 6044 cellular clones were cultured for 7 days with IPTG 500µM to pre-induce CK1α silencing. At the end of the pre-induction period, both cell lines were cultured in 6 well plates using STEM PRO medium (Invitrogen, CA, USA) for a total of 21 days in the continuous presence of IPTG. The STEM PRO medium contains the supplements needed to induce stromal cells differentiation into the osteogenic lineage. Alizarin Red staining was used to verify the presence of calcium deposits, produced by differentiated cells.

6.19 ALIZARIN RED STAINING

Alizarin Red S 2% (Alizarin Red Staining Kit, Sciencell™ Research Laboratories, USA) is an anthraquinone dye used to detect calcium deposits that are indicators of the presence of mature osteocytes. Alizarin Red S forms a complex with calcium that causes birefringence. At the end of 21 days of STEM PRO/RPMI or DMEM medium culture condition, both HS-5 and MSC hTERT cells were washed twice with H2O deionized (dH2O), fixed with formaldehyde 3,7% (Sigma-Aldrich, USA) in PBS for 30' under gentle agitation at room temperature. At the end, after 2 washes with dH2O, the cells were incubated for 25' with 1 mL of Alizarin Red S 2%, always in slight agitation. The dye was then removed and 3 washes were carried out with dH2O before acquiring images with the Olympus BX60 Microscope (Olympus Corporation, Japan).

6.20 ALKALINE PHOSPHATASE ASSAY

The colorimetric alkaline phosphatase assay kit (Abcam, UK) uses p-nitrophenyl phosphate (*p*NPP) as a phosphatase substrate which turns yellow (ODmax=405nm) when dephosphorylates by ALP. The assay was performed using supernatants collected after Lena treatment of primary MSC isolated from MM/MGUS/SMM patients' samples. For each assay it is mandatory to use a fresh set of standards in order to obtain a standard curve (Fig. 22) , preparing a 1mM *p*NPP standard by diluiting 40µL *p*NPP 5mM in 160µL of Assay Buffer. Using 1mM standard a standard curve dilution has been prepared as described in the table below in a microplate 96 wells. Each dilution had enough amount of standard to set up duplicate readings.

Standard#	pNPP 1 mM Standard (µL)	Assay Buffer (µL)	Final volume standard in well (µL)	End amount pNPP in well (nmol/well)
1	0	300	120	0
2	10	290	120	4
3	20	280	120	8
4	30	270	120	12
5	40	260	120	16
6	50	250	120	20

Table II. ALP assay, standard curve preparation.

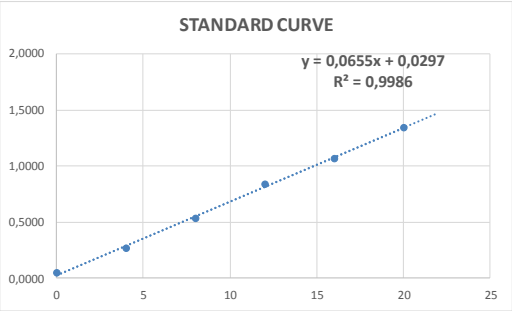

Fig.22 Example of standard curve.

After standard curve setup, in each sample wells reaction, 80µL of each supernatant sample was added in the microplate. To initiate ALP reaction 50µL of 5mM *p*NPP solution to each well containing sample and 10µL of ALP enzyme solution to each *p*NPP standard well were added. After 60' of incubation in the dark and at room temperature, the enzyme was able to convert *p*NPP substrate to an equal amount of colored p-Nitrophenol (*p*NP*)*. The reaction has been stopped in the sample wells and standard wells by adding 20µL of stop solution. Spectrophotometry reading was performed at OD 405nm (Variokan LUX multimode Microplate reader, Thermo Fisher, USA). ALP activity in the samples was calculated as: (B/ΔT*V)*D, where B=amount of *p*NP in sample well calculated from standard curve, ΔT=reaction time (minutes), V=original sample volume added into the reaction well (mL), D=sample dilution factor.

6.21 STATISTICAL ANALYSIS

All the data are expressed as mean ± SD (standard deviation). Data obtained were evaluated for their statistical significance with the two-tail unpaired Student's t test. Values were considered statistically significant at p values below < 0.05. All analysis were performed using GraphPad Prism 8.0.1.

6.22 CLINICAL AND PATHOLOGICAL FEATURES OF PATIENTS ANALYZED

The table below indicates the main clinical features of the patients' samples collected. Primary MSC were isolated from bone marrow of patients listed and treated with Lena 2.5µM for 1 week in order to investigate *RUNX2* and *ALP* mRNA expression levels. For all patients, bone disease was evaluated by CT scan analysis.

MM#	DIAGNOSIS	SEX	AGE	ISS	R-ISS	PARAPROTEIN	PCs %	KARIOTYPE	BONE DISEASE	LENA	RELAPSE/NEW DIAGNOSIS
1	MM	F	72	I	I	IgG/λ	20	monosomy 13	N	N	ND
2	MM	F	41	I	I	IgG/κ	50	gain(1q)	Y	N	ND
3	MM	F	56	I	I	IgA/κ	80	Standard	N	N	R
4	MM	F	78	I	I	IgA/κ	80	t(11;14), gain(1q)	N	N	ND
5	MM	F	69	I	I	IgA/λ	52	hyperdiploidy	Y	N	R
6	MM	M	82	II	II	IgG/λ	35	del(17)	Y	N	ND
7	MM	F	71	III	III	IgG/κ	100	t(4;14), gain(1q)	Y	N	R
8	MM	F	69	I	II	IgA/κ	30	del(17p), gain1q)	N	N	ND
9	MGUS	M	83			κ	6	ND	N	N	ND
10	MGUS	M	56			IgG/κ	5	ND	N	N	ND
11	MGUS	M	49			IgG/κ	6	ND	N	N	ND
12	SMM	F	54			κ	30	gain1q	N	N	ND
13	MM	M	67	I	I	IgG/κ	20	less of Y	Y	N	R
14	SMM	M	66			IgG/κ + κ	13	normal	N	N	ND
15	MM	M	71	I	II	IgG/κ	30	t(4;14), gain1q	Y	N	ND
16	SMM	M	80			IgG/λ	15-20	hyperdiploidy	N	N	ND
17	MM	F	66	I	I	IgG/κ	65-70	t(4;14), gain1q	Y	N	R
18	SMM	M	58			IgG/λ	15	normal	N	N	ND
19	MGUS	F	50			IgG/κ	<1	t(14;16)	N	N	ND
20	MM	M	60	III	III	κ	70	t(11;14)	Y	N	ND

Table III. Clinical features of patients analyzed. Clinical staging was performed according to the Internationl Staging System (ISS) and the Revised International Staging System (R-ISS). All features are reported as data at diagnosis. M=male, F=female, PC=Plasma Cell, Y=Yes/Present, N=No/Absent, Lena=Lenalidomide treatment, R=relapse, ND= new diagnosis.

7. RESULTS

7.1 CK1α SILENCING POSITIVELY REGULATES THE EXPRESSION OF POTENTIAL OSTEOGENIC DIFFERENTIATION MARKERS

The Wnt/β-catenin pathway plays a pivotal role in the osteogenic differentiation of MSC towards the osteoblastic lineage, since its activation modulates the expression of *RUNX2*, the main gene regulator of the differentiation process [23]. Considering that protein kinase CK1α negatively regulates Wnt/β-catenin signaling cascade, promoting β-catenin proteasomal degradation [86], we investigated whether CK1α gene silencing could modulate the osteogenic potential differentiation of MSC through β-catenin stabilization.

We performed the experiments using two different MSC cell lines, HS-5 and MSC hTERT. Specifically, we generated two *CSNK1A1* shRNA IPTG inducible MSC cellular clones (through lentiviral particles transduction), called respectively MSC hTERT 6044 and HS-5 6044**.** We carried out a time course of CK1α silencing in both MSC hTERT shRNA 6044 and HS-5 shRNA 6044, through the addition of IPTG 500μM at the culture medium up to 21 days for the HS-5 shRNA 6044 cells and up to 28 days for the MSC hTERT shRNA 6044 cellular clone. Over the time course, expression analysis of *CSNK1A1* and the osteogenic differentiation markers such as *RUNX2*, the master gene regulator of the osteogenic differentiation process and the others later osteogenic markers such as *ALP*, *SPP1* and *BGLAP* was carried out by qRT-PCR. We confirmed the *CSNK1A1* silencing over the time and we observed an upregulation of the different osteogenic markers investigated in both MSC hTERT shRNA 6044 (Fig.23A) and in HS-5 shRNA 6044 (Fig.23B). To evaluate the specificity of the CK1α silencing method used, we treated both MSC hTERT WT and HS-5 WT with IPTG 500μM respectively for 10 days and 7 days, observing no significant changes neither in *CSNK1A1* expression nor in *RUNX2,* excluding possible effects of IPTG *per se* on the expression of the osteogenic differentiation markers analyzed (Fig.23C).

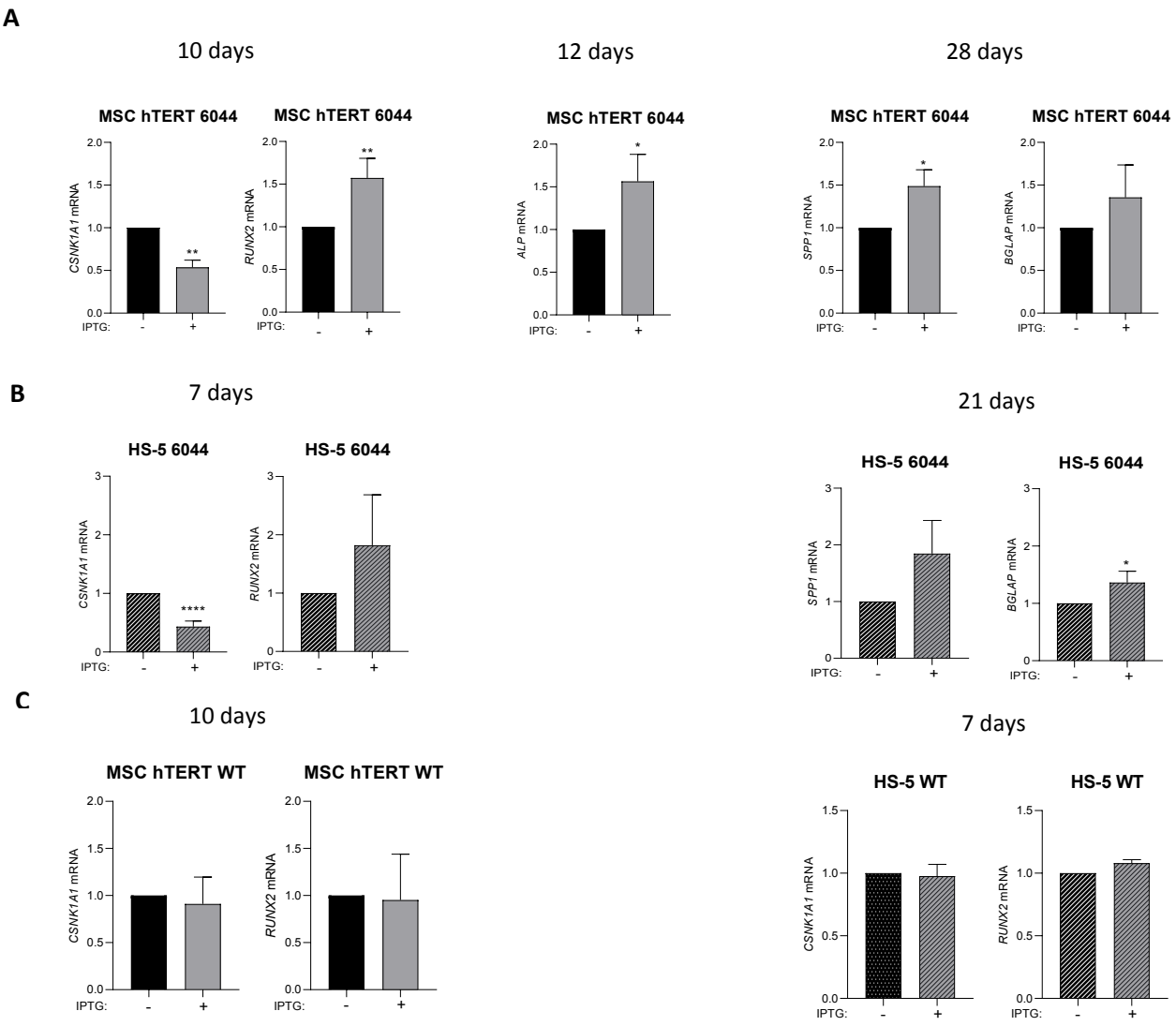

Fig.23 CK1α silencing modulates the expression of osteogenic differentiation markers in MSC hTERT 6044 and HS-5 6044 cell lines.

qRT-PCR analysis of *CSNK1A1*, *RUNX2*, *ALP*, *SPP1*, *BGLAP* mRNA in MSC hTERT 6044 cells (A) and of *CSNK1A1*, *RUNX2*, *SPP1* and *BGLAP* mRNA in HS-5 6044 cells (B) treated with IPTG 500µM over a time course. The different time points of CK1α silencing are indicated in each graph. Analysis of *CSNK1A1* and *RUNX2* after 10 days of IPTG 500µM treatment in MSC hTERT WT cells (C, left panel) and for 7 days in HS-5 WT cells (C, right panel). GAPDH was used as reference gene. Data represent mean± SD of n=8 independent experiments for *RUNX2* and *CSNK1A1* (panel A, left), of n=3 of independent experiments for *RUNX2, CSNK1A1* (panel B, left), *ALP* (panel A, middle), for *SPP1* and *BGLAP* analysis both in MSC hTERT 6044 and in HS-5 6044 cells (panel A/B, right), for *RUNX2 and CSNK1A1* analysis performed as control in panel C. *=p<0.05, ** =p<0.01, ****=p<0.0001 compared to untreated cells.

Since we observed in both MSC hTERT 6044 cells and HS-5 6044 cells an increased m-RNA expression of the potential osteogenic differentiation markers upon CK1α silencing, we next focused the analysis on the β-

catenin expression. Its expression levels were detected by WB analysis at different time points of CK1α silencing.

Surprisingly, CK1α silencing induced an oscillatory expression of β-catenin over the time being increased at 72h of CK1α silencing, reduced upon 6 days of silencing and increased at 8 days of silencing. As reported in Fig.24, the same trend was reproduced also in HS-5 6044.

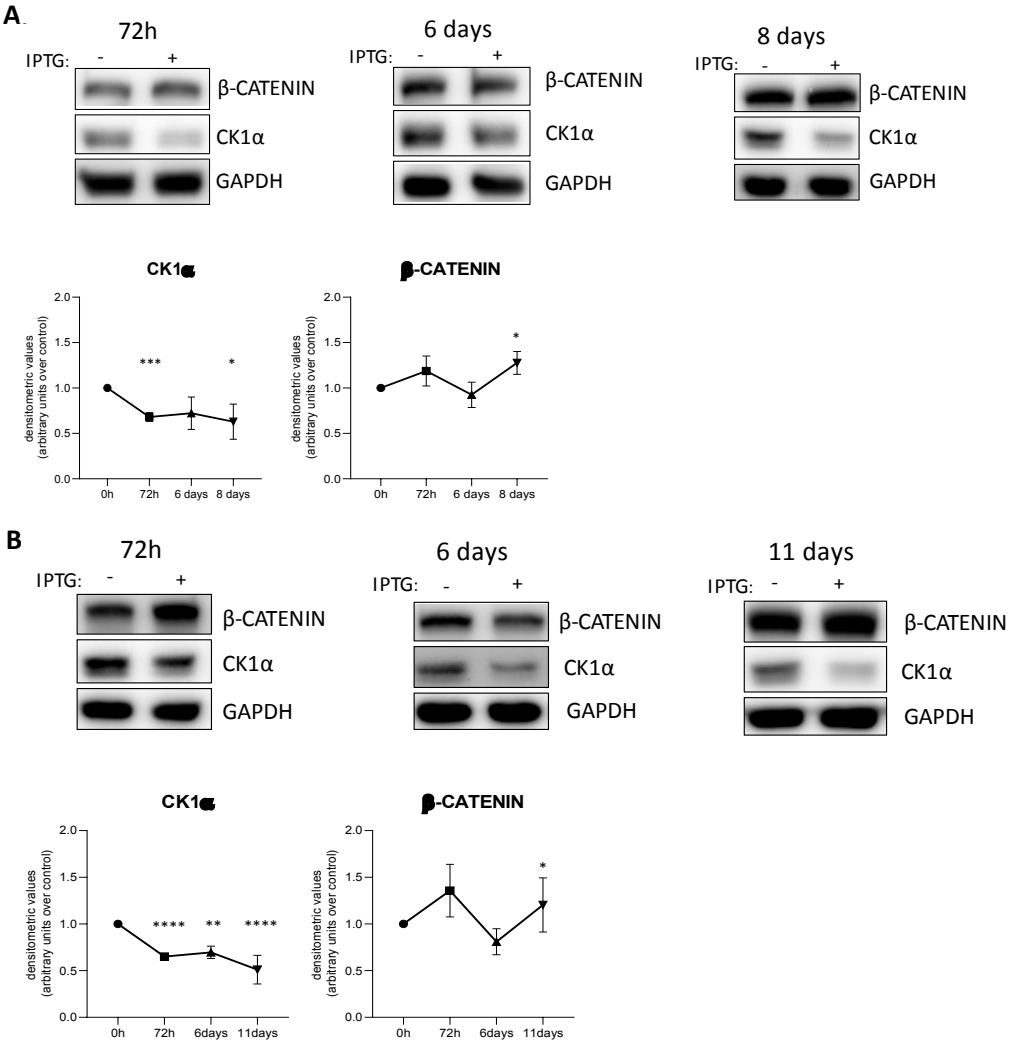

Fig.24 Time course of β-catenin expression levels upon CK1α silencing in MSC hTERT 6044 and HS-5 6044 cell lines. Protein expression of CK1α and β-catenin in MSC cell lines MSC hTERT 6044 (A) and HS-5 6044 (B) treated with IPTG 500µM over a time course. The different time points are indicated in each graph. GAPDH was used as loading control. The figure shows representative WB (A/B, upper panel) and densitometric analysis (A/B, lower panel) expressed as arbitrary units over untreated cells, indicated as mean±SD of n=3 independent experiments for MSC hTERT 6044 (A) and HS-5 6044 (B) cells. *=p<0.05, ** =p<0.01, ***=p<0.001, ****=p<0.0001 compared to untreated cells.

7.2 CK1α SILENCING IN STROMAL CELLS MODULATES OSTEOGENIC DIFFERENTIATION

To confirm the role of CK1α in the differentiation of MSC hTERT 6044 and HS-5 6044 into the osteoblastic lineage, we treated stromal cells with the STEM PRO osteogenic culture medium in CK1α silencing conditions. In detail, both MSC hTERT 6044 and HS-5 6044 were cultured for 7 days with IPTG 500µM to pre-induce CK1α silencing. At the end of the pre-induction period, both cell lines were cultured in the basal medium RPMI (for MSC hTERT 6044)/DMEM (for HS-5 6044) or in STEM PRO for a total of 21 days in the continuous presence of IPTG. The STEM PRO medium contains the supplements needed to induce stromal cells differentiation into the osteogenic lineage. Alizarin Red staining was used to verify the presence of calcium deposits, produced by differentiated cells. In the IPTG-treated cells maintained basal medium conditions, it is possible to observe the presence of initial foci of calcification compared to untreated cells (Fig.25 A/B NT vs IPTG RPMI/DMEM condition). Cells maintained in the osteogenic differentiation medium STEM PRO appeared more calcified compared to the ones in basal medium, as demonstrated by the presence of red calcium deposits (Fig.25 A/B RPMI/DMEM NT vs STEM PRO NT). A clear difference was most evident in MSC hTERT 6044 and HS-5 6044 cells cultured in STEM PRO treated with IPTG where a further increase in calcium deposits was observed compared to STEM PRO only treated cells (Fig.25 A/B STEM PRO NT vs STEM PRO IPTG), pointing to a putative role of CK1α kinase in osteogenic differentiation. As expected, in control MSC hTERT WT and HS-5 WT differences were observed only between cells grown in basal medium compared the STEM PRO condition, while treatment with IPTG was not associated with a marked increase in foci of calcification compared to STEM PRO only treated cells.

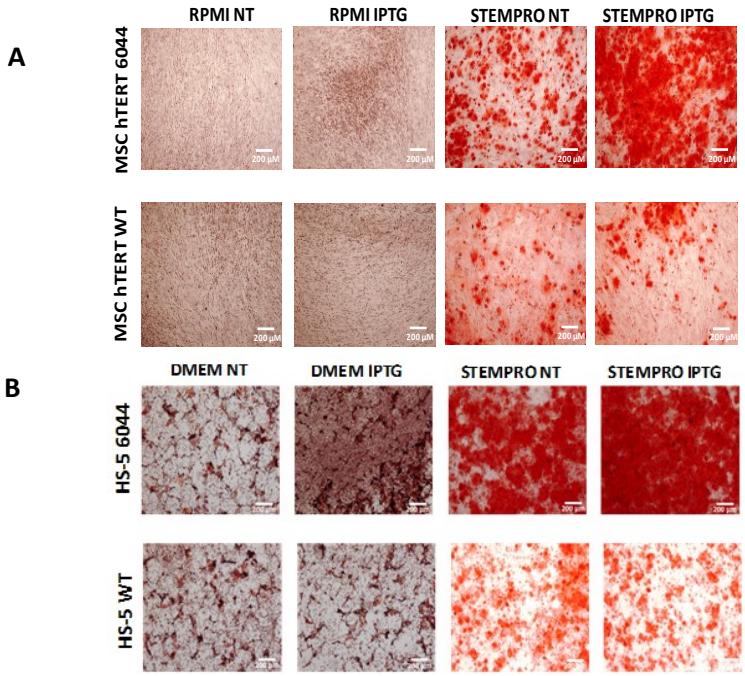

Fig.25 CK1α silencing increases calcium deposits of MSC cell lines pushed to differentiate into the osteoblastic lineage. Alizarin Red staining of MSC hTERT 6044 and HS-5 6044 cellular clones (upper panel A/B) and WT (lower panel A/B), as

control, cultured in RPMI or in STEM PRO osteogenic differentiation medium for 21 days. NT: untreated. Images were obtained by Olympus CKX53 microscopy, objective 4X. Bar size: 200µm.

7.3 WNT/β-CATENIN SIGNALING PATHWAY SUSTAINS RUNX2 EXPRESSION IN STROMAL CELLS

Considering the pivotal role of Wnt/β-catenin pathway in the control of RUNX2 expression in other cells [60] we further investigated Wnt/β-catenin/RUNX2 axis in our experimental model.

We stimulated MSC hTERT and HS-5 cells with Wnt-3A recombinant protein to investigate if RUNX2 expression could be modulated by the activation of Wnt/β-catenin pathway. We seeded both MSC lines and, accordingly to the literature [151], we used Wnt-3A at 200ng/mL for different time points to further detect RUNX2 expression. The analysis of β-catenin and its target gene expression was performed by qRT-PCR and WB.

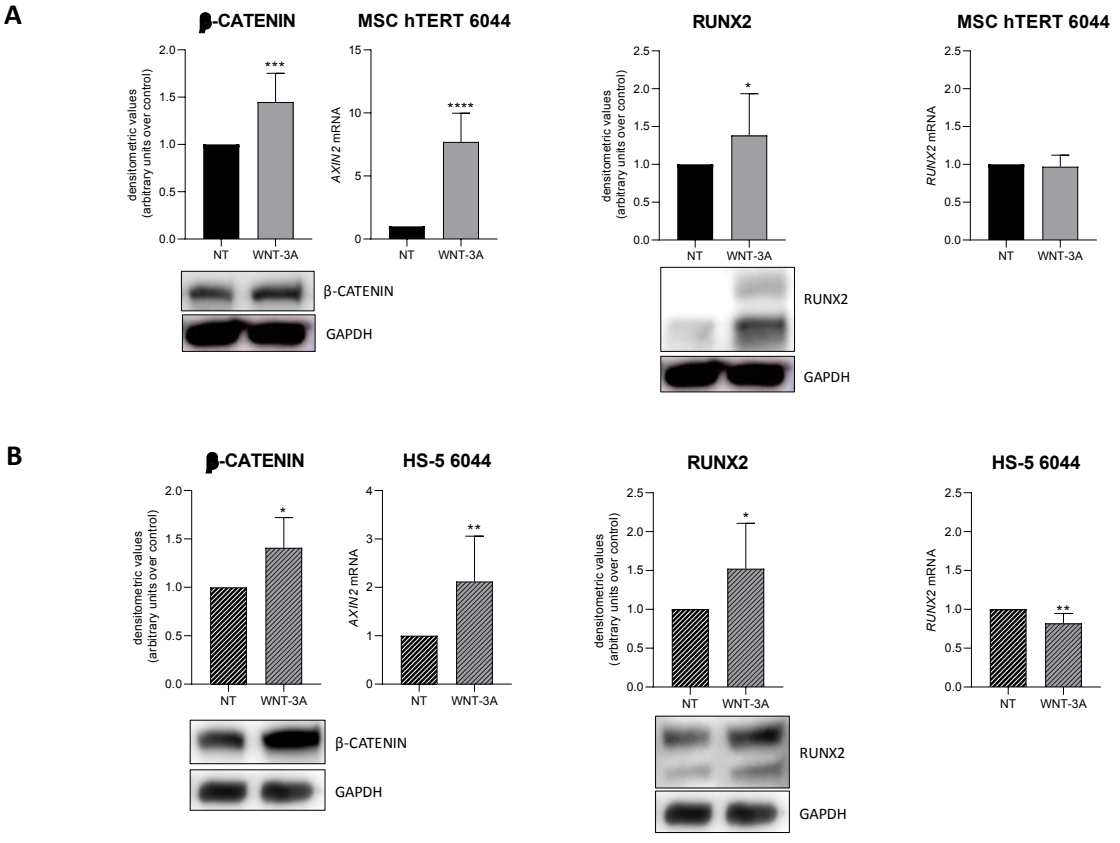

Fig.26 Wnt/ β-catenin pathway stimulation increases RUNX2 expression in MSC lines. Protein expression of β-catenin and RUNX2 in MSC cell lines MSC hTERT 6044 (A) and HS-5 6044 (B) treated with Wnt-3A 200 ng/mL for 8h (A) and 4h (B). GAPDH was used as loading control. The figure shows the representative WB and densitometric analysis expressed as arbitrary units over untreated cells (mean±SD) of n=10 independent experiments for MSC hTERT 6044 (A) and n=7

independent experiments for HS-5 6044 (B) cells. qRT-PCR analysis of *AXIN2* (A/B, left) *RUNX2* mRNA (A/B, right) in MSC hTERT 6044 cells (A) and in HS-5 6044 cells (B) treated with Wnt-3A at the same concentration and time reported above. GAPDH was used as housekeeping gene. Data represent mean± SD of n=9 independent experiments for MSC hTERT 6044 and n=7 independent experiments for HS-5 6044 (B) cells *=p<0.05, ** =p<0.01, ***=p<0.001, ****=p<0.0001 compared to untreated cells.

We confirmed the Wnt/β-catenin signaling cascade activation in both MSC cell lines through the increased protein expression of β-catenin and its downstream target *AXIN2* (Fig.26 A/B, left).
Regarding RUNX2 analysis, after 8h of Wnt-3A treatment in MSC hTERT 6044 cells and after 4h in HS-5 6044 cells, RUNX2 protein expression was increased (Fig.26 A/B, middle). On the contrary, at the same points for both MSC cell lines, surprisingly, the transcriptional levels of *RUNX2* were unchanged in MSC hTERT 6044 cells or slightly reduced in HS-5 6044 cells (Fig.26 A/B, right). It has been demonstrated a transcriptional autoregulation loop of *RUNX2* gene, upon overexpression of RUNX2 protein, able to downregulate its promoter activity, inhibiting its transcription [59]. In light of this RUNX2 autoregulation feedback loop, in our model the enforced RUNX2 protein expression may be therefore sufficient to block *RUNX2* transcriptional activity, especially in HS-5 6044 cells, where the RUNX2 protein was increased of 52% compared to untreated cells (Fig.26 A, middle).
Nevertheless, our data confirmed the central role of Wnt/β-catenin pathway in the control of RUNX2 expression, thus the involvement of this signaling cascade in the osteogenic differentiation also in our experimental model.

7.4 ROLE OF CK1α IN THE PLASMA CELL-STROMAL CELL CROSS TALK IN A BONE MARROW MICROENVIRONMENTAL MODEL

To deeply investigate whether CK1α could regulate osteoblastogenesis in the context of MMABD, we reproduced a bone marrow microenvironment model by co-culturing the IL-6 dependent INA-6 cells and the stromal cell lines MSC hTERT or HS-5 as a feeder layer. In particular, we created three different models of co-culture in which CK1α silencing was achieved in the MM compartment (model 1), in the MSC compartment (model 2) or in both populations (model 3), as represented in Fig.20 (chapter material and methods).
Considering that RUNX2 expression in MM cells sustains cell survival and tumor progression, leading to a worse aggressive phenotype of MMABD [46], we asked whether CK1α silencing, in the different models of co-culture, could modulate RUNX2 expression both in MM cells and in the stromal counterpart.

The stromal compartment was reproduced using MSC hTERT cells GFP or HS-5 cells mcherry as reported in Fig.27. The GFP or mcherry fluorescence in the stromal cells allowed to purify and obtain MSC and MM pure populations from each model of co-culture, by fluorescence activated cell sorting.

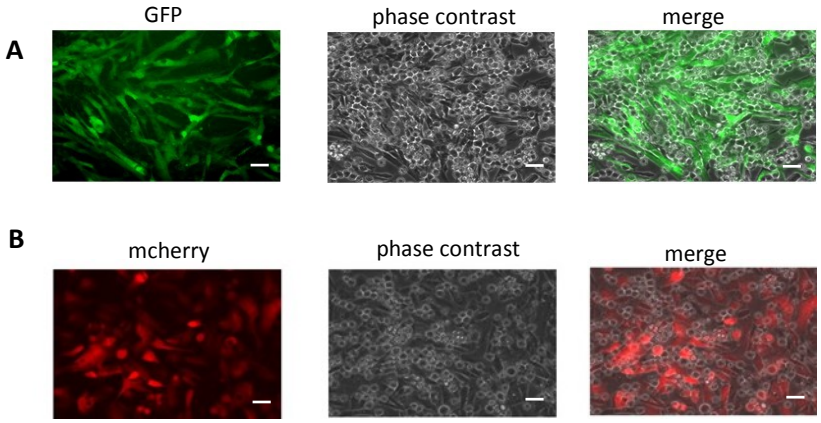

Fig.27 Microscopy analysis of INA-6/stromal cells models of co-culture. Images of MSC hTERT GFP+ (upper panel) and HS-5 mcherry+ cells (lower panel) co-cultured with INA-6 MM cells (phase contrast, middle panel). Images were obtained by Olympus CKX53 microscopy, objective 4X. Bar size: 200 µm.

- **MODEL 1**

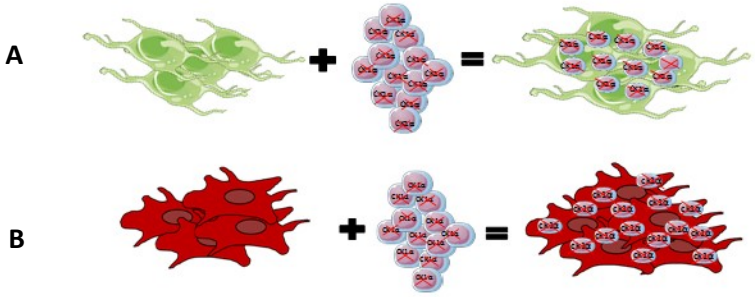

In the first model of co-culture, we investigated whether CK1α silencing in MM cells could overcome the microenvironment dependent protection of MSC and could regulate *RUNX2* gene expression in MM or stromal cell population. CK1α-deficient INA-6 6044 cells, pre silenced 7 days for CK1α through the addition of IPTG to the culture medium, were subsequently cultured on MSC hTERT WT or HS-5 WT for 3 days, in the continuous presence of CK1α silencing. After the harvest, MSC and MM pure populations were obtained through fluorescence activated cell sorting of GFP (A) or mcherry (B) which are expressed in the stromal compartment. The figure above shows a scheme of the experimental design.

MODEL 1.A CK1α-deficient INA-6 6044 cells co-cultured with CK1α-proficient MSC hTERT WT.

In model 1.A we observed that RUNX2 mRNA and protein expression in MM plasma cells was controlled by CK1α through β-catenin levels. Indeed, both β-catenin and RUNX2 protein levels were reduced in the CK1α silenced MM cells (Fig.28). On the contrary, in the MSC hTERT WT counterpart, while CK1α expression was not affected, RUNX2 mRNA levels were increased, with a trend towards upregulation both for β-catenin and RUNX2 protein expression (Fig.29).

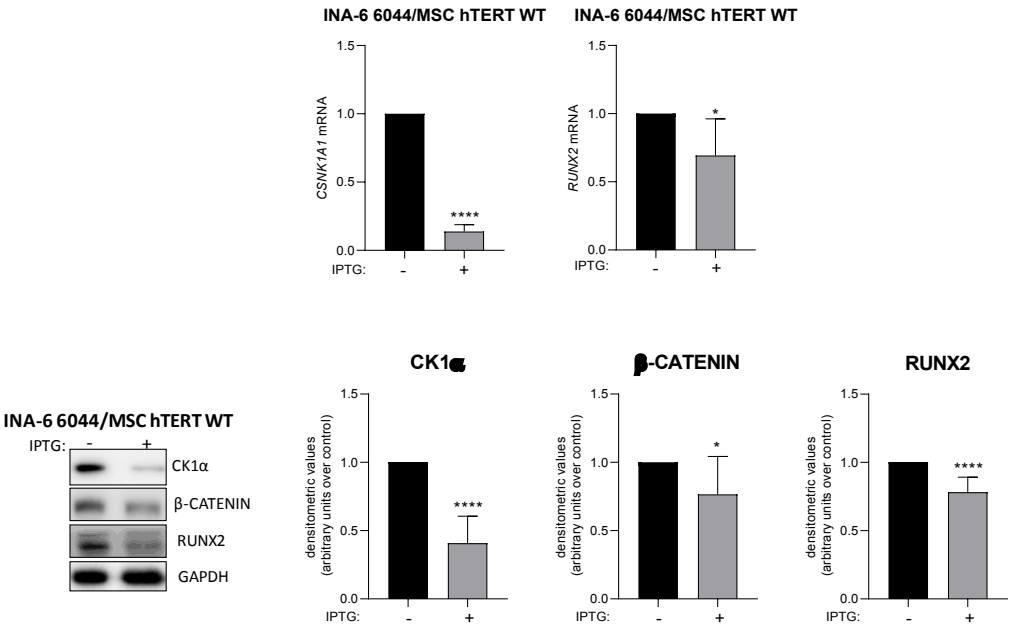

Fig.28 CK1α silencing in INA-6 plasma cells regulates the expression levels of RUNX2 in MM cells in a co-culture model with MSC hTERT. qRT-PCR analysis (upper panel) of *CSNK1A1* and *RUNX2* mRNA in INA-6 6044 (INA-6 6044/MSC hTERT WT) silenced for *CSNK1A1* by treatment with IPTG 500μM for 1 week and subsequently grown on a feeder layer of MSC hTERT WT in the continuous presence of IPTG for additional 3 days. GAPDH was used as housekeeping gene. Data represent mean±SD of n=6 independent experiments. The lower panel shows the representative WB (left) and densitometric analysis (right) of CK1α, β-catenin and RUNX2 proteins expressed as arbitrary units over untreated cells (mean±SD) of n=8 independent experiments. GAPDH was used as loading control. *=p<0.05, ****=p<0.0001 compared to untreated cells.

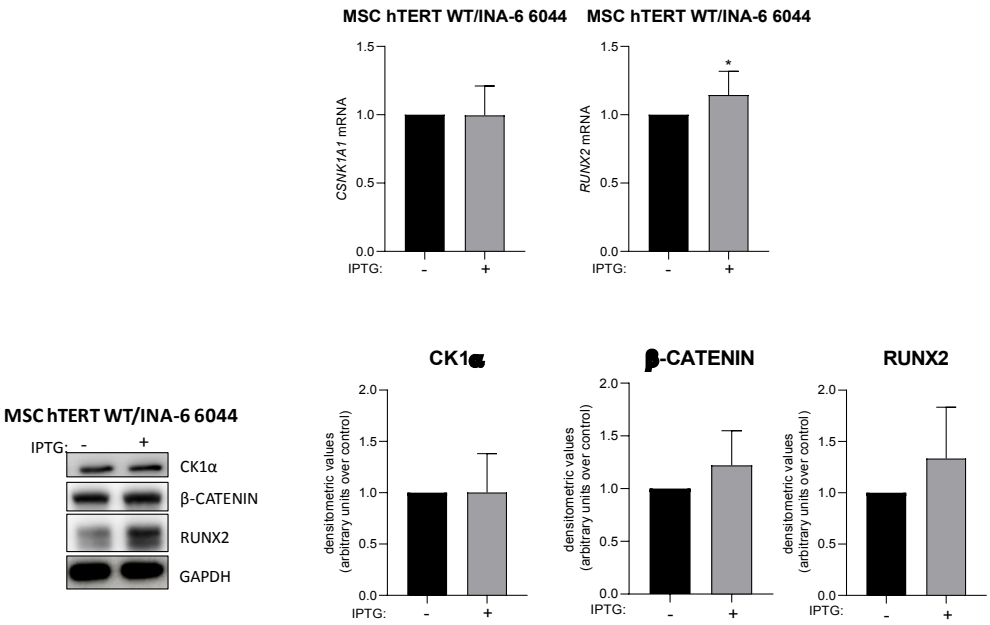

Fig.29 CK1α silencing in INA-6 plasma cells regulates the expression levels of RUNX2 in MSC in a co-culture model with MSC hTERT. qRT-PCR analysis (upper panel) of *CSNK1A1* and *RUNX2* mRNA in stromal cells MSC hTERT WT (MSC hTERT WT/INA-6 6044) cells co-cultured with CK1α silenced INA-6 6044 as described in Fig.28 legend. GAPDH was used as housekeeping gene. Data represent mean± SD of n=11 independent experiments. The lower panel shows the representative WB (left) and densitometric analysis (right) of CK1α, β-catenin and RUNX2 (lower panel) expressed as arbitrary units over untreated cells (mean±SD) of at least n=6 independent experiments. GAPDH was used as loading control. MSC hTERT WT pure population was obtained through cell sorting of GFP which is expressed in MSC hTERT WT cells. *=p<0.05 compared to untreated cells.

MODEL 1.B CK1α-deficient INA-6 6044 cells co-cultured with CK1α-proficient HS-5 WT.

Oppositely from model 1.A, in model 1.B we observed that CK1α silencing in INA-6 6044 cells co-cultured with HS-5 WT stromal cells (instead of MSC hTERT) upregulated β-catenin protein and RUNX2 mRNA expression in MM plasma cells (Fig.30). On the contrary, in the HS-5 WT counterpart, which as expected did not show any differences in CK1α levels, β-catenin and RUNX2 expression was slightly reduced (Fig.31).

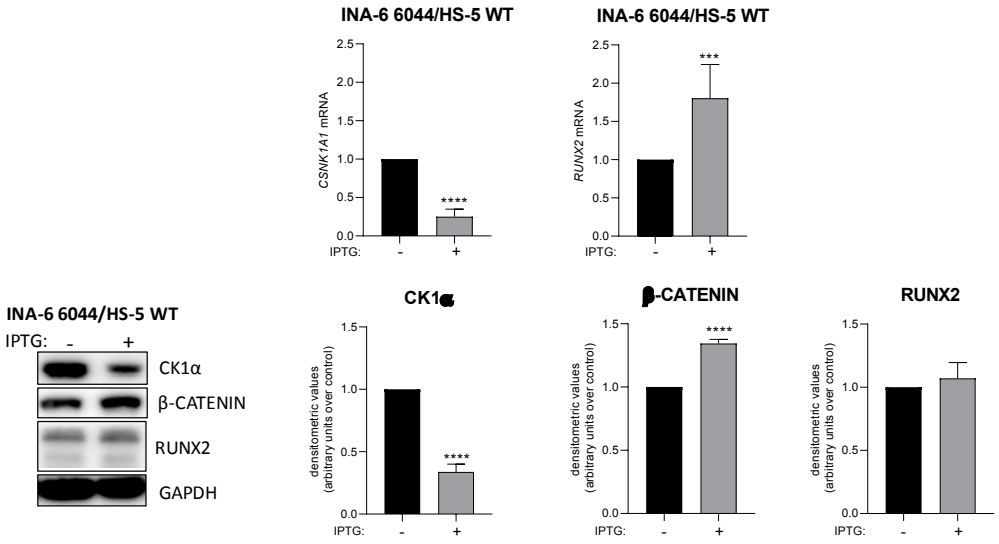

Fig.30 CK1α silencing in INA-6 plasma cells regulates the expression levels of RUNX2 in MM cells in a co-culture model with HS-5 cells. qRT-PCR analysis (upper panel) of *CSNK1A1* and *RUNX2* mRNA in plasma cells INA-6 6044 (INA- 6044/HS-5 WT) silenced for *CSNK1A1* by treatment with IPTG 500μM for 1 week and subsequently grown on a feeder layer of HS-5 WT cells in the continuous presence of IPTG for 3 days. GAPDH was used as housekeeping gene. Data represent mean± SD of n=7 independent experiments. The lower panel shows the representative WB (left) and densitometric analysis (right) of CK1α, β-catenin and RUNX2 expressed as arbitrary units over untreated cells (mean±SD) of n=3 independent experiments. GAPDH has been used as loading control. ***=p<0.001, ****=p<0.0001 compared to untreated cells.

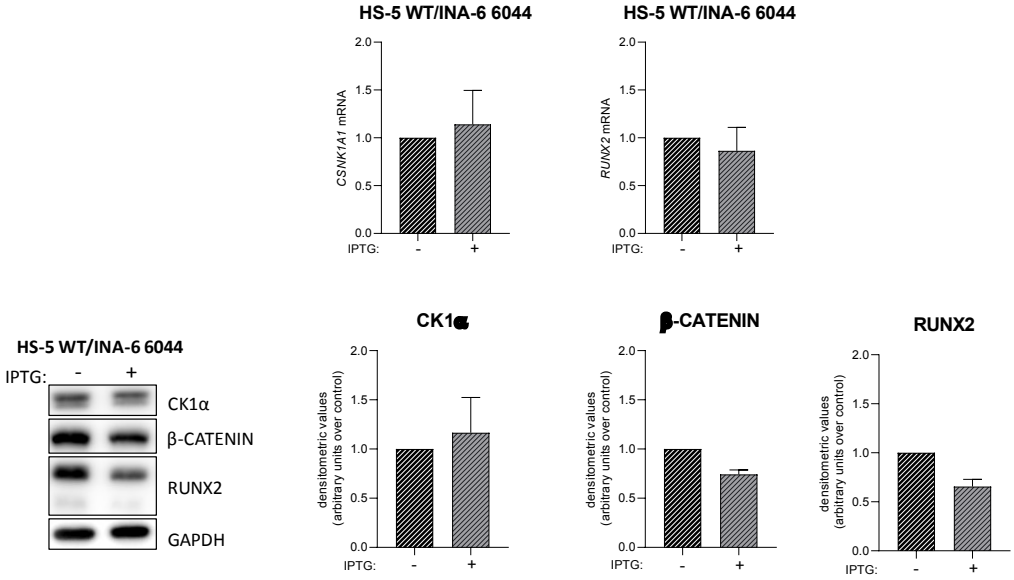

Fig.31 CK1α silencing in INA-6 plasma cells regulates the expression levels of RUNX2 in MSC in a co-culture model with HS-5 cells. qRT-PCR analysis (upper panel) of *CSNK1A1* and *RUNX2* mRNA in stromal cells HS-5 WT (HS-5 WT/INA-6 6044) co-cultured with CK1α silenced INA-6 cells as described in Fig.30 legend. GAPDH was used as housekeeping gene. Data represent the mean± SD of n=5 independent experiments. The lower panel shows the representative WB

(left) and densitometric analysis (right) of CK1α, β-catenin and RUNX2 expressed as arbitrary units over untreated cells (mean±SD) of n=2 independent experiments. GAPDH was used as loading control. HS-5 WT pure population was obtained through cell sorting of mcherry which is expressed in HS-5 WT cells.

- **MODEL 2**

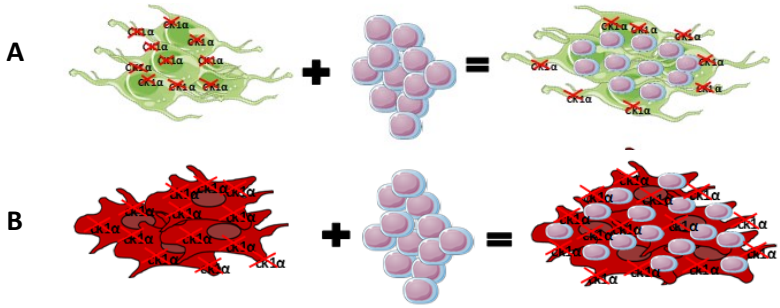

In the second model of co-culture, CK1α-proficient INA-6 WT cells were cultured on a feeder layer of CK1α-deficient MSC hTERT 6044 or HS-5 6044 stromal cells, previously silenced for 7 days with the addition of IPTG 500µM to the culture medium. CK1α silencing was maintained during the whole co-cultured period. After 3 days of co-culture, analysis was performed on the two cell populations (plasma cells and stromal cells) harvested through cell sorting considering the expression of GFP (A) or mcherry (B) protein in the stromal compartment. The figure above shows a scheme of the experimental design.

MODEL 2.A CK1α-proficient INA-6 WT cells co-cultured with CK1α-deficient MSC hTERT 6044 cells.

In this model, as expected, we did not observed any changes in CK1α mRNA expression in INA-6 WT cells. Consequently, also any transcriptional variation in *RUNX2* expression in MM compartment was not detected. (Fig.32 upper panel). Surprisingly, CK1α protein expression in CK1α proficient INA-6 WT was decreased. Accordingly, both β-catenin and RUNX2 protein expression was reduced (Fig.32, lower panel), as observed in the model 1.A where CK1α protein reduction in MM cells led to decreased β-catenin and RUNX2.

Focusing on the stromal compartment, we confirmed CK1α silencing of about 67% at the mRNA and 54% at protein level (Fig.33), which led to a reduction of RUNX2 mRNA level, but surprisingly not at the protein level. Indeed, RUNX2 protein levels were increased of the 68% compared to untreated cells while β-catenin protein levels were reduced of about 33% (Fig.33, lower panel). This result is in line with the previous data shown in Fig.26 where it seemed that high levels of RUNX2 protein were sufficient to block its transcriptional expression. Oppositely, for the first time a reduced expression of β-catenin, not in line with RUNX2 protein upregulation, was observed.

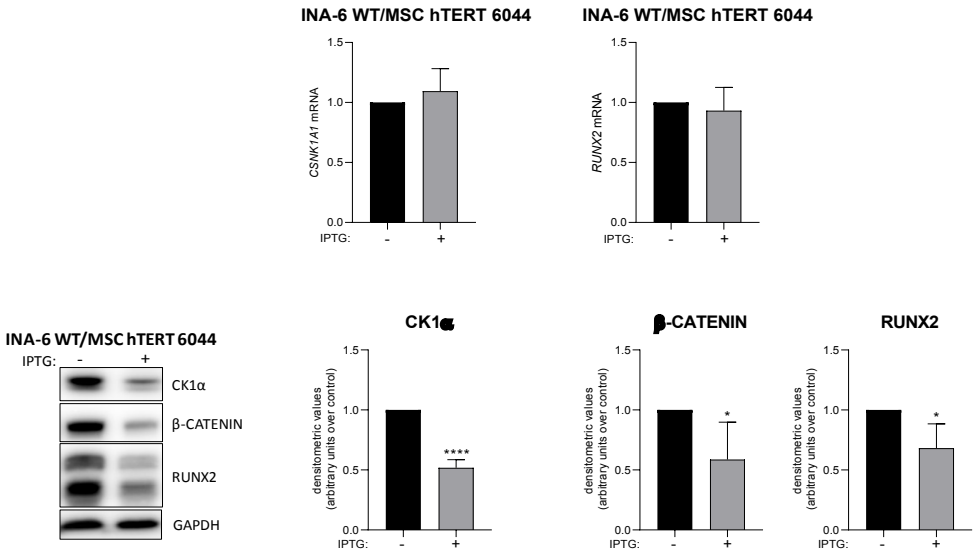

Fig.32 CK1α silencing in MSC hTERT in a co-culture model with CK1α-proficient INA-6 WT regulates the expression levels of RUNX2 in MM cells. qRT-PCR analysis (upper panel) of *CSNK1A1* and *RUNX2* mRNA in CK1α-proficient INA-6 WT (INA-6 WT/MSC hTERT 6044) co-cultured with CK1α-deficient MSC hTERT 6044 (silenced for *CSNK1A1* by treatment with IPTG 500μM for 1 week and subsequently used as a feeder layer for INA-6 WT in the continuous presence of IPTG for additional 3 days). GAPDH was used as housekeeping gene. Data represent mean± SD of n=6 independent experiments. The lower panel shows the representative WB (left) and densitometric analysis (right) of CK1α, β-catenin and RUNX2 expressed as arbitrary units over untreated cells (mean±SD) of n=4 independent experiments. GAPDH has been used as loading control.*=p<0.05, ****=p<0.0001 compared to untreated cells.

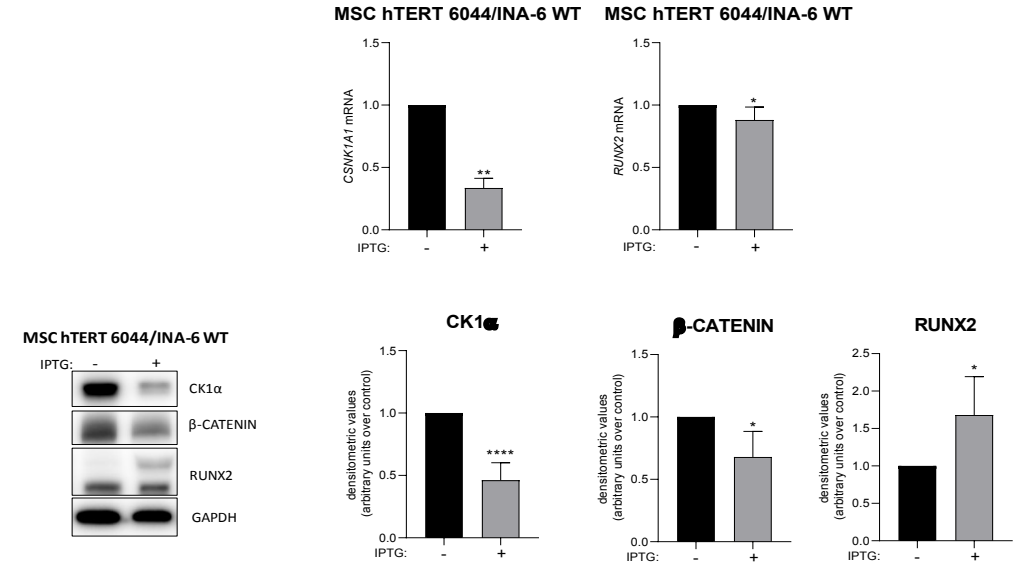

Fig.33 CK1α silencing in MSC hTERT in a co-culture model regulates the expression levels of RUNX2 in MSC. qRT-PCR analysis (upper panel) of *CSNK1A1* and *RUNX2* mRNA in CK1α-deficient MSC hTERT 6044 (MSC hTERT 6044/INA-6 WT) co-cultured with CK1α-proficient INA-6 WT as described in Fig. 32 legend. GAPDH was used as housekeeping gene. Data represent mean± SD of n=6 independent experiments. The lower panel shows the representative WB (left) and

densitometric analysis (right) of CK1α, β-catenin and RUNX2 expressed as arbitrary units over untreated cells (mean±SD) of n=4 independent experiments. GAPDH has been used as loading control. MSC hTERT 6044 pure population was obtained through cell sorting of GFP which is expressed in MSC hTERT 6044 cells. *=p<0.05 **=p<0.01, ****=p<0.0001 compared to untreated cells.

MODEL 2.B CK1α-proficient INA-6 WT cells co-cultured with CK1α-deficient HS-5 6044 cells.

Oppositely from MODEL 2.A, we observed that CK1α silencing in a different model of stromal cells, the HS-5 6044 co-cultured with INA-6 WT MM cells, upregulated *RUNX2* gene expression in INA-6 WT cells (Fig.34 upper panel) without significantly affecting CK1α expression in plasma cells. Consistently, a trend towards increase in β-catenin and a statistically significant upregulation of RUNX2 protein was observed, even if the increase in protein levels was lower than what observed at the transcriptional level (Fig. 32 lower panel). In CK1α-deficient HS-5 6044 cells no significant changes were detected in β-catenin levels, but a trend towards reduction in RUNX2 expression was observed (Fig.35).

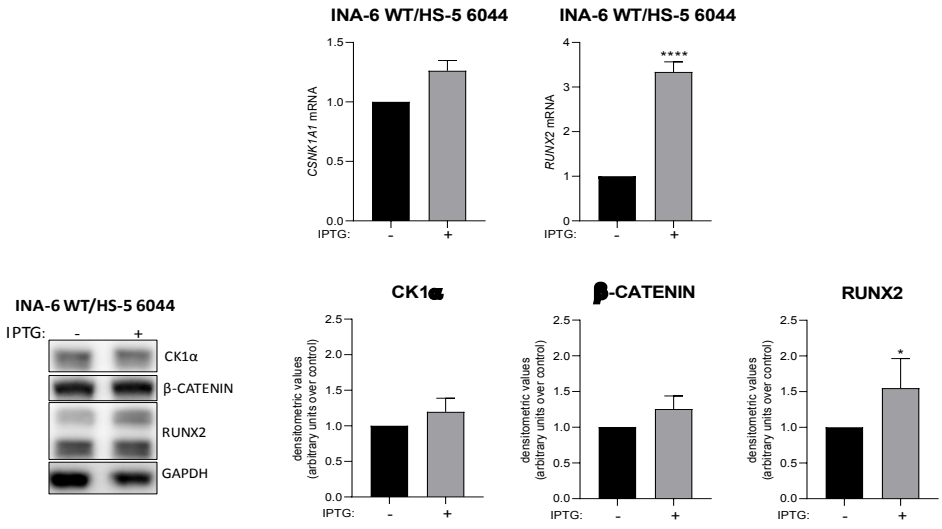

Fig.34 CK1α silencing in HS-5 cells in a co-culture model with INA-6 WT regulates the expression levels of RUNX2 in MM cells. qRT-PCR analysis (upper panel) of *CSNK1A1* and *RUNX2* mRNA in CK1α-proficient INA-6 WT (INA-6 WT/HS-5 6044) co-cultured with CK1α-deficient HS-5 6044 (silenced for *CSNK1A1* through IPTG 500μM treatment for 1 week and subsequently used as a feeder layer for INA-6 WT cells in the continuous presence of IPTG for another 3 days). GAPDH was used as housekeeping gene. Data represent mean± SD of n=3 independent experiments. The lower panel shows the representative WB (left) and densitometric analysis (right) of CK1α, β-catenin and RUNX2 expressed as arbitrary units over untreated cells (mean±SD) of n=3 independent experiments. GAPDH has been used as loading control.*=p<0.05, ****=p<0.0001 compared to untreated cells.

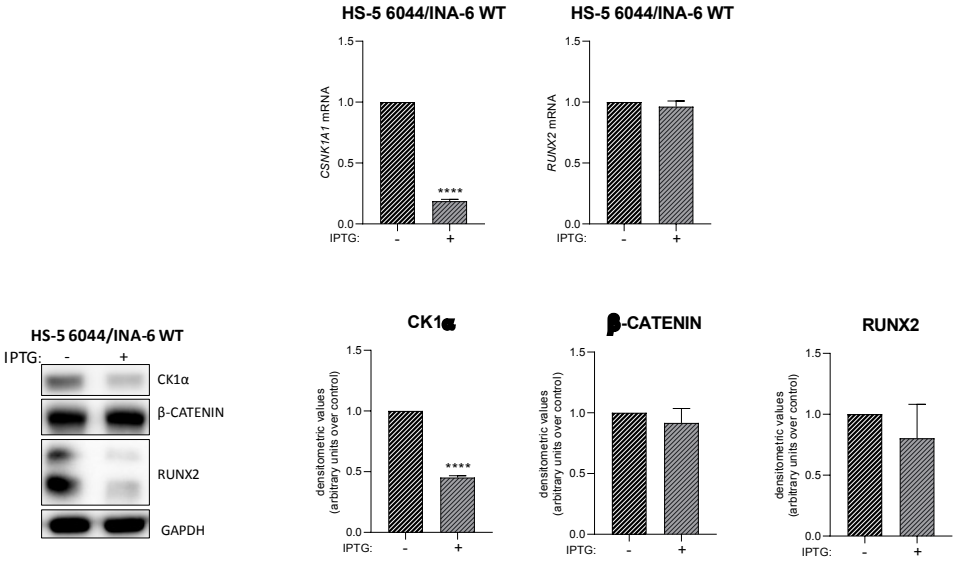

Fig.35 CK1α silencing in HS-5 in a co-culture model with INA-6 WT cells regulates the expression levels of RUNX2 in MSC cells. qRT-PCR analysis (upper panel) of *CSNK1A1* and *RUNX2* mRNA in CK1α-deficient HS-5 6044 (HS-5 6044/INA-6 WT) co-cultured with CK1α-proficient INA-6 WT as described in Fig.34 legend. GAPDH was used as housekeeping gene. Data represent mean± SD of n=3 independent experiments. The lower panel shows the representative WB (left) and densitometric analysis (right) of CK1α, β-catenin and RUNX2 expressed as arbitrary units over untreated cells (mean±SD) of n=3 independent experiments. GAPDH has been used as loading control. HS-5 6044 pure population was obtained through cell sorting of mcherry which is expressed in HS-5 6044 cells. ****=p<0.0001 compared to untreated cells.

- **MODEL 3**

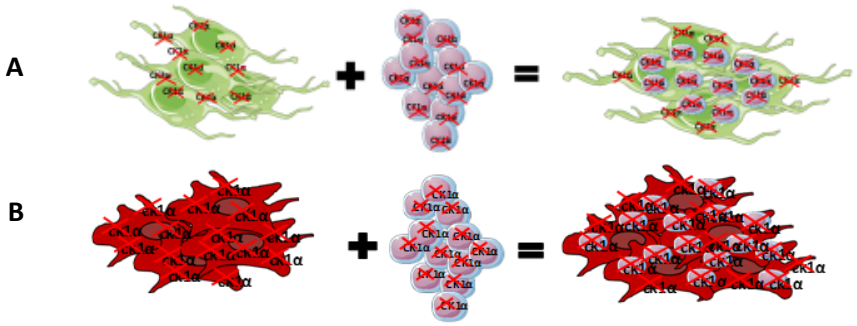

In the third model of co-culture, we investigated if CK1α silencing both in plasma cells and in the stromal compartment could regulate RUNX2 gene expression in both cell populations. The INA-6 6044 cells and the stromal cells MSC hTERT 6044 or HS-5 6044 have been pre silenced 7 days for CK1α through the addition of IPTG 500μM at the culture medium. After 1 week of pre-induction, the cells populations were co-cultured for additional 3 days, keeping CK1α silencing until the harvesting. After the harvest, MSC and MM pure

populations were obtained through fluorescence activated cell sorting of GFP (A) or mcherry (B) which are expressed in the stromal compartment. Figure above shows a scheme of the experimental design.

MODEL 3.A CK1α-deficient INA-6 6044 cells co-cultured with CK1α-deficient MSC hTERT 6044 cells.

In this model, as expected *CSNK1A1* silencing was obtained both in INA-6 6044 cells and in the stromal compartment MSC hTERT 6044 (Fig.36, 37). Unexpectedly, β-catenin was increased in CK1α-deficient INA-6 6044 leading to augmented RUNX2 expression both at mRNA and at protein levels (Fig.36). In the MSC hTERT stromal counterpart *RUNX2* mRNA expression was moderately upregulated, but this increment did not seem to translate into protein upregulation. A slightly decrease β-catenin expression was instead observed upon CK1α silencing (Fig.37).

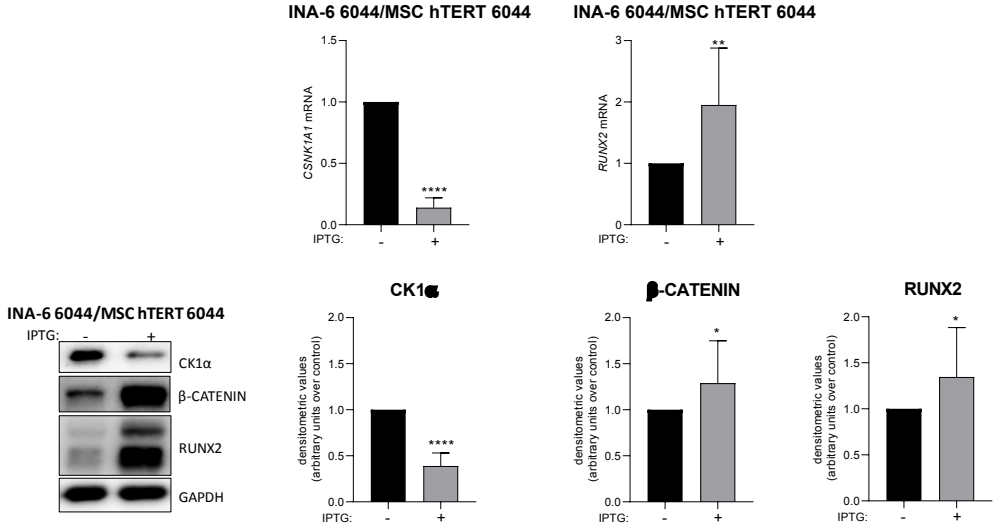

Fig.36 CK1α silencing in both INA-6 and MSC hTERT cells co-cultured regulates the expression levels of RUNX2 in MM cells. qRT-PCR analysis (upper panel) of *CSNK1A1* and *RUNX2* mRNA in CK1α-deficient INA-6 6044 (INA-6 6044/MSC hTERT 6044) silenced for *CSNK1A1* treated with IPTG 500μM for 1 week and subsequently cultured on a feeder layer of CK1α-deficient stromal cells MSC hTERT 6044 (silenced for *CSNK1A1* in the same manner of INA-6 6044) in the continuous presence of IPTG for additional 3 days of co-culture. GAPDH was used as housekeeping gene. Data represent mean± SD of n=13 independent experiments. The lower panel shows the representative WB (left) and densitometric analysis (right) of CK1α, β-catenin and RUNX2 (expressed as arbitrary units over untreated cells (mean±SD) of n=11 independent experiments. GAPDH has been used as loading control. *=p<0.05, **=p<0.01, ****=p<0.0001 compared to untreated cells.

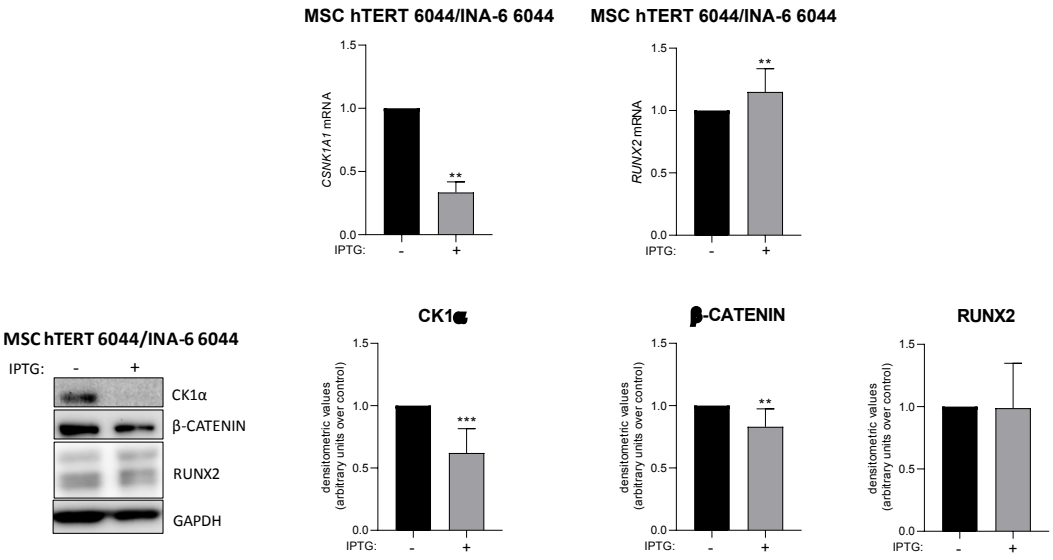

Fig.37 CK1α silencing in both INA-6 and MSC hTERT co-cultured regulates the expression levels of RUNX2 in MSC cells. qRT-PCR analysis (upper panel) of *CSNK1A1* and *RUNX2* mRNA in CK1α-deficient MSC hTERT 6044 (MSC hTERT 6044/INA-6 6044) silenced for *CSNK1A1* treated with IPTG 500μM for 1 week and subsequently used as a feeder layer for CK1α-deficient INA-6 6044 (silenced for *CSNK1A1* in the same manner of MSC hTERT 6044) in the continuous presence of IPTG for additional 3 days of co-culture. GAPDH was used as housekeeping gene. Data represent mean± SD of n=13 independent experiments. The lower panel shows the representative WB (left) and densitometric analysis (right) of CK1α, β-catenin and RUNX2 (lower panel) expressed as arbitrary units over untreated cells (mean±SD) of n=7 independent experiments. GAPDH has been used as loading control. MSC hTERT 6044 pure population was obtained through cell sorting of GFP which is expressed in MSC hTERT 6044 cells. **=p<0.01, ***=p<0.001 compared to untreated cells.

MODEL 3.B CK1α-deficient INA-6 6044 cells co-cultured with CK1α-deficient HS-5 6044 cells.

In this model we used the stromal cell line HS-5 instead of MSC hTERT. CK1α silencing in the co-culture between INA-6 6044 and HS-5 6044 was performed as described for model 3.A. Both *CSNK1A1* mRNA and protein expression were reduced in all the cell populations analyzed (Fig.38, 39). In contrast to the data obtained in the model 3.A, in which the stromal cells used were hTERT 6044 cells, both RUNX2 and β-catenin expression were decreased in plasma cells (Fig.38). Moreover, in the stromal counterpart, a trend towards increase of β-catenin led to RUNX2 mRNA and protein upregulation (Fig.39).

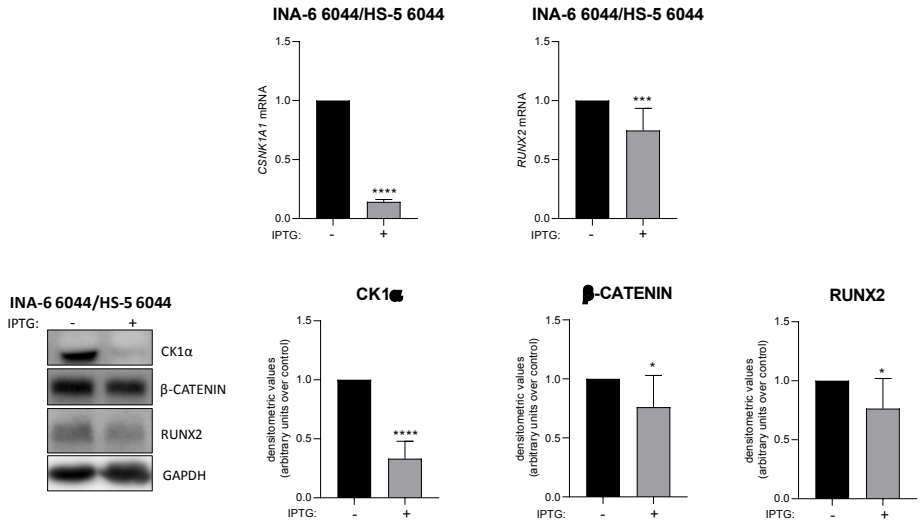

Fig.38 CK1α silencing in both INA-6 and HS-5 co-cultured regulates the expression levels of RUNX2 in MM cells. qRT-PCR analysis (upper panel) of *CSNK1A1* and *RUNX2* mRNA in CK1α-deficient INA-6 6044 (INA-6 6044/HS-5 6044) silenced for *CSNK1A1* by treatment with IPTG 500μM for 1 week and subsequently cultured on a feeder of CK1α-deficient stromal cells HS-5 6044 (silenced for *CSNK1A1* in the same manner of INA-6 6044) in the continuous presence of IPTG for additional 3 days of co-culture. GAPDH was used as housekeeping gene. Data represent mean± SD of n=10 independent experiments. The lower panel shows the representative WB (left) and densitometric analysis (right) of CK1α, β-catenin and RUNX2 expressed as arbitrary units over untreated cells (mean±SD) of at least n=7 independent experiments. GAPDH has been used as loading control.*=p<0.05, ***=p<0.001, ****=p<0.0001 compared to untreated cells.

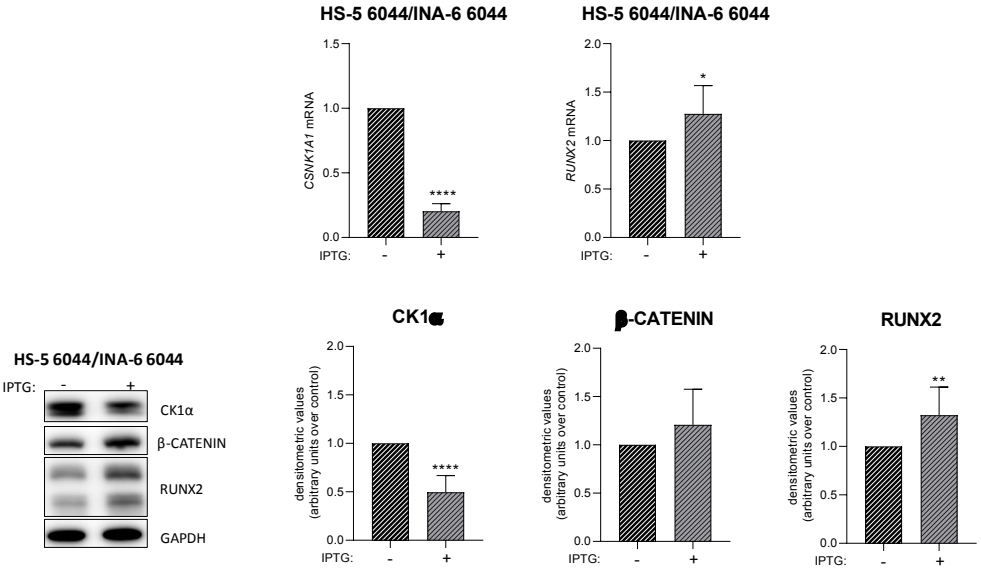

Fig.39 CK1α silencing in both INA-6 and HS-5 co-cultured regulates the expression levels of RUNX2 in MSC cells. qRT-PCR analysis (upper panel) of *CSNK1A1* and *RUNX2* mRNA in CK1α-deficient HS-5 6044 (HS-5 6044/INA-6 6044) silenced for *CSNK1A1* by treatment with IPTG 500μM for 1 week and subsequently used as a feeder layer for CK1α-deficient INA-6 6044 plasma cells (silenced for *CSNK1A1* in the same manner of HS-5 6044) in the continuous presence of IPTG. GAPDH

was used as housekeeping gene. Data represent mean± SD of n=8 independent experiments. The lower panel shows the representative WB (left) and densitometric analysis (right) of CK1α, β-catenin and RUNX2 expressed as arbitrary units over untreated cells (mean±SD) of at least n=7 independent experiments. GAPDH has been used as loading control. HS-5 6044 pure population was obtained through cell sorting of mcherry which is expressed in HS-5 6044 cells. *=p<0.05, **=p<0.01, ****=p<0.0001 compared to untreated cells.

For each model of co-culture, appropriate controls were performed. In particular, we investigated in the co-culture model between CK1α-proficient INA-6 WT cells and CK1α-proficient MSC hTERT WT or CK1α-proficient HS-5 WT cells whether IPTG addition could induce *per se* significant changes in RUNX2 expression in both cells populations as expected. As expected, IPTG did not induce CK1α silencing neither in stromal cell WT nor in INA-6 WT population without causing any changes in RUNX2 expression (data not shown). A schematic representation of the results obtained in all the three models tested is summarized in Fig. 40.

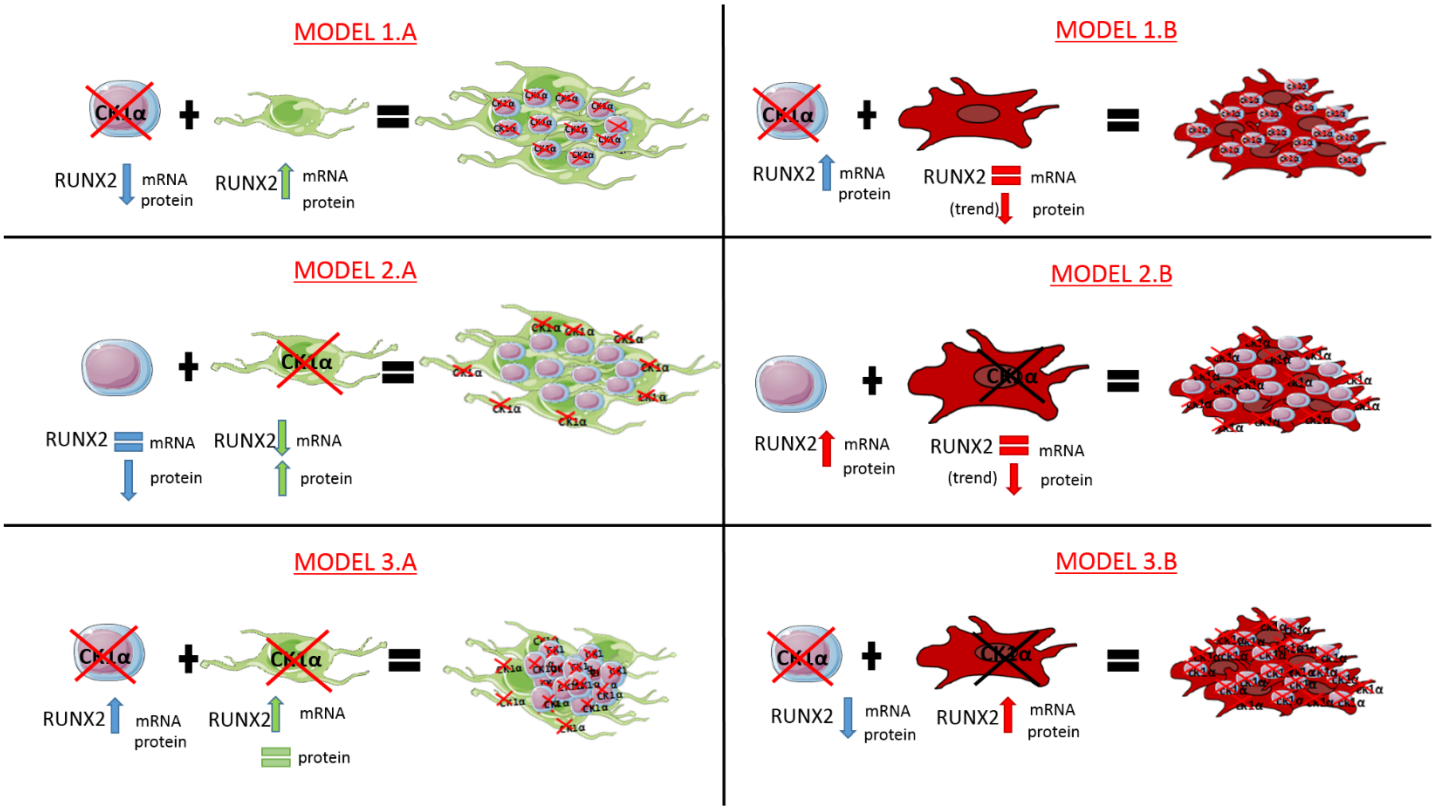

Fig. 40 Schematic representation of the results obtained on RUNX2 expression both in plasma cells and in stromal cells in each model of co-culture performed.

To better investigate the role of CK1α silencing in model 3.A of co-culture and to explain the unexpected high boost of RUNX2 expression in plasma cells after co-silencing CK1α in the MM cells and in MSC hTERT population, we decided to reproduce the same experiment by using a transwell system as described in Fig.21 (chapter material and methods). The transwell tool prevents cell-to cell contact between MM cells and stromal cells in the co-culture, allowing their cross-talk only through the soluble factors released in the

medium. Reproducing the same experimental protocol of the model 3, but with the introduction of the transwell, we investigated RUNX2 expression in CK1α-deficient INA-6 6044 cells and in CK1α-deficient MSC hTERT 6044 co-cultured. As reported in Fig.41, CK1α silencing in MM cells and in stromal compartments was confirmed. Surprisingly, *RUNX2* gene expression was significantly decreased in plasma cells, in contrast to its upregulation observed in Fig.36 when cell-to cell contact was preserved. Moreover, also the *RUNX2* transcriptional activity in MSC was mildly reduced (Fig.41) with an opposite trend compared to the data shown in Fig.37 (upper panel). These opposite results obtained avoiding MSC-MM cell contact could suggest the importance of the physical cell interactions established in the BM *niche,* in the control of RUNX2 expression both in MM cells and in MSC cells.

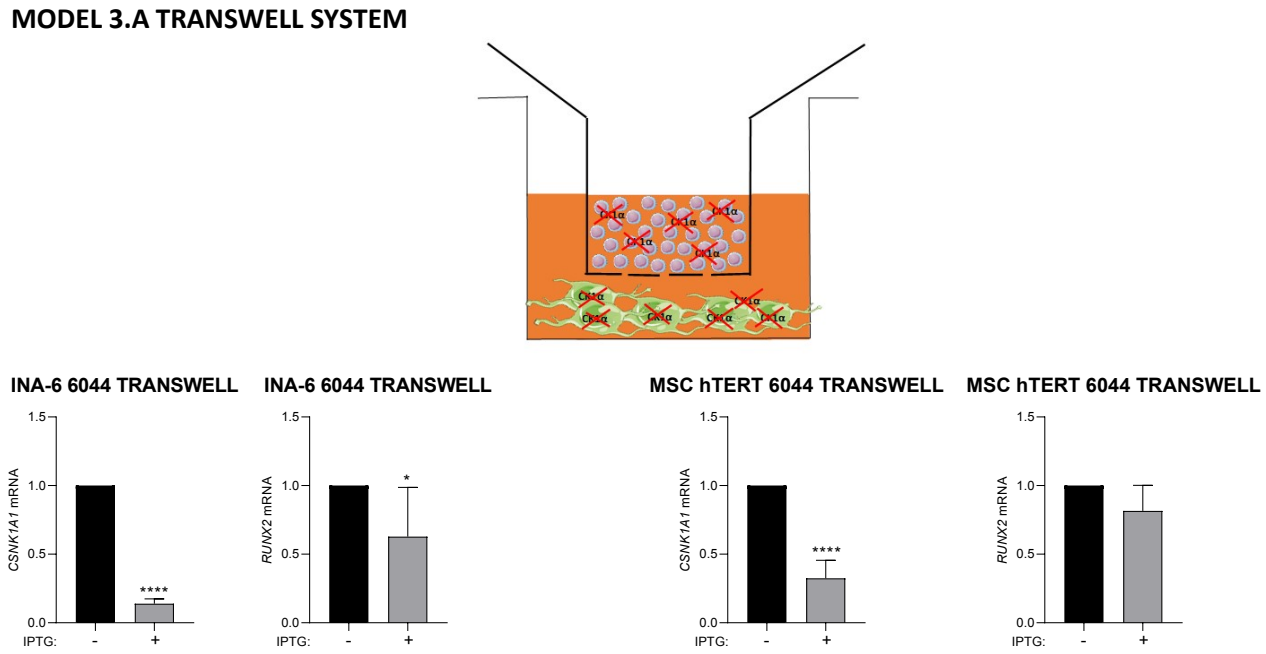

Fig.41 CK1α silencing in INA-6 and MSC hTERT cells, in a co-culture model using a transwell system, regulates the expression levels of RUNX2. Upper panel: schematic representation of the experimental design. Lower panel: qRT-PCR analysis of *CSNK1A1* and *RUNX2* mRNA in CK1α-deficient INA-6 6044 (left panel) and MSC hTERT 6044 cells (right panel), both silenced for *CSNK1A1* with IPTG 500μM for 1 week and subsequently co-cultured for additional 3 days using a transwell system, in the continuous presence of IPTG. GAPDH was used as housekeeping gene. Data represent mean± SD of n=6 (for INA-6 6044 analysis) and n=5 (for MSC hTERT 6044 analysis) independent experiments. *=p<0.05, ****=p<0.0001 compared to untreated cells.

Next, we performed the same experiment using the HS-5 6044 stromal cell model co-cultured with INA-6 6044 cells, keeping the transwell system. As reported in Fig.42 CK1α silencing in MM cells and in stromal compartment was confirmed. *RUNX2* gene expression was significantly decreased in plasma cells (Fig.42, left

panel), as observed with MSC hTERT co-culture, but upregulated in the HS-5 6044 counterpart (Fig.42, right panel).

The data indicate how CK1α modulation could differentially affect RUNX2 expression in the context of bone marrow microenvironment in the presence or absence of physical cell interactions between plasma cells and stromal cells.

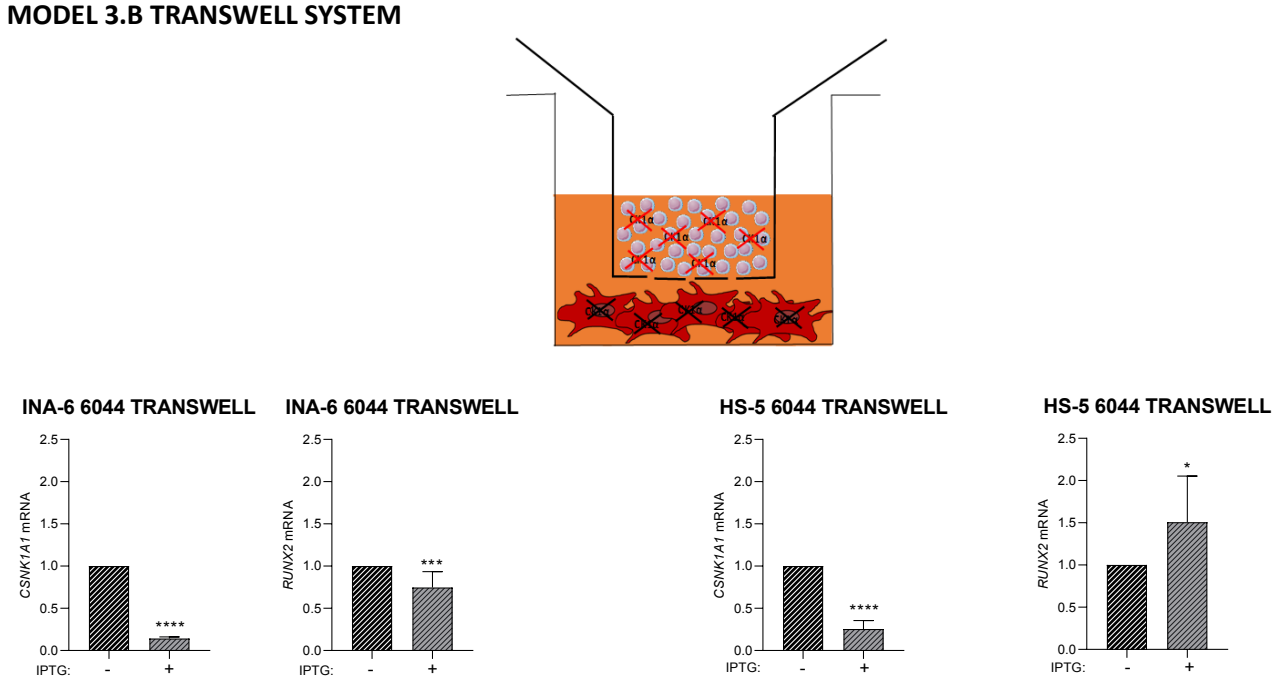

Fig.42 CK1α silencing in INA-6 and HS-5 in a co-culture model using a transwell system, regulates the expression levels of RUNX2. Upper panel: schematic representation of the experimental design. Lower panel: qRT-PCR analysis of *CSNK1A1* and *RUNX2* mRNA in CK1α-deficient INA-6 6044 (left panel) and HS-5 6044 cells (right panel), both silenced for *CSNK1A1* with IPTG 500μM for 1 week and subsequently co-cultured by a transwell system for additional 3 days, in the continuous presence of IPTG. GAPDH was used as housekeeping gene. Data represent mean± SD of n=8 (for INA-6 6044 analysis) and n=10 (for HS-5 6044 analysis) independent experiments. *=p<0.05, ***=p<0.001, ****=p<0.0001 compared to untreated cells.

Taken together, the data showed that in all models (1/2/3) of co-culture performed, the use of HS-5 or MSC hTERT cells, as stromal feeder layer of plasma cells in a co-culture system, led to opposite results on RUNX2 expression both in MM cells and in the stromal compartment.

7.5 CELL ADHESION SUSTAINS RUNX2 EXPRESSION IN MM CELLS

The data obtained regarding RUNX2 expression in all the studied models of co-culture have suggested as RUNX2 presented opposite trend of expression in the two different cellular populations of MM and stromal cells. Indeed, when RUNX2 expression was upregulated in MM cells, its expression on the stromal compartment was reduced or unchanged. On the contrary, RUNX2 upregulation on the stromal compartment seem to be supported by its down modulation in plasma cells.

To deeply investigate the role of soluble factors and the cell-to cell contact on the modulation of RUNX2 expression, we compared the expression of RUNX2 both in MSC and in MM cells, in different experimental conditions:

- alone: MM cells grown without MSC feeder layer or MSC grown without MM cells;
- co-culture: MM cells grown on a feeder layer of MSC in which the cross-talk is mediated both by soluble factors and by cell-to cell interactions;
- transwell co-culture: MM cells and MSC grown in co-culture but physically separated by a porous membrane, that prevents cell-to cell contact. In this last condition the cross-talk is mediated only by soluble factors.

Interestingly, co-culturing INA-6 with MSC hTERT stromal cells allowing cell-to cell contact, led to the increase of both β-catenin and RUNX2 expression in the MM cell population compared to its expression when INA-6 cells were grown without the MSC hTERT feeder layer (grown alone). Using the transwell system RUNX2 expression returned to the basal level of MM grown alone (Fig.43, upper panel). The same trend was detected also for β-catenin, confirming its main role on sustaining RUNX2 basal expression. On the contrary, RUNX2 expression in the MSC hTERT counterpart was decreased when grown in the traditional co-culture system compared to MSC grown alone and it was further decreased when grown in the transwell system condition (Fig.43, lower panel). Focusing on β-catenin protein expression in MSC, no significant changes were observed in the different tested basal experimental conditions.

These results suggest that in a context of the BM *niche* both cell adhesion and soluble factors could cooperate to control RUNX2 expression in the stromal compartment while its expression in MM cells could be mainly sustained by cell adhesion and cell- o cell contact, mainly through Wnt/ β-catenin pathway activation.

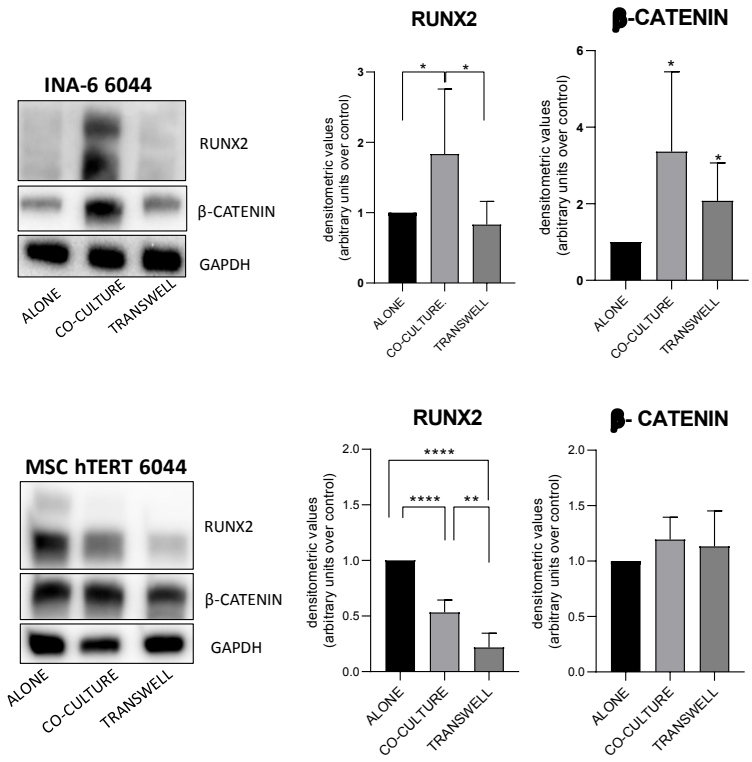

Fig.43 Cell adhesion sustains RUNX2 expression in MM cells lowering its expression in the stromal cell MSC hTERT. Representative WB (left panel) and densitometric analysis (right panel) of RUNX2 and β-catenin expression in alone/co-culture/transwell conditions, both in INA-6 6044 (upper panel) and in MSC hTERT counterpart (lower panel). Protein expression data represent mean± SD of n=5 independent experiments. *=p<0.05; **=p<0.01; ****=p<0.0001 compared to alone/co-culture condition.

Next, we reproduced the same experiments using HS-5 cells instead of MSC hTERT as feeder layer of INA-6 6044 cells in co-culture, analyzing the same previous conditions. In line with what observed with MSC hTERT, RUNX2 expression in MM cells co-cultured was supported by elevated levels of β-catenin (Fig.44, upper panel). Moreover, using the transwell system, RUNX2 expression as well as β-catenin returned to the basal level of MM cells grown alone. In contrast with MSC hTERT cells, the expression of RUNX2 in HS-5 was not modified neither culturing the cells in the traditional co-culture with plasma cells nor with the transwell system. Infact, neither cell-to cell contact nor soluble factors seem to affect RUNX2 expression in stromal cells. Indeed, both RUNX2 and β-catenin expression did not present any significant differences in the different experimental conditions (Fig.44 lower panel).

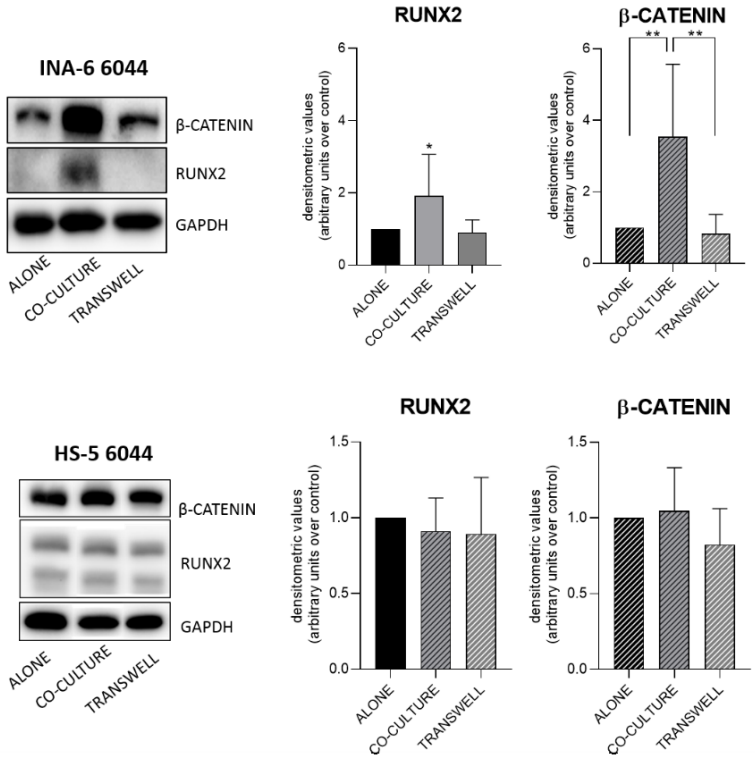

Fig.44 Cell adhesion sustains RUNX2 expression in MM cells without affecting its expression in the stromal cell HS-5. Representative WB (left panel) and densitometric analysis (right panel) of RUNX2 and β-catenin expression in alone/co-culture/transwell conditions, both in INA-6 6044 (upper panel) and in HS-5 6044 counterpart (lower panel). Protein expression data represent mean± SD of at least n=7 independent experiments. *=p<0.05, **=p<0.01 compared to alone condition/co-culture condition.

7.6 ROLE OF LENALIDOMIDE ON STROMAL CELL OSTEOGENIC DIFFERENTIATION POTENTIAL

7.6.A LENALIDOMIDE DOES NOT AFFECT MSC VIABILITY AND CELL CYCLE

If the effects of the use of IMiDs in the treatment of the hematological PCs disease have been widely studied and established, those on the mesenchymal stromal differentiation towards osteogenic lineage are still debated and unclear. For this reason, first we investigated in our experimental models whether Lena could affect MSC viability and if it could induce cell cycle perturbations.

We treated MSC hTERT and HS-5 cells for 7 days with different concentrations of Lena. As a positive control of Lena activity, we used the Lena sensitive MM cell line H929. Treatment with Lena while increasing H929 Annexin V positive cells, did not cause any toxicity of the two MSC lines analyzed (Fig.45)

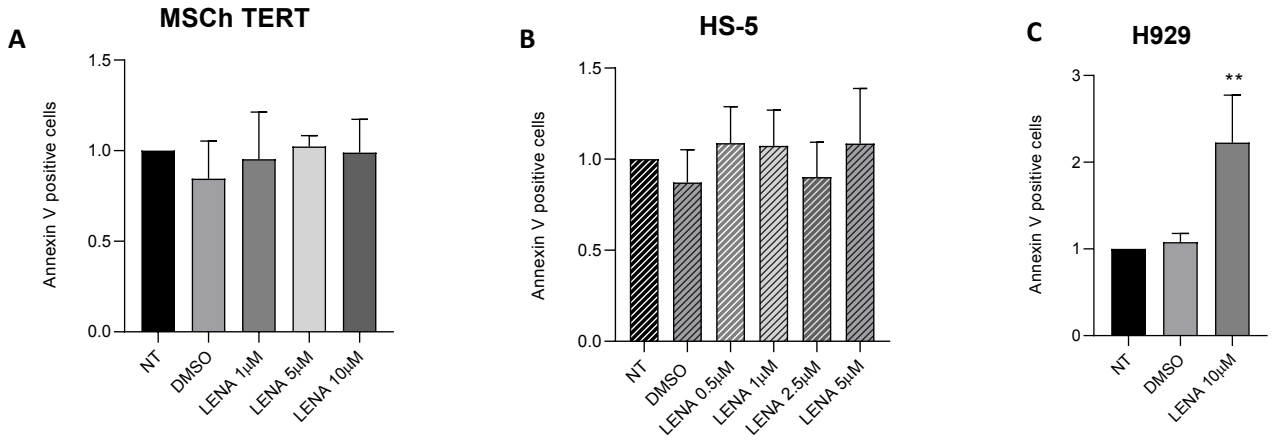

Fig.45 Lena treatment does not cause apoptosis on MSC. Quantification of apoptosis through Annexin V staining and FACS analysis in MSC hTERT (A) and HS-5 (B) cell lines treated with different concentrations of Lena (ranging from 0.5 to 10µM) for 7 days. H929 cells were used as positive control of Lena efficacy (C). Data are represented as the mean ± SD of n=8 independent experiments (A) and n=4 independent experiments (B/C) and are normalized over untreated cells. DMSO 0.0002% V/V was tested to exclude vehicle-induced toxicity. **= p<0.01 compared to untreated cells.

In parallel to cell toxicity experiments, we performed cell cycle analysis after treatment of MSC hTERT WT and HS-5 cell lines with 1µM, 5µM and 10µM Lena for 7 days. As represented in Fig.46, Lena treatment did not induce any changes in the different cell cycle phases in both MSC lines tested.

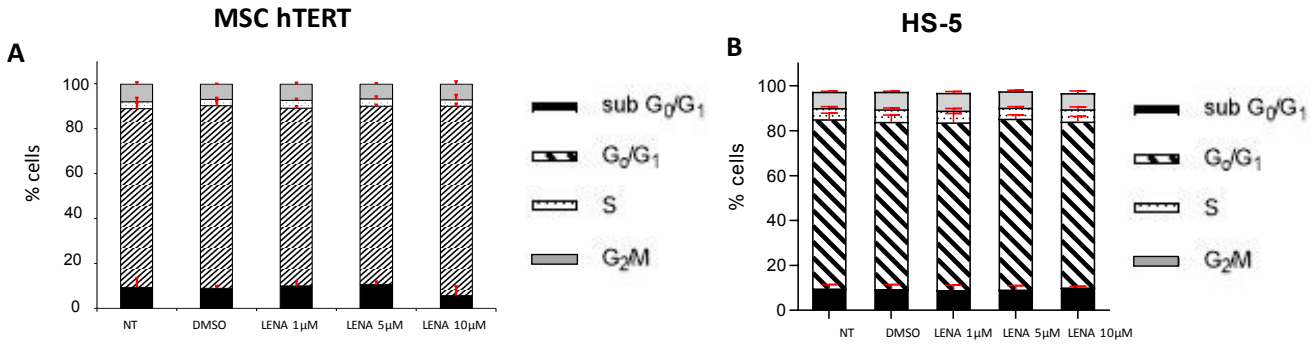

Fig.46 Lena treatment does not induce any significant changes in the cell cycle phases. Quantification of cell cycle phases through PI staining and FACS analysis in MSC hTERT (A) and HS-5 (B) after treatment of Lena at different concentrations (1/5/10µM) for 7 days. Data are represented as mean ± SD of n=4 independent experiments for MSC hTERT (A) and of n=6 independent experiments for HS-5 cells (B). DMSO 0.0002% V/V was tested to exclude vehicle-induced toxicity.

7.6.B LENALIDOMIDE TREATMENT INDUCES CK1α DEGRADATION IN MSC

It has been previously reported that Lena acts by a novel mechanism, modulating Cereblon (CRBN) E3 ubiquitin ligase and inducing the proteasomal degradation of Ikaros, Aiolos and CK1α leading to MM cells death [14]. Therefore, we asked whether this holds true also in stromal cells. We treated both MSC hTERT and HS-5 cells with different concentrations of Lena to detect any modulations in CK1α protein expression levels. CK1α was significantly reduced after treatment of Lena starting from the concentration of 1μM in both cell lines (Fig.47).

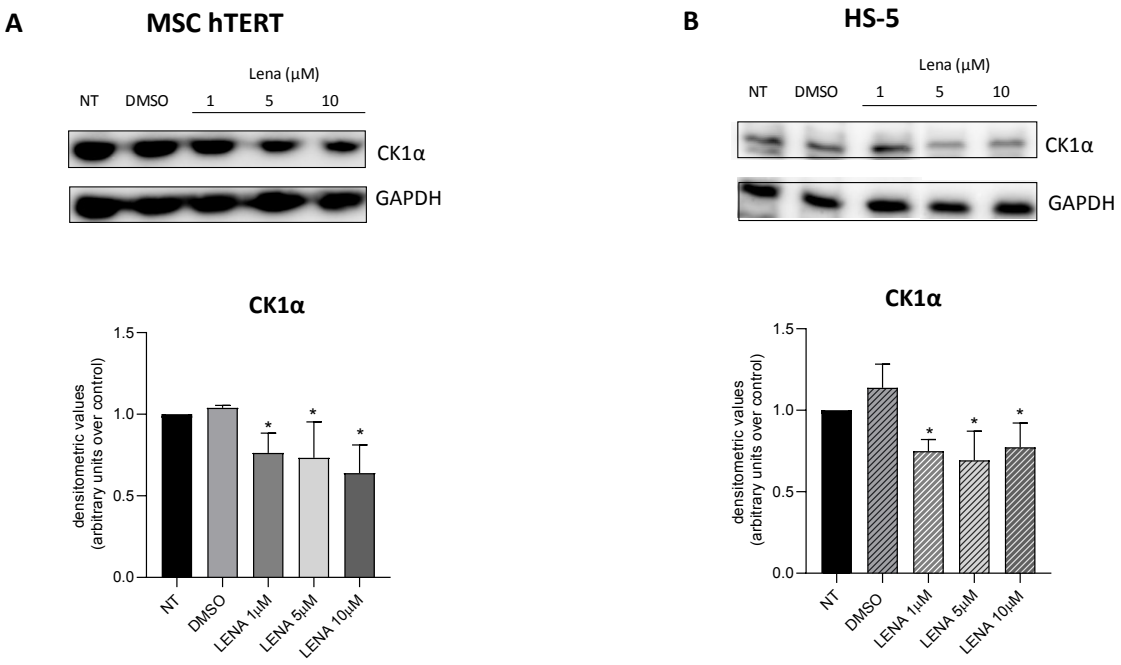

Fig.47 Lenalidomide treatment induces CK1α degradation in MSC cell lines. Representative WB (upper panel) and densitometric analysis (lower panel) of CK1α expression after Lena treatment (ranging from 1 to 10μM) for 7 days, in MSC hTERT cells (A) and in HS-5 cells (B). Data represent the mean ± SD of n=4 independent experiments. DMSO 0.0002% V/V was tested to exclude vehicle induced toxicity.*=$p<0.05$ compared to untreated condition.

7.6.C ROLE OF LENALIDOMIDE IN THE OSTEOGENIC DIFFERENTIATION POTENTIAL

The effects of the use of IMiDs on MSC differentiation and bone remodeling is still debated and controversial [76][78]. Therefore, we tried to elucidate the possible effects of Lena on MSC osteogenic potential considering that Lena reduced CK1α level of expression in MSC (Fig.47). We treated MSC hTERT for 7 days with the same concentrations of Lena used in the previous experiments, finding that treatment of stromal cells with Lena significantly reduced *RUNX2* mRNA levels starting from 5μM concentration (Fig.48A). We decided to use this concentration (5μM), to investigate if Lena could change RUNX2 expression also in the other stromal cell available (HS-5). Unexpectedly, *RUNX2* transcriptional expression was significantly

incremented in HS-5 cells, underlying an opposite effect compared to what we observed in MSC hTERT cells (Fig.48B).

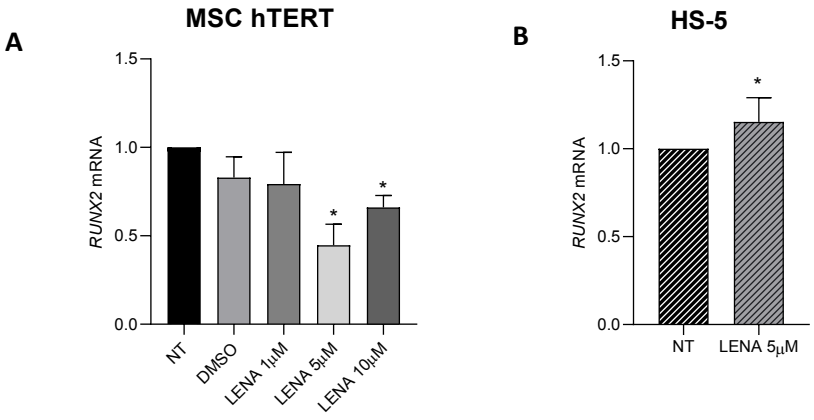

Fig.48 Lena differently regulates RUNX2 gene expression in MSC hTERT and HS-5 cells. qRT-PCR of RUNX2 mRNA expression in MSC hTERT (A) and HS-5 cells (B). GAPDH was used as reference gene. Data represent the mean ± SD of n=4 independent experiments (A) and n=6 independent experiments (B). *=$p<0.05$ compared to untreated condition.

To better explore the effects of Lena on MSC osteogenic potential, we collected bone marrow samples from a cohort of patients affected by MGUS/SMM/MM, in order to purify primary MSC. The cohort of 20 patients was stratified according to the disease stage, considering bone disease in case of active MM (table III showed the clinical features of MM patients analyzed). The isolated primary MSC were treated with Lena 2.5μM for 7 days and *RUNX2* gene expression was analyzed. A trend towards reduction of *RUNX2* was observed in each stage of the disease, especially in MGUS and active MM with bone disease (Fig.49A). To further study the potential negative role of Lena treatment on the MSC osteogenic potential, we also investigated gene expression of *ALP*, another osteogenic differentiation marker, both in MSC hTERT cells and in primary patients stromal cells. *ALP* mRNA was reduced in MSC hTERT treated with Lena at different doses (Fig.49B, left) and in primary MSC from MGUS or MM patients, with or without bone disease (Fig.49B, right). However, the SMM condition presented more biological variability (Fig.49B, right). We next used also the colorimetric ALP assay to detect the enzyme activity in the different supernatants collected after Lena treatment of primary MSC. Even if preliminarily, the analysis revealed a trend towards reduction of ALP activity in each stage of the disease (Fig.49C), excluding the MGUS stage, for which we did not have sufficient samples to the analysis. These data confirmed the previous results obtained by transcriptional analysis for both *RUNX2* and *ALP* mRNA, pointing to a negative regulatory role of Lena on MSC differentiation potential.

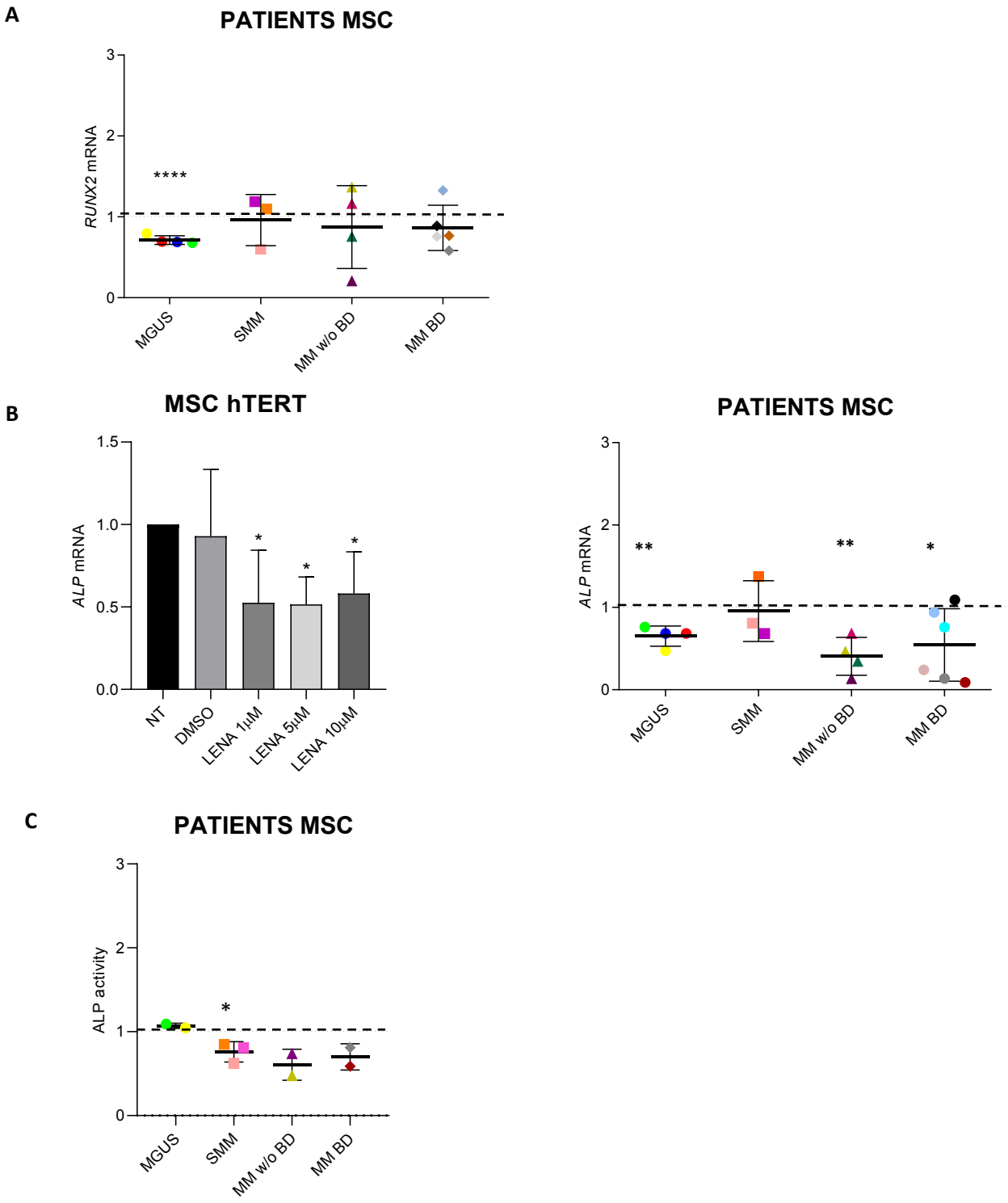

Fig.49 Lena determines *RUNX2* and *ALP* reduction in MSC hTERT line and in primary patient derived MSC.

A. Dispersion graph of *RUNX2* expression quantified by qRT-PCR in patient derived MSC with MGUS, SMM, MM not affected (MM w/o BD) or affected (MM BD) by bone disease (BD), treated with Lena 2,5µm for 7 days. DMSO 0.00005% V/V has been used to confirm the non-toxicity of the vehicle. Data was normalized on the *GAPDH* housekeeping gene and compared to DMSO condition, indicated by the dotted line. **B.** qRT-PCR of *ALP* expression in MSC hTERT (left panel) treated with Lena 1,5,10 µM for 7 days. Data represent the mean ± SD of n=4 independent experiments and were compared to untreated condition. GAPDH was used as reference gene. DMSO 0.0002% V/V has been used to confirm the non-toxicity of the vehicle. Dispersion graph of *ALP* expression quantified by qRT-PCR in patient derived MSC (right

panel) treated with Lena 2,5µm for 7 days. DMSO 0.00005% V/V has been used to confirm the non-toxicity of the vehicle. Data was normalized on the *GAPDH* housekeeping gene and compared to DMSO condition, indicated by the dotted line. **C.** Dispersion graph of ALP secreted activity quantified by the colorimetric ALP assay kit performed on the supernatants of patient derived MSC treated with DMSO or Lena 2,5µM for 7 days. The data was normalized to ALP activity in the DMSO condition, indicated by the dotted line. *=p<0.05, **=p<0.01, ****=p<0.0001 compared to DMSO condition.

7.7 COMPARISON BETWEEN MSC hTERT AND HS-5 STROMAL CELL LINES

All the experiments performed in this thesis work, made use of two models of stromal cells: the MSC hTERT and the HS-5 cell lines. Performing co-culture experiments, with the different combination of CK1α silencing in MM cells and in MSC populations, it was found that the use of these 2 different mesenchymal cell lines, led to opposite results both in the MM cell population and in the stromal counterpart. Moreover, also Lena caused opposite results about the expression of the potential osteogenic markers, in the two mesenchymal stromal cell lines. Looking for potential differences in the two cell lines, we found that the HS-5 immortalization method uses HPV-16 E6/E7 expression (ATCC bio resources and [152]). Differently, MSC hTERT immortalization method uses the enforced expression of the catalytic subunit of telomerase [150]. Focusing on the HS-5 immortalization method, it has been reported that the E6/E7 gene products interfere with the function of p53 and Rb1, respectively, thereby preventing cell cycle progression [153]. Considering that CK1α is a major regulator of MDM2-p53 signaling and that it is reported that p53 negatively regulates *RUNX2* expression [136], [154], we asked if p53 could be differentially activated in both HS-5 and MSC hTERT cells upon an apoptotic stimulus. Doxorubicin (Doxo) 1,2 µM was added to the cell culture medium of HS-5 6044, MSC hTERT 6044 and INA-6 6044 cells for 18 hours , the latter used as postive control of p53 induction. As expected, Doxo led to increased Annexin V positive cells in INA-6 6044 cells, with an increased apoptosis rate of 90% (Fig.50 left panel A). While MSC hTERT 6044 have been shown very sensitive to Doxo treatment with a strong increment of apoptotic cells (Fig.50, middle panel A), HS-5 6044 have been proven to be resistant to the treatment with no significant changes in apoptosis observed upon Doxo treatment (Fig.50 right panel A). The analysis of PARP cleavage confirmed the apoptotic effect of Doxo only in MSC hTERT cells (Fig.50, B panel).

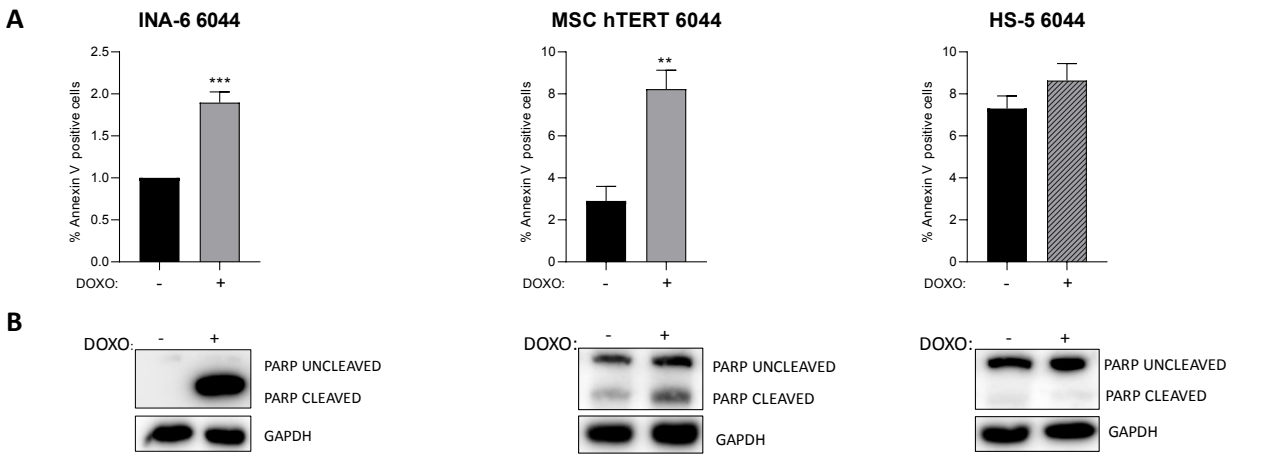

Fig.50 Doxorubicin treatment differently modulates cell apoptosis in MSC hTERT 6044 and in HS-5 cell lines. A. Quantification of apoptosis through Annexin V staining and FACS analysis in INA- 6 6044 cells (left panel), MSC hTERT 6044 (middle panel) and HS-5 6044 (right panel) cells, treated with 1.2µM of Doxo for 18h. Data represent the mean ± SD of n=3 independent experiments and are presented as arbitrary values over untreated cells. **=p< 0.01, ***=p<0.001 compared to untreated cells. **B.** Representative WB of Parp cleavage expression after Doxo treatment in INA-6 6044, MSC hTERT WT and in HS-5 WT cells.

To further investigate the possible mechanism of resistance of HS-5 cells to Doxo treatment, we analyzed p53 and related protein expression in the tested models. We found that p53 and its downstream target p21 were expressed and upregulated only in MSC hTERT cells after Doxo treatment (Fig.51), confirming the possible resistance of HS-5 cells to cell cycle progression inhibitory agents. The same protein analysis was performed using the INA-6 6044 cells as positive control, sensitive to Doxo treatment, which increased p53 protein level upon Doxo treatment (data not shown).

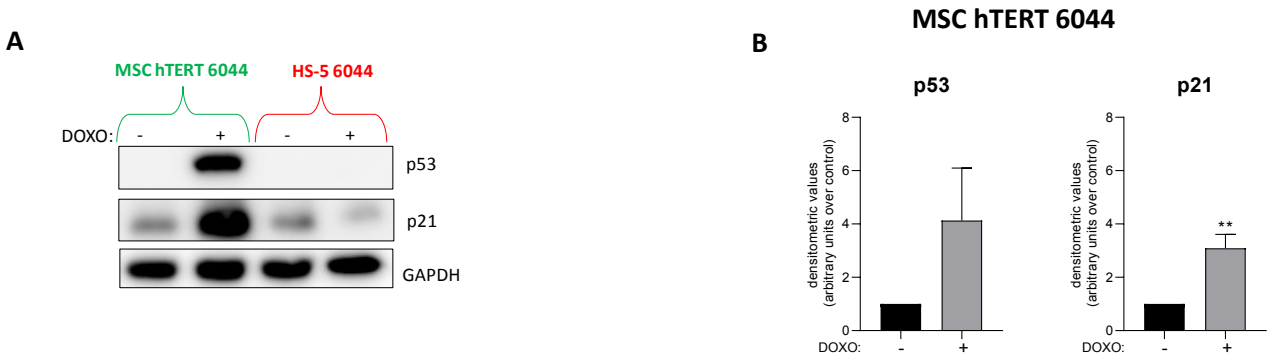

Fig.51 Doxorubicin differentially modulates p53 and p21 expression levels in MSC hTERT and in HS-5 cell lines. A. Representative WB of p53, p21 expression after Doxo 1.2µM treatment for 18 hours, of MSC hTERT 6044 cells and HS-5 6044 cells. **B.** Densitometric analysis of p53 and p21 protein expression in the Doxo sensitive MSC hTERT 6044 cells. GAPDH was used as housekeeping protein. Data represent the mean ± SD of n=3 independent experiments. **=p<0.01 compared to untreated cells.

7.8 CK1α SILENCING IN CO-CULTURE SYSTEM AFFECTS PLASMA CELLS VIABILITY

Finally, to conclude our investigation, we examined the rate of apoptosis in MM cells in the different models (indicated in Fig.40) to determine the impact of the different CK1α silencing conditions on MM cells viability. We focused our analysis only on MM cells co-cultured with MSC hTERT cell line. Indeed, our initial aim was to determine if CK1α silencing could induce a double positive effects in a bone marrow *niche* context: the plasma cells death and, at the same time, a potentially recovery of an osteoblastic phenotype in the stromal compartment.

Apoptosis was investigated by Annexin V/PI staining or by trypan blue staining. The rate of apoptosis was increased in the INA-6 MM population both in model 1.A and in 2.A, accordingly with the down modulation of RUNX2 (Fig.52 A/B). In the model 3.A, the strong upregulation of RUNX2 in MM cells correlated with a reduced MM cells apoptosis (Fig. 52C).

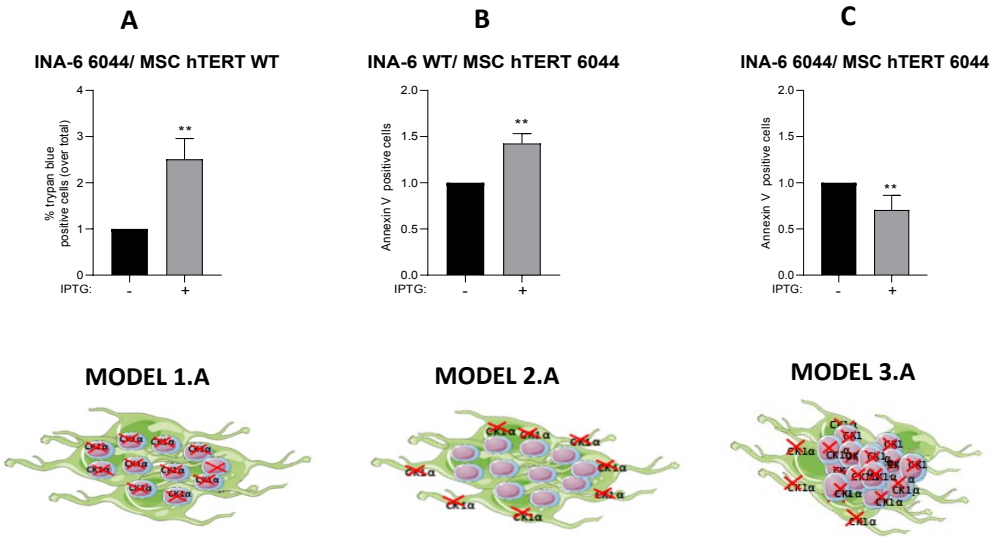

Fig.52 CK1α silencing differentially modulates apoptosis in the different co-culture models studied. Quantification of apoptosis through: -trypan blue staining in CK1α-deficient INA-6 6044 cells co-cultured with CK1α-proficient MSC hTERT WT (A); -Annexin V staining and FACS analysis in CK1α-proficient INA-6 WT cells co-cultured with CK1α-silenced MSC hTERT 6044 (B), in CK1α-deficient INA-6 6044 cells co-cultured with CK1α-silenced MSC hTERT 6044 (C). Data represent the mean ± SD of n=3 independent experiments for A/B conditions, n=4 for C condition. **=p<0.01 compared to untreated cells.

8. DISCUSSION AND CONCLUSIONS

In this work, we investigated whether the kinase CK1a could regulate osteoblastogenesis in the context of MMABD.

To assess how CK1α inactivation could affect osteoblastogenesis, we used two different IPTG-inducible CK1α directed shRNA MSC lines, namely MSC hTERT and HS-5. We observed that the osteogenic differentiation markers *RUNX2* (early) and *ALP*, *SPP1 and BGLAP* (late) were upregulated at different time points, both in CK1α-deficient MSC hTERT 6044 cells or HS-5 cells (Fig.23). In particular, the increase of the osteogenic differentiation markers was detected at shorter CK1α silencing time points in HS-5 cells compared to the MSC hTERT cells, suggesting that the osteogenic differentiation induced by CK1α silencing starts quicker in HS-5 cells compared to MSC hTERT cells.

Komori et al. demonstrated that *RUNX2* expression enhances MSC proliferation and induces their commitment into the osteoblastic lineage also through the regulation of Wnt/β-catenin pathway [30]. Moreover, *T.Gaur et al*. have reported that *RUNX2* is a gene target of β-catenin/TCF1, suggesting a direct regulation between canonical Wnt/β-catenin pathway and the early events of osteogenesis [60]. For these reasons, we focused our investigation on β-catenin protein expression.

Surprisingly, we found that β-catenin expression followed an "oscillatory wave" over a time course of CK1α silencing and it was not always upregulated over time. The same oscillatory expression was confirmed in both MSC lines used (Fig.24). It has previously been shown a negative feedback loop involving AXIN2, a β-catenin transcriptional target gene that could itself inhibit β-catenin abundance and activity, regulating Wnt signaling in HEK293 cells [155] [156]. Therefore, this could be the case in our tested models when high level of β-catenin induced by CK1α silencing could be down regulated by AXIN2 protein expression. Future experiments will be performed to monitor AXIN2 expression level in the tested conditions.
The antagonistic role of CK1α towards osteogenesis has been further confirmed culturing CK1α-proficient or deficient stromal cells in osteogenic medium. Indeed, Alizarin Red staining showed more foci of calcification induced by CK1α silencing (Fig.25). Even if a quantitative analysis will be necessary to calculate the rate of calcium deposits, these data suggest a putative role of CK1α in the osteogenic differentiation process.

Considering that Wnt/β-catenin regulates the osteogenic differentiation in different models of MSC through *RUNX2* expression [60], to verify the link between Wnt/β-catenin and RUNX2 axis in our experimental model we stimulated both MSC hTERT and HS-5 with the recombinant protein Wnt-3A. The data showed increased

protein expression of RUNX2 after β-catenin activation but surprisingly the *RUNX2* mRNA levels had a opposite trend of expression (Fig.26). *Drissi*'s *et al.* study revealed an auto-regulatory feedback loop of RUNX2, since its protein overexpression was sufficient to inhibit the activity on its own promoter, reducing its transcriptional expression [59]. Therefore, future experiments also including chromatin immunoprecipitation assays will be necessary to better investigate the putative RUNX2 feedback loop of autoregulation also in our experimental model.

We next evaluated how CK1α inactivation in a recreated BM microenvironment could be exploited to implement the osteoblastogenic potential of MSC using three different models of co-culture between MSC and MM cells. CK1α silencing was achieved in 1) the MM compartment (model 1), 2) the MSC compartment (model 2) or 3) both cell types (model 3). Each model has been performed using both MSC hTERT and HS-5 cell lines as the feeder layer of MM cells.

Our results revealed that CK1α inactivation in the BM *niche* modulates RUNX2 expression through Wnt/β-catenin signaling cascade. However, the data showed unexpected opposite results with regards to RUNX2 expression both in MM cell population and in the stromal counterpart when comparing MSC hTERT cells and HS-5 cells.

Focusing on the results obtained from the model 1, CK1α silencing in MM cells co-cultured with MSC hTERT WT, reduced both β-catenin and RUNX2 expression in PCs, potentially counteracting the MSC osteogenic differentiation block induced by malignant PCs (Fig.28). Indeed, RUNX2 expression was found increased in the stromal counterpart that was sustained by β-catenin upregulation (Fig.29). Corroborating our data, it was reported that the inhibitory effect of MM cells on osteoblast differentiation appears to be mediated in part also by the capability of MM cells to constrain RUNX2 activity in human MSC and osteoprogenitor cells [38]. Moreover, evidences confirm that RUNX2 expression and activity in MM cells sustain angiogenesis, cell survival and tumor progression, leading to poor prognosis [72].

Surprisingly, opposite results were obtained using HS-5 WT as feeder layer for CK1α-deficient PCs. The data revealed a strong activation of Wnt/β-catenin pathway and increased *RUNX2* transcriptional expression in MM cells (Fig.30) whereas in the stromal counterpart there was a trend towards reduction for both β-catenin and RUNX2 expression (Fig.31). From these preliminary data it appears that the use of either MSC hTERT or HS-5 cells as stromal cells feeder layer of CK1α-silenced MM cells could lead to opposite results regarding Wnt/β-catenin activation and RUNX2 expression.

Model 2 studied the effects of CK1α silencing in the stromal compartment but in the context of BM microenvironment. Surprisingly, in this model, when CK1α silencing was achieved in stromal cells we could determine CK1α protein reduction also in plasma cells, thus potentially negatively regulating RUNX2. In fact, an unexpected CK1α post translation modulation in CK1α-proficient MM cells co-cultured with CK1α-

deficient MSC hTERT 6044 was detected (Fig.32), leading to the subsequent RUNX2 upregulation in the stromal counterpart (Fig.33). Future experiments are needed to discover whether CK1α protein reduction in MM cells could be caused by proteasome activity or by caspase activation. Differently from the results obtained in model 1, for the first time, β-catenin levels did not correlate with RUNX2 levels in stromal cells. As recently reviewed by *K. Sweeney*, Wnt/β-catenin pathway could control RUNX2 expression that in turn regulates not only osteoblastogenic related genes, but also a variety of Wnt ligands, Wnt inhibitors and TCF/LEF co-activators, thus modulating also β-catenin itself signaling pathway [45]. Intriguingly, it has been shown that after an initial RUNX2 upregulation, its prolonged overexpression negatively affects the capability of preosteoblasts to differentiate into mature osteoblasts. Thus osteoblastic cells need to reduce the levels of β-catenin and inhibit its transcriptional activity to complete the differentiation process [157]. Therefore, the strong upregulation of RUNX2 protein detected in the stromal compartment (+68% compared to untreated cells, the highest increment observed in all models of co-culture performed) could be sufficient to regulate Wnt inhibitors expression to further reducing β-catenin activity also in our experimental model. Indeed, in the MSC hTERT 6044 compartment, RUNX2 protein upregulation seemed to be sufficient to block both its gene transcription and β-catenin expression level (Fig.33). Therefore, this data seem to confirm the transcriptional autoregulation loop of RUNX2 [59], previously observed in both MSC hTERT and HS-5 cells after Wnt-3A stimulation (Fig.26).

Opposite from the last results obtained with MSC hTERT, the use of CK1α-deficient HS-5 6044 cells as feeder layer of MM cells, led to augmented RUNX2 expression in PCs (Fig.34). This increased RUNX2 expression could in turn be sufficient to inhibit its activation in the stromal compartment, potentially negatively affecting the MSC osteogenic differentiation. Indeed, in this model we could observe a trend towards a reduction of RUNX2 in the HS-5 stromal compartment (Fig.35).

Finally, with the model 3 of co-culture we tried to reproduce *in vitro* a model of CK1α inactivation in the bone marrow microenvironment as closest as possible to that hypothetically obtainable *in vivo* through the use of a CK1α specific inhibitor on patients. Unexpectedly, we found that co-silencing of CK1α both in MM cells and in MSC hTERT 6044 produced a strong upregulation of RUNX2 in MM cells (Fig.36) and an inhibition of the Wnt/β-catenin signaling activity in the stromal compartment. This was accompanied by a slight increase of RUNX2 mRNA levels, but not RUNX2 protein expression (Fig.37). *Trotter et al.* reported that the RUNX2-PI3K/AKT axis in MM cells is an important driving force for the tumor progression as well as for poor prognosis [72]. Moreover, *K. A. Cohen-Solal et al.* reported that PI3K/AKT pathway stimulates RUNX2 activity by controlling the expression of different proteins such as SMURF2, FOXO1, FOXO3, indirectly related to RUNX2 stability. Interestingly, in a mutual activation, RUNX2 enhances PI3K/AKT signaling by up-regulating p85, p110β, AKT protein levels and components of mTORC2 complex in the context of mouse osteoblast and chondrocyte differentiation [47]. Finally, it has been reported that RUNX2 promotes MM cell proliferation

and protects cells from cytotoxic drugs *via* the AKT/GSK-3β pathway activation [158]. Therefore, the increment of RUNX2 expression in MM cells could be sustained also by other pathways different from the Wnt/β-catenin, such as PI3K/AKT axis or soluble factors and adhesion molecules involved in MM/MSC cross talk. Preliminary data in our laboratory showed that the AKT axis might be upregulated in MM cells in CK1α co-silenced MM and MSC hTERT conditions (data not shown).

Extremely important in the PCs/MSC cross talk in the BM microenvironment are both soluble factors and cell-to cell interactions, which could support MM clonal expansion. To better explain the increased RUNX2 expression in CK1α-deficient MM cells co-cultured with CK1α-deficient MSC hTERT 6044 cells, we cultured the same MM and MSC CK1α silenced cells in a transwell system, to avoid the physical interactions between MM and MSC cells populations, allowing their cross talk only through the soluble factors released in the medium. In these settings, opposite expression of RUNX2 both in MM cells and in MSC counterpart was achieved, compared to the data obtained maintaining cell-to cell adhesion (Fig.41). These results highlighted the importance of cell adhesion in the control of RUNX2 expression and suggest how the effects of CK1α silencing could be bypassed by the absence of cells interactions.

Oppositely from the results obtained using CK1α-deficient MSC hTERT 6044, the data of model 3.B (CK1α-deficient INA-6 6044 co-cultured with CK1α-deficient HS-5 6044) showed a double positive effect of CK1α silencing on the differentiation potential of stromal cells and on the hematological disease. Indeed, CK1α silencing in this model was able to reduce both β-catenin and RUNX2 expression in MM cells (Fig.38), which in turn promoted their increment in the HS-5 6044 counterpart (Fig.39), corroborating the idea of a possible reduction of malignant plasma cells clonal expansion along with the sustaining of MSC osteogenic differentiation potential.

Considering the different results obtained with the use of MSC hTERT and HS-5 cells in each of the three co-culture models, we reproduced the third model between CK1α-deficient INA-6 6044 and CK1α-deficient HS-5 6044 also using the transwell system. Differently from the results obtained with MSC hTERT cells (opposite RUNX2 expression observed with the use of the transwell system compared to traditional co-culture both in MM cells and MSC populations), the RUNX2 expression was reduced in MM cells and increased in HS-5 stromal compartment (Fig.42), reproducing the same results obtained with the traditional co-culture model 3.B in the presence of cell adhesion. Therefore, in this setting, neither cell-to cell contact nor soluble factors seem to interfere in the control of RUNX2 expression, mainly modulated by CKα silencing.

Focusing the analysis on RUNX2 basal expression in MM cells and in MSC compartment, without considering CK1α silencing conditions, we observed that RUNX2 and β-catenin were sustained by cell-to cell interaction instead of soluble factors (Fig.43/44 upper panels) in all the models analyzed. Interestingly, very recently *Pei Pei Zhang et al.* demonstrated that RUNX2 was highly expressed in adherent B-NHL and MM cell lines compared to cells grown in suspension and knocking down the expression of RUNX2, could reverse CAM-DR,

suggesting it as a promising therapeutic target to bypass the drug resistance [158]. In our experimental conditions RUNX2 protein bands in MM cells were technically detectable only in the co-culture condition, barely recognizable both in the "alone" and in transwell settings. Moreover, soluble factors did not significantly affect RUNX2 expression in MM cells (Fig.43/44). If the data on the MM populations are consistent using both MSC hTERT and HS-5, the data regarding the MSC hTERT and HS-5 populations depicted two different *scenario*s of RUNX2 basal expression. In fact, the co-culture and the transwell system conditions prevented RUNX2 expression in MSC hTERT cells, suggesting that both cell adhesion and soluble factors are involved in the control of RUNX2 activity in this MSC line (Fig.43, lower panel). Moreover, not significant changes in β-catenin protein expression were observed in MSC hTERT cells (Fig.43, lower panel). On the contrary, RUNX2 basal expression in HS-5 cells did not seem to be modulated by cell adhesion and soluble factors since no changes in its expression were observed comparing "alone", co-culture and transwell settings (Fig.44, lower panel). As observed in MSC hTERT cells, β-catenin expression did not change in the different settings also in HS-5 cells (Fig.44, lower panel).

Considering the importance of both cell adhesion and soluble factors in the control of RUNX2 basal expression in MSC hTERT cell line, future investigations will be needed to try to identify the main soluble factors that could be involved. Furthermore, to investigate the possibility that CK1α could regulate the secretion of soluble factors participating in the establishment of the MM/MSC cross talk, we have already collected supernatants to be tested with a human cytokine array, in order to identify the main cytokines that could be modulated by CK1α in this context.

After investigating the effects of CK1α inactivation in the different CK1α silenced co-culture models on MSC osteogenic potential, we focused our investigation on Lenalidomide (Lena). Indeed, while the positive effects of Lena and its derivatives on MM hematological disease are widely known, the effects of the use of IMiDs on MSC differentiation potential and bone remodeling are still debated and controversial [76], [77], [78], [79], [80]. Considering that Lenalidomide could reduce CK1α protein levels in different hematological disease [135] [127], we investigated its effects on our MSC models.

We have proved that Lena did not cause any toxicity on the MSC lines tested (Fig.45,46) and we confirmed that it caused CK1α degradation also in MSC (Fig.47). Therefore, we investigated if the expression of potential osteogenic markers could be modulated after CK1α degradation-induced by Lena.

In HS-5 cells Lena induced *RUNX2* transcriptional upregulation (Fig.48B), while in MSC hTERT it caused RUNX2 reduction (Fig.48A), confirming once again, the different behavior of the two available stromal cell line models. The transcriptional analysis performed in MSC isolated from a cohort of 20 patients stratified according to the disease stages in MGUS, SMM and active MM, with or without MMABD showed a trend towards reduction of *RUNX2* in each stage of the disease (Fig.49A). These preliminary data suggested that MSC hTERT cell line could better mimic disease related stromal cells. For this reason, we investigated the

osteogenic potential after Lena treatment only in MSC hTERT cell line and confirmed that other osteogenic markers expression (Fig.49B) and secretion such as *ALP* (Fig.49C), were reduced both in MSC hTERT cells and in primary MSC from patients. Thus, these data suggest a negative role of Lena in sustaining the osteoblastogenic potential of stromal cells and a consequent likely negative effect on MMABD.
Along this line, high levels of activin A secretion, critical in MM-induced osteolysis, were identified after Lena treatment of BMSC [77]. The increased activin A secretion could be abrogated by the addition of activin A-neutralizing antibody, which effectively restored osteoblast function [77]. Activin A was investigated also by *Bolomski et al.*'s study, who discovered how ALP activity and matrix mineralization were reduced after Lena treatment of BMSC in *in vitro* experiments. Moreover, they reported that beta A, DKK-1, gremlin 1 and activin A molecules were up regulated, while *RUNX2* and *DLX5* downregulated, underlying the negative effects of Lena on osteoblastogenesis [76]. Future experiments will be therefore necessary to investigate whether elevated levels of Wnt/β-catenin pathway inhibitors could be present in the collected culture medium treated with Lena. Indeed, high levels of DKKs and SFRPs in supernatants could be sufficient to overcome the potential beneficial effects of MSC osteogenic differentiation induced by CK1α degradation, likely leading to a negative effect of Lena in counteracting the MMABD.

All the experiments performed in this study, made use of two models of stromal cells, the MSC hTERT and HS-5 cell lines, which led to opposite results considering the expression of the potential osteogenic markers (Fig.40). A possible explanation for this discrepancy could rely on the different immortalization method used in the two cell lines: the enforced expression of the catalytic subunit of telomerase for MSC hTERT cell line [150] and the HPV-16 E6/E7 expression for HS-5 cells, able to deregulate p53 and Rb1, preventing cell cycle arrest [152][153]. In particular, the immortalization method of HS-5 cells, which determined a p53 degradation, could be responsible for the different results. Indeed, protein kinase CK1α regulates p53 levels [127] which in turn was also reported to modulate RUNX2, thus the osteogenic differentiation [154]. Many studies have demonstrated that the tumour suppressor p53 exerts a repressive effect on bone development and remodeling. *N. Artigas et al.* demonstrated that p53 is able to physically interact both with RUNX2 and OSX, inhibiting the transcriptional activity of the main controllers of the early phases of osteoblastogenesis [159]. *C. J. Lengner et al.* observed increased osteoblast differentiation and elevated RUNX2 expression in osteoblast progenitor cells derived from p53-null mice. Moreover, they discovered that deletion of p53 in osteoblasts induced hyperproliferation, elevated levels of RUNX2 expression and increased bone maturation *in vitro*, indicating p53 as a negative regulator of bone development [154]. *J. Huang's* group reported that murine p53 deficient MSC have enhanced osteogenic differentiation compared to MSC with wild-type p53. Furthermore, p53 indirectly represses the expression of RUNX2 by activating the miRNA-34 family [160]. Very recently, *N. Liao et al.* confirmed a critical and tumorigenesis-independent function of p53 as a key regulator of mesenchymal cell differentiation and unraveled how an osteoblast-specific inactivation of p53 results in

locally increased bone formation in mouse models [161]. Indeed, in our experimental conditions, only MSC hTERT cells were responsive to Doxorubicin showing a strong increased apoptosis (Fig.50) and expression of p53 and its downstream target p21, while p53 was not modulated in HS-5 cells (Fig.51). The results obtained by Lena treatment and the findings about p53 expression, suggest that, from the translational point of view, the MSC hTERT could represent the best model of stromal cells to use in our *in vitro* experiments to mimic disease related MCS.

To summarize our initial aim was to determine whether through CK1α inactivation in a context of BM *niche,* it could be possible to treat the hematological disease, but also regulating osteoblastogenesis, to possibly ameliorate MMABD.

In our laboratory it has already been demonstrated that CK1α silencing or inhibition in MM cells induces plasma cells apoptosis and cell cycle arrest, also overcoming bone marrow microenvironment dependent protection [127]. We found that the rate of apoptosis in MM cells, in all the BM microenvironment models tested, correlated with RUNX2 expression levels. Indeed, in the co-cultures models in which MSC hTERT have been used as a feeder layer of plasma cells and CK1α silencing was achieved in MM cells or in MSC compartment, RUNX2 downregulation in MM cells was associated with an increased rate of apoptosis (Fig.52). On the contrary, in the model where CK1α inactivation was obtained in both MM and in MSC hTERT, RUNX2 upregulation in MM cells reduced plasma cell apoptosis (Fig.52).

Altogether, the data obtained from this thesis work suggest that the protein kinase CK1α is a key regulator of MM pathophysiology, since not only it supports the malignant plasma cells survival, but also sustains their cross talk with the microenvironment. A specific CK1α inactivation in MM cells or in the MSC counterpart could support the osteogenic transcriptional program, with the potential to counteract the MMABD. We also found that Lena treatment did not seem to have a positive role on the expression of osteoblastic related genes, potentially negatively impacting on the MSC osteogenic differentiation potential. Therefore, CK1α inhibition could be suggested not only to enhance the pro-apoptotic effect of Lena on the haematological plasma cell clonal expansion, but it could also interfere with the undesirable effects of this drug on the MSC osteogenic differentiation potential, likely ameliorating MMABD.

9. BIBLIOGRAFY

[1] O. Castaneda and R. Baz, “Multiple Myeloma Genomics - A Concise Review,” *Acta Med. Acad.*, vol. 48, no. 1, pp. 57–67, 2019.

[2] J. Corre, N. Munshi, and H. Avet-Loiseau, “Genetics of multiple myeloma: Another heterogeneity level?,” *Blood*, vol. 125, no. 12, pp. 1870–1876, 2015.

[3] K. Brigle and B. Rogers, “Pathobiology and Diagnosis of Multiple Myeloma,” *Semin. Oncol. Nurs.*, vol. 33, no. 3, pp. 225–236, 2017.

[4] N. Tageja *et al.*, “Smoldering multiple myeloma: Present position and potential promises,” *Eur. J. Haematol.*, vol. 92, no. 1, pp. 1–12, 2014.

[5] D. Kazandjian, “Multiple myeloma epidemiology and survival: A unique malignancy,” *Semin. Oncol.*, vol. 43, no. 6, pp. 676–681, 2016.

[6] C. M. E. Medical Masterclass Contributors, “ORIGINAL Haematology : multiple myeloma,” *Clin. Med. (Northfield. Il).*, vol. 19, no. 1, pp. 58–60, 2019.

[7] K. C. Anderson and R. D. Carrasco, “Pathogenesis of myeloma,” *Annu. Rev. Pathol. Mech. Dis.*, vol. 6, pp. 249–274, 2011.

[8] C. J. Neuse *et al.*, “Genome instability in multiple myeloma,” *Leukemia*, vol. 34, no. 11, pp. 2887–2897, 2020.

[9] M. Bhutani, D. M. Foureau, S. Atrash, P. M. Voorhees, and S. Z. Usmani, “Extramedullary multiple myeloma,” *Leukemia*, vol. 34, no. 1, pp. 1–20, 2020.

[10] M. T. Gundesen, T. Lund, H. E. H. Moeller, and N. Abildgaard, “Plasma Cell Leukemia: Definition, Presentation, and Treatment,” *Curr. Oncol. Rep.*, vol. 21, no. 1, 2019.

[11] A. García-Ortiz *et al.*, “The role of tumor microenvironment in multiple myeloma development and progression,” *Cancers*, vol. 13, no. 2. pp. 1–22, 2021.

[12] S. Marino and G. D. Roodman, “Multiple myeloma and bone: The fatal interaction,” *Cold Spring Harb. Perspect. Med.*, vol. 8, no. 8, pp. 1–21, 2018.

[13] S. V. Rajkumar, “Multiple myeloma: 2020 update on diagnosis, risk-stratification and management,” *Am. J. Hematol.*, vol. 95, no. 5, pp. 548–567, 2020.

[14] E. C. Fink and B. L. Ebert, “The novel mechanism of lenalidomide activity,” *Blood*, vol. 126, no. 21,

pp. 2366–2369, 2015.

[15] V. Kotla *et al.*, “Mechanism of action of lenalidomide in hematological malignancies,” *J. Hematol. Oncol.*, vol. 2, pp. 1–10, 2009.

[16] F. Accardi, D. Toscani, M. Bolzoni, B. D. Palma, F. Aversa, and N. Giuliani, “Mechanism of Action of Bortezomib and the New Proteasome Inhibitors on Myeloma Cells and the Bone Microenvironment : Impact on Myeloma-Induced Alterations of Bone Remodeling,” vol. 2015, 2015.

[17] S. Gandolfi, J. P. Laubach, T. Hideshima, D. Chauhan, K. C. Anderson, and P. G. Richardson, “The proteasome and proteasome inhibitors in multiple myeloma,” *Cancer Metastasis Rev.*, vol. 36, no. 4, pp. 561–584, 2017.

[18] J. S. Du, C. H. Yen, C. M. Hsu, and H. H. Hsiao, “Management of myeloma bone lesions,” *Int. J. Mol. Sci.*, vol. 22, no. 7, pp. 1–14, 2021.

[19] N. Giuliani and F. Malavasi, “Editorial: Immunotherapy in Multiple Myeloma,” *Front. Immunol.*, vol. 10, no. August, pp. 1–4, 2019.

[20] A. M. Goodman, M. S. Kim, and V. Prasad, “Persistent challenges with treating multiple myeloma early,” *Blood*, vol. 137, no. 4, pp. 456–458, 2021.

[21] T. Hideshima, C. Mitsiades, G. Tonon, P. G. Richardson, and K. C. Anderson, “Understanding multiple myeloma pathogenesis in the bone marrow to identify new therapeutic targets,” *Nature Reviews Cancer*, vol. 7, no. 8. pp. 585–598, 19-Aug-2007.

[22] X. Feng, “Chemical and Biochemical Basis of Cell-Bone Matrix Interaction in Health and Disease,” *Curr. Chem. Biol.*, vol. 3, no. 2, pp. 189–196, 2012.

[23] J. Caetano-Lopes, H. Canhão, and J. E. Fonseca, “Osteoblasts and bone formation.,” *Acta Reum. Port.*, vol. 32, no. 2, pp. 103–110, 2007.

[24] C. Mazziotta *et al.*, “Micrornas modulate signaling pathways in osteogenic differentiation of mesenchymal stem cells,” *Int. J. Mol. Sci.*, vol. 22, no. 5, pp. 1–21, 2021.

[25] A. J. Friedenstein, R. K. Chailakhjan, and K. S. Lalykina, “THE DEVELOPMENT OF FIBROBLAST COLONIES IN MONOLAYER CULTURES OF GUINEA-PIG BONE MARROW AND SPLEEN CELLS,” *Cell Prolif.*, vol. 3, no. 4, 1970.

[26] C. A. Yoshida *et al.*, “Sp7 inhibits osteoblast differentiation at a late stage in mice,” *PLoS One*, vol. 7, no. 3, 2012.

[27] M. Wu, G. Chen, and Y. P. Li, “TGF-β and BMP signaling in osteoblast, skeletal development, and

bone formation, homeostasis and disease," *Bone Res.*, vol. 4, no. March, 2016.

[28] G. Chen, C. Deng, and Y. P. Li, "TGF-β and BMP signaling in osteoblast differentiation and bone formation," *Int. J. Biol. Sci.*, vol. 8, no. 2, pp. 272–288, 2012.

[29] M. Sciaudone, E. Gazzerro, L. Priest, A. M. Delany, and E. Canalis, "Notch 1 Impairs Osteoblastic Cell Differentiation," *Endocrinology*, vol. 144, no. 12, pp. 5631–5639, 2003.

[30] T. Komori, "Regulation of Proliferation, Differentiation and Functions of Osteoblasts by Runx2.," *Int. J. Mol. Sci.*, vol. 20, no. 7, Apr. 2019.

[31] Y.-T. Tsao, Y.-J. Huang, H.-H. Wu, Y.-A. Liu, Y.-S. Liu, and O. K. Lee, "Osteocalcin Mediates Biomineralization during Osteogenic Maturation in Human Mesenchymal Stromal Cells," *Int. J. Mol. Sci.*, vol. 18, no. 1, 2017.

[32] G. Hutchings *et al.*, "Bone Regeneration, Reconstruction and Use of Osteogenic Cells; from Basic Knowledge, Animal Models to Clinical Trials," *J. Clin. Med.*, vol. 9, no. 1, p. 139, 2020.

[33] N. A. Sims and T. J. Martin, "Osteoclasts Provide Coupling Signals to Osteoblast Lineage Cells through Multiple Mechanisms," *Annu. Rev. Physiol.*, vol. 82, pp. 507–529, 2020.

[34] M. Adhikari and J. Delgado-calle, "Role of Osteocytes in Cancer Progression in the Bone and the Associated Skeletal Disease," 2021.

[35] P. V. N. Bodine and B. S. Komm, "Wnt signaling and osteoblastogenesis," *Rev. Endocr. Metab. Disord.*, vol. 7, no. 1–2, pp. 33–39, 2006.

[36] Y. Kobayashi, S. Uehara, N. Udagawa, and N. Takahashi, "Regulation of bone metabolism by Wnt signals," *J. Biochem.*, vol. 159, no. 4, pp. 387–392, 2016.

[37] R. L. Jilka, "Molecular and cellular mechanisms of the anabolic effect of intermittent PTH," *Bone*, vol. 40, no. 6, pp. 1434–1446, 2007.

[38] N. Giuliani, M. Mangoni, and V. Rizzoli, "Osteogenic differentiation of mesenchymal stem cells in multiple myeloma: Identification of potential therapeutic targets," *Exp. Hematol.*, vol. 37, no. 8, pp. 879–886, 2009.

[39] B. Boyce, Z. Yao, and L. Xing, "Osteoclasts have multiple roles in bone in addition to bone resorption," *Crit. Rev. Eukaryot. Gene Expr.*, vol. 19, no. 3, pp. 171–180, 2009.

[40] B. F. Boyce and L. Xing, "Functions of RANKL/RANK/OPG in bone modeling and remodeling," *Arch. Biochem. Biophys.*, vol. 473, no. 2, pp. 139–146, 2008.

[41] N. Kobayashi *et al.*, “Segregation of TRAF6-mediated signaling pathways clarifies its role in osteoclastogenesis,” *EMBO J.*, vol. 20, no. 6, pp. 1271–1280, 2001.

[42] S. Aoki, M. Honma, M. Hayashi, Y. Sugamori, M. Khan, and Y. Kariya, “Coupling of bone resorption and formation by RANKL reverse signalling,” *Nature*, 2018.

[43] M. Tobeiha, M. H. Moghadasian, N. Amin, and S. Jafarnejad, “RANKL/RANK/OPG Pathway: A Mechanism Involved in Exercise-Induced Bone Remodeling,” *Biomed Res. Int.*, vol. 2020, 2020.

[44] M. Bruderer, R. G. Richards, M. Alini, and M. J. Stoddart, “Role and regulation of runx2 in osteogenesis,” *Eur. Cells Mater.*, vol. 28, pp. 269–286, 2014.

[45] K. Sweeney, E. R. Cameron, and K. Blyth, “Complex Interplay between the RUNX Transcription Factors and Wnt/β-Catenin Pathway in Cancer: A Tango in the Night,” *Molecules and cells*, vol. 43, no. 2. 2020.

[46] S. Colla *et al.*, “Human myeloma cells express the bone regulating gene Runx2/Cbfa1 and produce osteopontin that is involved in angiogenesis in multiple myeloma patients,” vol. 6, pp. 2166–2176, 2005.

[47] K. A. Cohen-Solal, R. K. Boregowda, and A. Lasfar, “RUNX2 and the PI3K/AKT axis reciprocal activation as a driving force for tumor progression,” *Mol. Cancer*, vol. 14, no. 1, p. 137, Dec. 2015.

[48] T. Fujita *et al.*, “Runx2 induces osteoblast and chondrocyte differentiation and enhances their migration by coupling with PI3K-Akt signaling,” *J. Cell Biol.*, vol. 166, no. 1, 2004.

[49] F. Kugimiya *et al.*, “GSK-3β controls osteogenesis through regulating Runx2 activity,” *PLoS One*, vol. 2, no. 9, pp. 1–10, 2007.

[50] D. Levanon, V. Negreanu, Y. Bernstein, I. Bar-Am, L. Avivi, and Y. Groner, “Aml1, aml2, and aml3, the human members of the runt domain gene-family: Cdna structure, expression, and chromosomal localization,” *Genomics*, vol. 23, no. 2. pp. 425–432, 1994.

[51] Z. S. Xiao, A. B. Hjelmeland, and L. D. Quarles, “Selective Deficiency of the ‘Bone-related’ Runx2-II Unexpectedly Preserves Osteoblast-mediated Skeletogenesis,” *J. Biol. Chem.*, vol. 279, no. 19, pp. 20307–20313, 2004.

[52] L. YL and X. ZS, “Advances in Runx2 Regulation and Its Isoforms,” *Med. Hypotheses*, vol. 68, no. 1, 2007.

[53] B. D. Gelb, E. Cooper, M. Shevell, and R. J. Desnick, “Genetic mapping of the cleidocranial dysplasia (CCD) locus on chromosome band 6p21 to include a microdeletion.,” *Am. J. Med. Genet.*, vol. 58, no.

2, pp. 200–205, 1995.

[54] V. Geoffroy, P. Ducy, and G. Karsenty, “A PEBP2α/AML-1-related factor increases osteocalcin promoter activity through its binding to an osteoblast-specific cis-acting element,” *J. Biol. Chem.*, vol. 270, no. 52, pp. 30973–30979, 1995.

[55] P. Ducy, R. Zhang, V. Geoffroy, A. L. Ridall, and G. Karsenty, “Osf2/Cbfa1: A transcriptional activator of osteoblast differentiation,” *Cell*, vol. 89, no. 5, pp. 747–754, 1997.

[56] K. Thirunavukkarasu *et al.*, “The osteoblast-specific transcription factor Cbfa1 contributes to the expression of osteoprotegerin, a potent inhibitor of osteoclast differentiation and function,” *J. Biol. Chem.*, vol. 275, no. 33, pp. 25163–25172, 2000.

[57] V. Geoffroy, M. Kneissel, B. Fournier, A. Boyde, and P. Matthias, “High Bone Resorption in Adult Aging Transgenic Mice Overexpressing Cbfa1/Runx2 in Cells of the Osteoblastic Lineage,” *Mol. Cell. Biol.*, vol. 22, no. 17, pp. 6222–6233, 2002.

[58] M. Kuhlwilm, A. Davierwala, and S. Pääbo, “Identification of Putative Target Genes of the Transcription Factor RUNX2,” vol. 8, no. 12, pp. 1–9, 2013.

[59] H. Drissi *et al.*, “Transcriptional autoregulation of the bone related CBFA1/RUNX2 gene,” *J. Cell. Physiol.*, vol. 184, no. 3, pp. 341–350, 2000.

[60] T. Gaur *et al.*, “Canonical WNT signaling promotes osteogenesis by directly stimulating Runx2 gene expression,” *J. Biol. Chem.*, vol. 280, no. 39, pp. 33132–33140, 2005.

[61] Y. Maehata *et al.*, “Both direct and collagen-mediated signals are required for active vitamin D3-elicited differentiation of human osteoblastic cells: Roles of osterix, an osteoblast-related transcription factor,” *Matrix Biol.*, vol. 25, no. 1, pp. 47–58, 2006.

[62] N. Bingham, A. Reale, and A. Spencer, “An Evidence-Based Approach to Myeloma Bone Disease.,” *Curr. Hematol. Malig. Rep.*, vol. 12, no. 2, pp. 109–118, Apr. 2017.

[63] T. Vejlgaard, N. Abildgaard, H. Jans, J. L. Nielsen, and L. Heickendorff, “Abnormal bone turnover in monoclonal gammopathy of undetermined significance: Analyses of type I collagen telopeptide, osteocalcin, bone-specific alkaline phosphatase and propeptides of type I and type III procollagens,” *Eur. J. Haematol.*, vol. 58, no. 2, pp. 104–108, 1997.

[64] N. Giuliani *et al.*, “Myeloma cells block RUNX2 / CBFA1 activity in human bone marrow osteoblast progenitors and inhibit osteoblast formation and differentiation,” vol. 106, no. 7, pp. 2472–2483, 2005.

[65] C. Panaroni, A. J. Yee, and N. S. Raje, “Myeloma and Bone Disease,” *Curr. Osteoporos. Rep.*, vol. 15, no. 5, pp. 483–498, 2017.

[66] B. A. Nierste, C. A. Glackin, and J. Kirshner, “Dkk-1 and IL-7 in plasma of patients with multiple myeloma prevent differentiation of mesenchymal stem cells into osteoblasts.,” *Am. J. Blood Res.*, vol. 4, no. 2, pp. 73–85, 2014.

[67] N. Giuliani *et al.*, “Human myeloma cells stimulate the receptor activator of nuclear factor- B ligand (RANKL) in T lymphocytes : a potential role in multiple myeloma bone disease,” vol. 100, no. 13, pp. 4615–4621, 2002.

[68] D. J. Heath *et al.*, “An osteoprotegerin-like peptidomimetic inhibits osteoclastic bone resorption and osteolytic bone disease in myeloma,” *Cancer Res.*, vol. 67, no. 1, pp. 202–208, 2007.

[69] P. I. Croucher *et al.*, “Osteoprotegerin inhibits the development of osteolytic bone disease in multiple myeloma,” *Blood*, vol. 98, no. 13, pp. 3534–3540, 2001.

[70] N. Giuliani, “Plenary paper Myeloma cells induce imbalance in the osteoprotegerin / osteoprotegerin ligand system in the human bone marrow environment,” vol. 98, no. 13, pp. 3527–3534, 2018.

[71] D. Toscani, M. Bolzoni, F. Accardi, F. Aversa, and N. Giuliani, “Review The osteoblastic niche in the context of multiple myeloma,” 2014.

[72] T. N. Trotter *et al.*, “Myeloma cell – derived Runx2 promotes myeloma progression in bone,” vol. 125, no. 23, pp. 3598–3609, 2019.

[73] M. Garayoa *et al.*, “Mesenchymal stem cells from multiple myeloma patients display distinct genomic profile as compared with those from normal donors,” *Leukemia*, vol. 23, no. 8, pp. 1515–1527, 2009.

[74] J. Adamik *et al.*, “EZH2 or HDAC1 inhibition reverses multiple myeloma-induced epigenetic suppression of osteoblast differentiation,” *Mol. Cancer Res.*, vol. 15, no. 4, pp. 405–417, 2017.

[75] N. Giuliani *et al.*, “Production of Wnt inhibitors by myeloma cells: Potential effects on canonical Wnt pathway in the bone microenvironment,” *Cancer Res.*, vol. 67, no. 16, pp. 7665–7674, 2007.

[76] A. Bolomsky *et al.*, “Immunomodulatory drugs thalidomide and lenalidomide affect osteoblast differentiation of human bone marrow stromal cells in vitro.,” *Exp. Hematol.*, vol. 42, no. 7, pp. 516–25, Jul. 2014.

[77] T. Scullen *et al.*, “Lenalidomide in combination with an activin A-neutralizing antibody: Preclinical

rationale for a novel anti-myeloma strategy," *Leukemia*, vol. 27, no. 8, pp. 1715–1721, 2013.

[78] M. Bolzoni *et al.*, "Immunomodulatory drugs lenalidomide and pomalidomide inhibit multiple myeloma-induced osteoclast formation and the RANKL/OPG ratio in the myeloma microenvironment targeting the expression of adhesion molecules.," *Exp. Hematol.*, vol. 41, no. 4, pp. 387–97.e1, Apr. 2013.

[79] I. Breitkreutz *et al.*, "Lenalidomide inhibits osteoclastogenesis, survival factors and bone-remodeling markers in multiple myeloma.," *Leukemia*, vol. 22, no. 10, pp. 1925–32, Oct. 2008.

[80] S. Munemasa *et al.*, "Osteoprogenitor differentiation is not affected by immunomodulatory thalidomide analogs but is promoted by low bortezomib concentration, while both agents suppress osteoclast differentiation," *Int. J. Oncol.*, vol. 33, no. 1, pp. 129–136, Jul. 2008.

[81] M. Wobus *et al.*, "Impact of lenalidomide on the functional properties of human mesenchymal stromal cells.," *Exp. Hematol.*, vol. 40, no. 10, pp. 867–76, Oct. 2012.

[82] I. Spaan, R. A. Raymakers, A. van de Stolpe, and V. Peperzak, "Wnt signaling in multiple myeloma: a central player in disease with therapeutic potential.," *J. Hematol. Oncol.*, vol. 11, no. 1, p. 67, 2018.

[83] R. Nusse *et al.*, "A new nomenclature for int-1 and related genes: the Wnt gene family.," *Cell*, vol. 64, no. 2, p. 231, Jan. 1991.

[84] K. S. Houschyar *et al.*, "Wnt Pathway in Bone Repair and Regeneration – What Do We Know So Far," *Front. Cell Dev. Biol.*, vol. 6, no. January, pp. 1–13, 2019.

[85] M. Frenquelli and G. Tonon, "WNT Signaling in Hematological Malignancies," *Front. Oncol.*, vol. 10, no. December, pp. 1–8, 2020.

[86] C. Shen *et al.*, "Casein kinase 1α as a regulator of wnt-driven cancer," *Int. J. Mol. Sci.*, vol. 21, no. 16, pp. 1–16, 2020.

[87] R. Baron and M. Kneissel, "WNT signaling in bone homeostasis and disease: from human mutations to treatments," *Nat. Med.*, vol. 19, no. 2, pp. 179–192, 2013.

[88] Y. Zhang and X. Wang, "Targeting the Wnt/β-catenin signaling pathway in cancer," *J. Hematol. Oncol.*, vol. 13, no. 1, pp. 1–16, 2020.

[89] P. Janovská, E. Normant, H. Miskin, and V. Bryja, "Targeting casein kinase 1 (Ck1) in hematological cancers," *Int. J. Mol. Sci.*, vol. 21, no. 23, pp. 1–19, 2020.

[90] A. S. Tsukamoto, R. Grosschedl, R. C. Guzman, T. Parslow, and H. E. Varmus, "Expression of the int-1 gene in transgenic mice is associated with mammary gland hyperplasia and adenocarcinomas in

male and female mice.," *Cell*, vol. 55, no. 4, pp. 619–25, Nov. 1988.

[91] M. Caspi, A. Wittenstein, M. Kazelnik, Y. Shor-Nareznoy, and R. Rosin-Arbesfeld, "Therapeutic targeting of the oncogenic Wnt signaling pathway for treating colorectal cancer and other colonic disorders," *Adv. Drug Deliv. Rev.*, vol. 169, pp. 118–136, 2021.

[92] S. He and S. Tang, "WNT/β-catenin signaling in the development of liver cancers," *Biomed. Pharmacother.*, vol. 132, no. October, p. 110851, 2020.

[93] A. Gajos-Michniewicz and M. Czyz, *Wnt signaling in melanoma*, vol. 21, no. 14. 2020.

[94] E. Ashihara *et al.*, "β-catenin small interfering RNA successfully suppressed progression of multiple myeloma in a mouse model," *Clin. Cancer Res.*, vol. 15, no. 8, pp. 2731–2738, 2009.

[95] K. Sukhdeo *et al.*, "Targeting the beta-catenin/TCF transcriptional complex in the treatment of multiple myeloma.," *Proc. Natl. Acad. Sci. U. S. A.*, vol. 104, no. 18, pp. 7516–21, May 2007.

[96] P. jun Choi, O. Yuseok, J. H. Her, E. Yun, G. Y. Song, and S. Oh, "Anti-proliferative activity of CGK012 against multiple myeloma cells via Wnt/β-catenin signaling attenuation," *Leuk. Res.*, vol. 60, no. July, pp. 103–108, 2017.

[97] C. C. Bjorklund *et al.*, "Evidence of a role for activation of Wnt/β-catenin signaling in the resistance of plasma cells to lenalidomide," *J. Biol. Chem.*, vol. 286, no. 13, pp. 11009–11020, 2011.

[98] H. van Andel, K. A. Kocemba, M. Spaargaren, and S. T. Pals, "Aberrant Wnt signaling in multiple myeloma: molecular mechanisms and targeting options," *Leukemia*, vol. 33, no. 5, pp. 1063–1075, 2019.

[99] C. S. Chim, R. Pang, T. K. Fung, C. L. Choi, and R. Liang, "Epigenetic dysregulation of Wnt signaling pathway in multiple myeloma," *Leukemia*, vol. 21, no. 12, pp. 2527–2536, 2007.

[100] K. Mahtouk *et al.*, "Growth factors in multiple myeloma: A comprehensive analysis of their expression in tumor cells and bone marrow environment using Affymetrix microarrays," *BMC Cancer*, vol. 10, no. Mmc, 2010.

[101] Z. Ren *et al.*, "Syndecan-1 promotes Wnt/b-catenin signaling in multiple myeloma by presenting Wnts and R-spondins," *Blood*, vol. 131, no. 9, pp. 982–994, 2018.

[102] M. Frenquelli *et al.*, "The WNT receptor ROR2 drives the interaction of multiple myeloma cells with the microenvironment through AKT activation," *Leukemia*, vol. 34, no. 1, pp. 257–270, 2020.

[103] Y. W. Qiang *et al.*, "Wnts induce migration and invasion of myeloma plasma cells," *Blood*, vol. 106, no. 5, 2005.

[104] M. P. Yavropoulou and J. G. Yovos, “The role of the Wnt signaling pathway in osteoblast commitment and differentiation.,” *Hormones (Athens).*, vol. 6, no. 4, pp. 279–294, 2007.

[105] S. J. Rodda and A. P. McMahon, “Distinct roles for Hedgehog and caronical Wnt signaling in specification, differentiation and maintenance of osteoblast progenitors,” *Development*, vol. 133, no. 16, pp. 3231–3244, 2006.

[106] J. B. Kim *et al.*, “Bone regeneration is regulated by Wnt signaling,” *J. Bone Miner. Res.*, vol. 22, no. 12, pp. 1913–1923, 2007.

[107] U. H. Lerner and C. Ohlsson, “The WNT system: Background and its role in bone,” *J. Intern. Med.*, vol. 277, no. 6, pp. 630–649, 2015.

[108] C. Bänziger, D. Soldini, C. Schütt, P. Zipperlen, G. Hausmann, and K. Basler, “Wntless, a conserved membrane protein dedicated to the secretion of Wnt proteins from signaling cells.,” *Cell*, vol. 125, no. 3, pp. 509–22, May 2006.

[109] Z. Zhong *et al.*, “Wntless functions in mature osteoblasts to regulate bone mass,” *Proc. Natl. Acad. Sci. U. S. A.*, vol. 109, no. 33, 2012.

[110] Y. Wan *et al.*, “Osteoblastic Wnts differentially regulate bone remodeling and the maintenance of bone marrow mesenchymal stem cells,” *Bone*, vol. 55, no. 1, pp. 258–267, 2013.

[111] S. Kang, C. N. Bennett, I. Gerin, L. A. Rapp, K. D. Hankenson, and O. A. MacDougald, “Wnt Signaling Stimulates Osteoblastogenesis of Mesenchymal Precursors by Suppressing CCAAT/Enhancer-binding Protein α and Peroxisome Proliferator-activated Receptor γ,” *J. Biol. Chem.*, vol. 282, no. 19, pp. 14515–14524, May 2007.

[112] G. J. Spencer, J. C. Utting, S. L. Etheridge, T. R. Arnett, and P. G. Genever, “Wnt signalling in osteoblasts regulates expression of the receptor activator of NFκB ligand and inhibits osteoclastogenesis in vitro,” *J. Cell Sci.*, vol. 119, no. 7, pp. 1283–1296, 2006.

[113] M. V. Semënov, X. Zhang, and X. He, “DKK1 antagonizes Wnt signaling without promotion of LRP6 internalization and degradation,” *J. Biol. Chem.*, vol. 283, no. 31, pp. 21427–21432, 2008.

[114] W. Wei *et al.*, “Biphasic and Dosage-Dependent Regulation of Osteoclastogenesis by -Catenin,” *Mol. Cell. Biol.*, vol. 31, no. 23, pp. 4706–4719, 2011.

[115] G. Manning, D. B. Whyte, R. Martinez, T. Hunter, and S. Sudarsanam, “The protein kinase complement of the human genome,” *Science (80-.).*, vol. 298, no. 5600, pp. 1912–1934, 2002.

[116] U. Knippschild *et al.*, “The CK1 family: Contribution to cellular stress response and its role in

carcinogenesis," *Front. Oncol.*, vol. 4 MAY, no. May, pp. 1–32, 2014.

[117] F. Piazza, S. Manni, A. Arjomand, A. Visentin, L. Trentin, and G. Semenzato, "New responsibilities for aged kinases in B-lymphomas," *Hematol. Oncol.*, vol. 38, no. 1, pp. 3–11, 2020.

[118] B. Schittek and T. Sinnberg, "Biological functions of casein kinase 1 isoforms and putative roles in tumorigenesis," *Mol. Cancer*, vol. 13, no. 1, pp. 1–14, 2014.

[119] B. del Valle-Perez, O. Arques, M. Vinyoles, A. G. de Herreros, and M. Dunach, "Coordinated Action of CK1 Isoforms in Canonical Wnt Signaling," *Mol. Cell. Biol.*, vol. 31, no. 14, pp. 2877–2888, 2011.

[120] L. J. Fulcher and G. P. Sapkota, "Functions and regulation of the serine/threonine protein kinase CK1 family: Moving beyond promiscuity," *Biochem. J.*, vol. 477, no. 23, pp. 4603–4621, 2020.

[121] U. Knippschild, A. Gocht, S. Wolff, N. Huber, J. Löhler, and M. Stöter, "The casein kinase 1 family: Participation in multiple cellular processes in eukaryotes," *Cell. Signal.*, vol. 17, no. 6, pp. 675–689, 2005.

[122] Z. Spinello, A. Fregnani, L. Q. Tubi, L. Trentin, F. Piazza, and S. Manni, "Targeting protein kinases in blood cancer: Focusing on ck1α and ck2," *Int. J. Mol. Sci.*, vol. 22, no. 7, pp. 1–17, 2021.

[123] S. Jiang, M. Zhang, J. Sun, and X. Yang, "Casein kinase 1α: Biological mechanisms and theranostic potential," *Cell Commun. Signal.*, vol. 16, no. 1, pp. 1–24, 2018.

[124] A. S. Alzahrani, "PI3K/Akt/mTOR inhibitors in cancer: At the bench and bedside," *Semin. Cancer Biol.*, vol. 59, no. April, pp. 125–132, 2019.

[125] G. Song, G. Ouyang, and S. Bao, "The activation of Akt/PKB signaling pathway and cell survival," *J. Cell. Mol. Med.*, vol. 9, no. 1, pp. 59–71, 2005.

[126] S. Duan *et al.*, "MTOR generates an auto-amplification loop by triggering the βTrCP- and CK1α-dependent degradation of DEPTOR," *Mol. Cell*, vol. 44, no. 2, pp. 317–324, 2011.

[127] S. Manni *et al.*, "Inactivation of CK1α in multiple myeloma empowers drug cytotoxicity by affecting AKT and β-catenin survival signaling pathways," *Oncotarget*, vol. 8, no. 9, pp. 14604–14619, 2017.

[128] V. N. Ngo *et al.*, "Casein kinase 1 a governs antigen-receptor-induced NF- k B activation and human lymphoma cell survival," vol. 458, no. March, 2009.

[129] D. Vrábel, L. Pour, and S. Ševčíková, "The impact of NF-κB signaling on pathogenesis and current treatment strategies in multiple myeloma," *Blood Rev.*, vol. 34, pp. 56–66, 2019.

[130] J. E. Cortes, R. Gutzmer, M. W. Kieran, and J. A. Solomon, "Hedgehog signaling inhibitors in solid and

hematological cancers," *Cancer Treat. Rev.*, vol. 76, no. April, pp. 41–50, 2019.

[131] Z. Liu *et al.*, "A critical role of autocrine sonic hedgehog signaling in human CD138+myeloma cell survival and drug resistance," *Blood*, vol. 124, no. 13, pp. 2061–2071, 2014.

[132] Y. Hu, W. Song, D. Cirstea, D. Lu, N. C. Munshi, and K. C. Anderson, "CSNK1α1 mediates malignant plasma cell survival," *Leukemia*, vol. 29, no. 2, pp. 474–482, Feb. 2015.

[133] A. Venerando, O. Marin, G. Cozza, V. H. Bustos, S. Sarno, and L. A. Pinna, "Isoform specific phosphorylation of p53 by protein kinase CK1," pp. 1105–1118, 2010.

[134] M. Järås *et al.*, "Csnk1a1 inhibition has p53-dependent therapeutic efficacy in acute myeloid leukemia," vol. 211, no. 4, pp. 605–612, 2014.

[135] R. K. Schneider *et al.*, "Role of casein kinase 1A1 in the biology and targeted therapy of del(5q) MDS," *Cancer Cell*, vol. 26, no. 4, pp. 509–520, 2014.

[136] X. Liu, Q. Huang, L. Chen, H. Zhang, E. Schonbrunn, and J. Chen, "Tumor-derived CK1α mutations enhance MDMX inhibition of p53," *Oncogene*, vol. 39, no. 1, pp. 176–186, 2020.

[137] A. M. Dulak *et al.*, "Exome and whole-genome sequencing of esophageal adenocarcinoma identifies recurrent driver events and mutational complexity," *Nat. Genet.*, vol. 45, no. 5, pp. 478–486, 2013.

[138] Y. Sato *et al.*, "Integrated molecular analysis of clear-cell renal cell carcinoma," *Nat. Genet.*, vol. 45, no. 8, pp. 860–867, 2013.

[139] K. Kataoka *et al.*, "Integrated molecular analysis of adult T cell leukemia/lymphoma," *Nat. Genet.*, vol. 47, no. 11, pp. 1304–1315, 2015.

[140] E. S. Okerberg *et al.*, "Identification of a tumor specific, active-site mutation in casein kinase 1α by chemical proteomics," *PLoS One*, vol. 11, no. 3, p. 172649, 2016.

[141] J. Luo, N. L. Solimini, and S. J. Elledge, "Principles of Cancer Therapy: Oncogene and Non-oncogene Addiction," *Cell*, vol. 136, no. 5, pp. 823–837, 2009.

[142] T. Sinnberg *et al.*, "Suppression of casein kinase 1α in melanoma cells induces a switch in β-catenin signaling to promote metastasis," *Cancer Res.*, vol. 70, no. 17, pp. 6999–7009, 2010.

[143] T. Sinnberg *et al.*, "B-Catenin Signaling Increases During Melanoma Progression and Promotes Tumor Cell Survival and Chemoresistance," *PLoS One*, vol. 6, no. 8, 2011.

[144] S. Manni *et al.*, "Protein Kinase CK1 a Sustains B-Cell Receptor Signaling in Mantle Cell Lymphoma," vol. 11, no. October, pp. 1–15, 2021.

[145] S. Manni, M. Carrino, and F. Piazza, “Role of protein kinases CK1α and CK2 in multiple myeloma: Regulation of pivotal survival and stress-managing pathways,” *J. Hematol. Oncol.*, vol. 10, no. 1, pp. 1–10, 2017.

[146] G. Rena, J. Bain, M. Elliott, and P. Cohen, “D4476, a cell-permeant inhibitor of CK1, suppresses the site-specific phosphorylation and nuclear exclusion of FOXO1a,” *EMBO Rep.*, vol. 5, no. 1, pp. 60–65, 2004.

[147] W. Minzel *et al.*, “Small Molecules Co-targeting CKIα and the Transcriptional Kinases CDK7/9 Control AML in Preclinical Models,” *Cell*, vol. 175, no. 1, pp. 171-185.e25, 2018.

[148] R. Burger *et al.*, “Gp130 and ras mediated signaling in human plasma cell line INA-6: A cytokine-regulated tumor model for plasmacytoma,” *Hematol. J.*, vol. 2, no. 1, pp. 42–53, 2001.

[149] A. F. Gazdar, H. K. Oie, I. R. Kirsch, and G. F. Hollis, “Establishment and characterization of a human plasma cell myeloma culture having a rearranged cellular myc proto-oncogene,” *Blood*, vol. 67, no. 6, pp. 1542–1549, 1986.

[150] K. Mihara *et al.*, “Development and functional characterization of human bone marrow mesenchymal cells immortalized by enforced expression of telomerase,” *Br. J. Haematol.*, vol. 120, no. 5, pp. 846–849, 2003.

[151] J. Caverzasio and D. Manen, “Essential Role of Wnt3a-Mediated Activation of Mitogen-Activated Protein Kinase p38 for the Stimulation of Alkaline Phosphatase Activity and Matrix Mineralization in C3H10T1/2 Mesenchymal Cells,” *Endocrinology*, vol. 148, no. 11, pp. 5323–5330, Nov. 2007.

[152] B. A. Roecklein and B. Torok-Storb, “Functionally distinct human marrow stromal cell lines immortalized by transduction with the human papilloma virus E6/E7 genes,” *Blood*, vol. 85, no. 4, pp. 997–1005, 1995.

[153] M. Tommasino and L. Crawford, “Human Papillomavirus E6 and E7: Proteins which deregulate the cell cycle,” *BioEssays*, vol. 17, no. 6, pp. 509–518, 1995.

[154] C. J. Lengner *et al.*, “Osteoblast differentiation and skeletal development are regulated by Mdm2-p53 signaling,” *J. Cell Biol.*, vol. 172, no. 6, pp. 909–921, 2006.

[155] E. Pedone and L. Marucci, “Role of β -Catenin Activation Levels and Fluctuations in Controlling Cell Fate,” vol. 3, pp. 1–22, 2019.

[156] J. B. C. Papers *et al.*, “Activation of AXIN2 Expression by Beta-Catenin-T Cell Factor,” *J. Biol. Chem.*, vol. 277, no. 24, pp. 21657–21665, 2002.

[157] C. Haxaire, E. Haÿ, and V. Geoffroy, “Runx2 Controls Bone Resorption through the Down-Regulation of the Wnt Pathway in Osteoblasts,” *Am. J. Pathol.*, vol. 186, no. 6, pp. 1598–1609, 2016.

[158] P. Zhang, Y. Wang, C. Cheng, F. Zhang, D. Ding, and D. Chen, “Runt-related transcription factor 2 in fl uences cell adhesion-mediated drug resistance and cell proliferation in B-cell non-Hodgkin ’ s lymphoma and multiple myeloma,” *Leuk. Res.*, vol. 92, no. March, p. 106340, 2020.

[159] N. Artigas *et al.*, “P53 inhibits SP7/Osterix activity in the transcriptional program of osteoblast differentiation,” *Cell Death Differ.*, vol. 24, no. 12, pp. 2022–2031, 2017.

[160] H. Yunlong *et al.*, “T ISSUE -S PECIFIC S TEM C ELLS p53 Loss Increases the Osteogenic Differentiation of Bone Marrow Stromal Cells,” *Stem Cells*, vol. 33, no. December 18, pp. 1304–1319, 2015.

[161] N. Liao *et al.*, “Osteoblast-specific inactivation of p53 results in locally increased bone formation,” *PLoS One*, vol. 16, no. 11 November, pp. 1–17, 2021.